
Report No. K-TRAN: KU-03-4R
REVISED FINAL REPORT

A MODEL STUDY OF BRIDGE HYDRAULICS, EDITION 2

A. David Parr, Ph.D.
Shannon Milburn
Travis Malone
Theodore Bender

The University of Kansas
Lawrence, Kansas

August 2010

A COOPERATIVE TRANSPORTATION RESEARCH PROGRAM
BETWEEN:

KANSAS DEPARTMENT OF TRANSPORTATION
KANSAS STATE UNIVERSITY
UNIVERSITY OF KANSAS



1 Report No. K-TRAN: KU-03-4R		2 Government Accession No.		3 Recipient Catalog No.	
4 Title and Subtitle A Model Study of Bridge Hydraulics, Edition 2				5 Report Date August 2010	
				6 Performing Organization Code	
7 Author(s) A. David Parr, Ph.D., Shannon Milburn, Travis Malone, Theodore Bender				8 Performing Organization Report No.	
9 Performing Organization Name and Address The University of Kansas Department of Civil, Environmental and Architectural Engineering 2150 Learned Hall, 1530 W 15th Street Lawrence, Kansas 66045-7609				10 Work Unit No. (TRAIS)	
				11 Contract or Grant No. C1357	
12 Sponsoring Agency Name and Address Kansas Department of Transportation Bureau of Materials and Research 700 SW Harrison Street Topeka, Kansas 66603-3745				13 Type of Report and Period Covered Revised Final Report July 2002 - June 2010	
				14 Sponsoring Agency Code RE-0318-01	
15 Supplementary Notes This report replaces K-TRAN: KU-03-4, which should have been destroyed. For more information write to address in block 9.					
16 Abstract <p>Most flood studies in the United States use the Army Corps of Engineers HEC-RAS (Hydrologic Engineering Center's River Analysis System) computer program. This study was carried out to compare results of HEC-RAS bridge modeling with laboratory experiments. A laboratory flume was constructed specifically for this purpose. Nine experiments were performed for each bridge type for a range of flow and tailwater conditions.</p> <p>This report is the second edition. The first edition of the report considered the laboratory model to be distorted with 1:100 horizontal scale and 1:20 vertical scale. The second edition considers both distorted and undistorted interpretations of the laboratory models. Moreover, more advanced HEC-RAS modeling techniques are used to better match the HEC-RAS and the laboratory results.</p> <p>HEC-RAS models were developed for the assumption of a distorted laboratory model and for the assumption of an undistorted laboratory model. The results were very close for the distorted and undistorted HEC-RAS models. The maximum difference in computed water surface elevation was about 2 percent (0.28 ft in prototype dimensions) at the downstream bounding cross section.</p> <p>Overall, HEC-RAS did very well in matching the laboratory results as long as the Froude number did not exceed 0.7 at the downstream bounding cross section. When the Froude number exceeded 0.7 at the downstream bounding cross section, the laboratory results still showed the effect of tailwater condition but the HEC-RAS models did not.</p>					
17 Key Words HEC-RAS, tailwater, bridge hydraulics			18 Distribution Statement No restrictions. This document is available to the public through the National Technical Information Service, Springfield, Virginia 22161		
19 Security Classification (of this report) Unclassified		20 Security Classification (of this page) Unclassified		21 No. of pages 114	
				22 Price	

A MODEL STUDY OF BRIDGE HYDRAULICS, EDITION 2

Revised Final Report

Prepared by

A. David Parr, Ph.D.
Shannon Milburn
Travis Malone
Theodore Bender

The University of Kansas
Lawrence, Kansas

A Report on Research Sponsored By

THE KANSAS DEPARTMENT OF TRANSPORTATION
TOPEKA, KANSAS

August 2010

© Copyright 2010, **Kansas Department of Transportation**

PREFACE

The Kansas Department of Transportation's (KDOT) Kansas Transportation Research and New-Developments (K-TRAN) Research Program funded this research project. It is an ongoing, cooperative and comprehensive research program addressing transportation needs of the state of Kansas utilizing academic and research resources from KDOT, Kansas State University and the University of Kansas. Transportation professionals in KDOT and the universities jointly develop the projects included in the research program.

NOTICE

The authors and the state of Kansas do not endorse products or manufacturers. Trade and manufacturers' names appear herein solely because they are considered essential to the object of this report.

This information is available in alternative accessible formats. To obtain an alternative format, contact the Office of Transportation Information, Kansas Department of Transportation, 700 SW Harrison, Topeka, Kansas 66603-3745 or phone (785) 296-3585 (Voice) (TDD).

DISCLAIMER

The contents of this report reflect the views of the authors who are responsible for the facts and accuracy of the data presented herein. The contents do not necessarily reflect the views or the policies of the state of Kansas. This report does not constitute a standard, specification or regulation.

REPORT

This revised final report completely replaces the K-TRAN: KU-03-4 report that was distributed in September of 2007. If you have a copy of this report with the September 2007 date, please destroy it and use only this report.

ABSTRACT

Most flood studies in the United States use the Army Corps of Engineers HEC-RAS (Hydrologic Engineering Center's River Analysis System) computer program. This study was carried out to compare results of HEC-RAS bridge modeling with laboratory experiments. A laboratory flume was constructed specifically for this purpose. The following three different bridge geometries were considered.

- Type 1 A regular bridge with abutments, bridge piers and roadway,
- Type 2 A simple bridge opening with weir flow in one overbank,
- Type 3 A simple skewed bridge.

Nine experiments were performed for each bridge type for a range of flow and tailwater conditions.

This report is the second edition. The first edition of the report considered the laboratory model to be distorted with 1:100 horizontal scale and 1:20 vertical scale. The second edition considers both distorted and undistorted interpretations of the laboratory models. Moreover, more advanced HEC-RAS modeling techniques are used to better match the HEC-RAS and the laboratory results. The advanced HEC-RAS models were based on review comments and model revisions by Mr. Gary W. Brunner (GWB), Senior Technical Hydraulic Engineer, Hydrologic Engineering Center (HEC).

The agreement between laboratory and HEC-RAS modeling was good for all cases except when the Froude number at the downstream bridge face cross section exceeded a Froude number of about 0.7. For these experiments, the HEC-RAS model results showed inlet control and the tailwater condition did not affect the water surface

profiles upstream from the bridge. The corresponding laboratory results did show the tailwater effect upstream from the bridge when the Froude number exceeded 0.7.

HEC-RAS models were developed for the assumption of a distorted laboratory model and for the assumption of an undistorted laboratory model. The results were very close for the distorted and undistorted HEC-RAS models. The maximum difference in computed water surface elevation was about 2 percent (0.28 feet in prototype dimensions) at the downstream bounding cross section.

Overall, HEC-RAS did very well in matching the laboratory results as long as the Froude number did not exceed 0.7 at the downstream bounding cross section. When the Froude number exceeded 0.7 at the downstream bounding cross section, the laboratory results still showed the effect of tailwater condition but the HEC-RAS models did not.

ACKNOWLEDGEMENTS

This project was supported by the Kansas Department of Transportation (KDOT). We greatly appreciate Brad Rognlie, Michael Orth and Rudy Reynolds of KDOT for their continued support and their genuine interest quality engineering. We would also like to express our appreciation to Jim Weaver with the University of Kansas for his help and advice on this project. Special thanks are due to Mr. Gary Brunner of Hydrologic Engineering Center (HEC) for his help and advice in the development of significantly improved HEC-RAS models that are discussed in this report.

TABLE OF CONTENTS

Abstract	iii
Acknowledgements	v
Table Of Contents	vi
List Of Tables	vii
List Of Figures	ix
Chapter 1 - Introduction.....	1
Chapter 2 - Laboratory Model	3
Chapter 3 - Modeling Criteria	8
Chapter 4 - Type 1 Experiments – Standard Bridge Flow	12
4.1 Regular Undistorted Type 1 HEC-RAS Models.....	16
4.2 Modified Undistorted Type 1 HEC-RAS Models.....	21
4.3 Distorted Type 1 HEC-RAS Models	30
4.4 Adjusting N-Values Through the Bridge Opening.....	35
Chapter 5 - Type 2 Experiments – Combination Bridge/Weir Flow	39
5.1 Regular Undistorted Type 2 HEC-RAS Models.....	46
5.2 Modified Distorted Type 2 HEC-RAS Models.....	49
5.3 Distorted Type 2 HEC-RAS Models	61
Chapter 6 - Type 3 Experiments – Skewed Bridge	65
6.1 Regular Distorted Type 3 HEC-RAS Models.....	68
6.2 Modified Distorted Type 3 HEC-RAS Models.....	76
6.3 Distorted Type 3 HEC-RAS Models	87
Chapter 7 - Summary And Conclusions	91
References	99

LIST OF TABLES

Table 4.1: Parameters for Type 1 Experiments.....	16
Table 4.2: Type 1 Laboratory Water Surface Profiles Expressed in Prototype Dimensions.....	18
Table 4.3: Laboratory Results for Regular Undistorted HEC-RAS Stations	18
Table 4.4: Regular Undistorted HEC-RAS Model Results.....	19
Table 4.5: Differences in Water Surface Elevations between HEC-RAS and Laboratory for the Regular Undistorted HEC-RAS Model (HR – Lab)	19
Table 4.6: Modified Undistorted HEC-RAS Model Results.....	25
Table 4.7: Laboratory Results for Modified Distorted HEC-RAS Stations	25
Table 4.8: Differences in Water Surface Elevations between HEC-RAS and Laboratory for the Modified Undistorted HEC-RAS Model (HR – Lab)	26
Table 4.9: Results for Undistorted and Distorted Regular Type 1 HEC-RAS Models.....	32
Table 4.10: Results for Undistorted and Distorted Modified GWB Type 1 HEC- RAS Models.....	33
Table 4.11: Parameters for the Modified Undistorted and Distorted HEC-RAS Models.....	34
Table 5.1: Parameters for Type 2 Experiments.....	44
Table 5.2: Laboratory Results for Type 2 Experiments	45
Table 5.3: Water Surface Profiles for the Regular Undistorted HEC-RAS Type 2 Experiments.....	48
Table 5.4: Lab Results for Type 2 Experiments at Undistorted HEC-RAS Stations	48
Table 5.5: Differences (HEC-RAS - Lab) for Regular Undistorted Model.....	48
Table 5.6: Water Surface Profiles for the Modified (GWB) Distorted HEC-RAS Type 2 Experiments.....	53
Table 5.7: Differences (HEC-RAS - Lab) for Modified Undistorted Model.....	53
Table 5.8: Differences between Modified and Regular Undistorted Type 2 HEC- RAS Models (Mod – Reg).....	54
Table 5.9: Results for Undistorted and Distorted Regular GWB Type 2 HEC-RAS Models.....	62
Table 5.10: Results for Undistorted and Distorted Modified GWB Type 2 HEC- RAS Models.....	63
Table 5.11: HEC-RAS Parameters for Undistorted and Distorted Modified GWB Type 2 HEC-RAS Models.....	64

Table 6.1: Bounding Cross Sections and Deck/Roadway Data Before and After Invoking the Skew Option in the Bridge Editor.....	68
Table 6.2: Reach Length and Contraction/Expansion Coefficient Tables for Type 3 Experiments.....	73
Table 6.3: Parameter for Type 3 Experiments.....	74
Table 6.4: Lab Results for Type 3 Experiments	75
Table 6.5: Lab Results for Type 3 Experiments at HEC-RAS Undistorted Stations	75
Table 6.6: Regular Undistorted Type 3 HEC-RAS Results.....	75
Table 6.7: Differences (HEC-RAS - Lab) for Regular Undistorted Type 3 Model	76
Table 6.8: Modified Undistorted Type 3 HEC-RAS Results.....	79
Table 6.9: Lab Results for Type 3 Experiments at HEC-RAS Undistorted Stations	79
Table 6.10: Differences (HEC-RAS - Lab) for Modified Undistorted Type 3 Model	79
Table 6.11: Results for Modified Undistorted and Distorted Type 3 HEC-RAS Models.....	88
Table 6.12: Results for Undistorted and Distorted Modified GWB Type 2 HEC- RAS Models.....	89
Table 6.13: HEC-RAS Parameters for Undistorted and Distorted Modified GWB Type 3 HEC-RAS Models (No Interpolated Xsecs)	90
Table 7.1: Portion of Table 4.11 for Type 1 Experiments	93
Table 7.2: Portion of Table 5.11 for Type 2 Experiments	94
Table 7.3: Portion of Table 6.13 for Type 3 Experiments	96
Table 7.4: Project, Plan and File Names	98

LIST OF FIGURES

Figure 2.1: Plan View of Laboratory Flume	3
Figure 2.2: Calibration Curve for Flume Inflow Pipe	4
Figure 2.3: Locations of Piezometers in Test Reach	5
Figure 2.4: Piezometer Bank Location and Construction	6
Figure 2.5: Manometer Bank for a Typical Experiment	7
Figure 3.1: Derivation of Equation for the Prototype Main Channel n-value in Terms of the n-value from the Laboratory Model – Distorted Model	10
Figure 3.2: Derivation of Equations for Prototype Overbank n-values in Terms of the n-value from the Laboratory Model – Distorted Model	11
Figure 4.1: Model and Prototype Roadway Embankments for Type 1 Experiments	12
Figure 4.2: Bridge Model for Type 1 Experiments	13
Figure 4.3: Distorted Prototype Dimensions of Bridge for Type 1 Experiments.....	14
Figure 4.4: Upstream and Downstream Views of a Type 1 Experiment	15
Figure 4.5: Screen Captures of the Regular Distorted HEC-RAS Model for Type 1 Experiments	17
Figure 4.6: Laboratory and Regular Distorted HEC-RAS Results for Type1 Experiments	20
Figure 4.7: Dye Streakline Showing Nonlinear Flow Pattern.....	23
Figure 4.8: Plan, Bridge and n-value Table for Modified GWB HEC-RAS Model	24
Figure 4.9: Water Surface Profiles for the Laboratory, Regular Distorted HEC- RAS Model and Modified Distorted HEC-RAS Model – Low Flow	27
Figure 4.10: Water Surface Profiles for the Laboratory, Regular Distorted HEC- RAS Model and Modified Distorted HEC-RAS Model – Middle Flow	28
Figure 4.11: Water Surface Profiles for the Laboratory, Regular Distorted HEC- RAS Model and Modified Distorted HEC-RAS Model – High Flow.....	29
Figure 4.12: Derivation of Equations for Type 1 Bridge Overbank n-values in Terms of the n-value from the Laboratory Model	36
Figure 4.13: Derivation of Equations for Type 3 Bridge Overbank n-values in Terms of the n-value from the Laboratory Model	37
Figure 4.14: Derivation of Equations for Type 2 Main Channel n-values in Terms of the n-value from the Laboratory Model	38
Figure 5.1: Bridge Model for Type 2 Experiments	40
Figure 5.2: Prototype of Bridge Model for Type 2 Experiments.....	41

Figure 5.3: Illustration of Containment Region for Measuring the Weir Discharge	42
Figure 5.4: Weir and Bridge for a Type 2 Experiment	43
Figure 5.5: Type 2 Experiment	45
Figure 5.6: Plan, Bridge and n-value Table for Regular Distorted Type 2 HEC-RAS Model	47
Figure 5.7: Plan View and Bridge for Regular Distorted HEC-RAS Type 2 Model	52
Figure 5.8: Lab and Undistorted Regular and Modified HEC-RAS Results for Type 2 Experiments - Low Flow	55
Figure 5.9: Lab and Undistorted Regular and Modified HEC-RAS Results for Type 2 Experiments - Middle Flow	56
Figure 5.10: Lab and Undistorted Regular and Modified HEC-RAS Results for Type 2 Experiments - High Flow	57
Figure 5.11: Lab and Undistorted Regular and Modified HEC-RAS Results for Type 2 Experiments - Low Flow	58
Figure 5.12: Lab and Undistorted Regular and Modified HEC-RAS Results for Type 2 Experiments - Middle Flow	59
Figure 5.13: Lab and Undistorted Regular and Modified HEC-RAS Results for Type 2 Experiments - High Flow	60
Figure 6.1: Laboratory and Prototype Bridge Geometry for Type 3 Experiments	66
Figure 6.2: Type 3 Laboratory Bridge Model in Flume	67
Figure 6.3: Upstream View of Skewed Bridge for Type 3 Experiments	67
Figure 6.4: Screen Captures for Regular Undistorted Type 3 HR Model with No Bridge Skew	70
Figure 6.5: Screen Captures for Regular Undistorted Type 3 HR Model with 30° Bridge Skew	71
Figure 6.6: Plan View of RS 150 and RS 346.13 for Skewed Bridge	72
Figure 6.7: Lab and HEC-RAS Undistorted Results for Type 3 Experiments - Low Flow	80
Figure 6.8: Lab and HEC-RAS Undistorted Results for Type 3 Experiments - Middle Flow	81
Figure 6.9: Lab and HEC-RAS Undistorted Results for Type 3 Experiments - High Flow	82
Figure 6.10: Lab and HEC-RAS Undistorted Results for Type 3 Experiments (No Skew for Regular and 30 Deg Skew for Modified) - Low Flow	84
Figure 6.11: Lab and HEC-RAS Undistorted Results for Type 3 Experiments (No Skew for Regular and 30 Deg Skew for Modified) - Middle Flow	85

Figure 6.12: Lab and HEC-RAS Undistorted Results for Type 3 Experiments (No Skew for Regular and 30 Deg Skew for Modified) - High Flow	86
--	----

CHAPTER 1 - INTRODUCTION

Most analyses of bridge hydraulics for flood flows are performed using the Army Corps of Engineers HEC-RAS (Hydrologic Engineering Center's River Analysis System) computer program. This study was carried out to compare results of HEC-RAS bridge modeling with experiments performed in a laboratory flume. The study was intended to add some insight into the effect of bridge hydraulic features such as ineffective flow regions, weir overflow and flow through skewed bridges. This insight should be useful for bridge engineers in HEC-RAS bridge modeling endeavors.

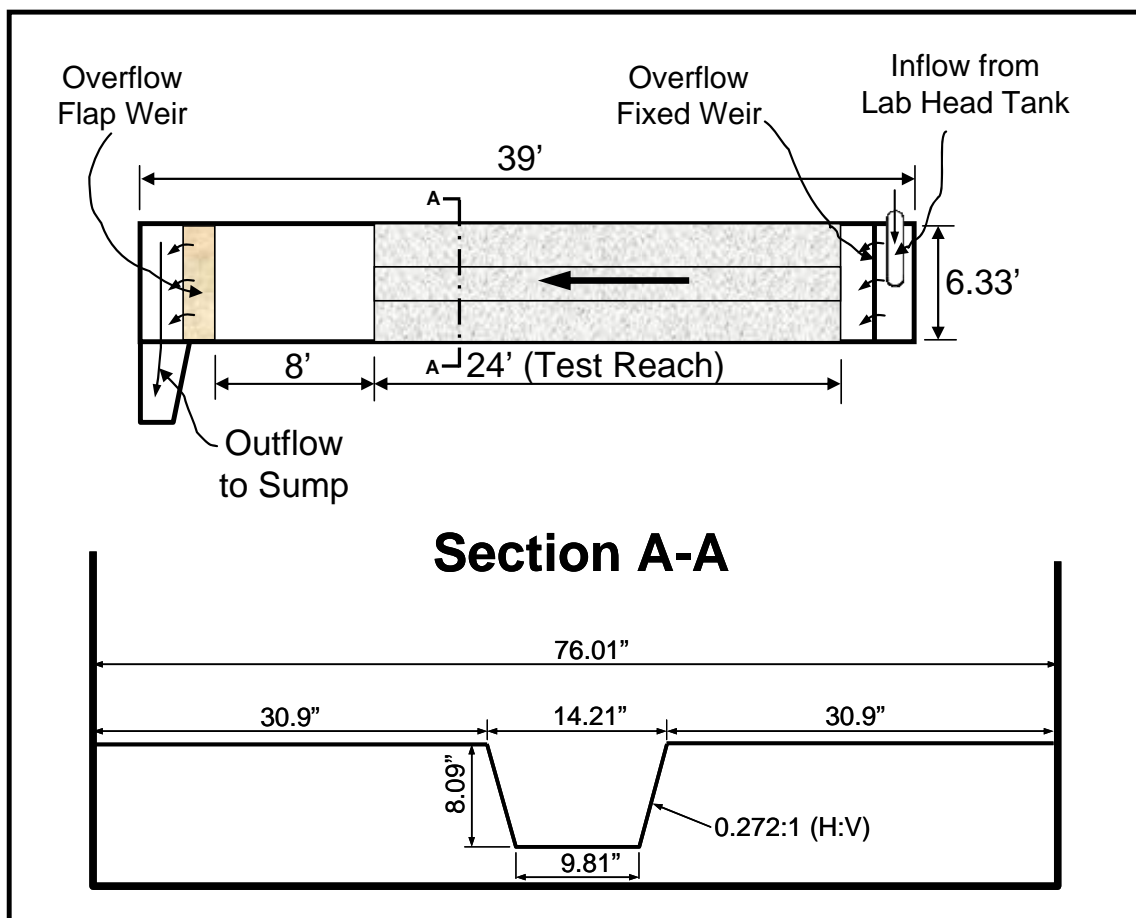
A laboratory flume was constructed specifically for this project. The flume cross section has a main channel region and relatively wide left and right overbank regions. Different bridge scenarios were modeled. Froude number similarity was used to "scale up" model parameters and create prototype HEC-RAS hydraulic models simulating laboratory model conditions. Water surface profiles were compared for corresponding HEC-RAS and laboratory results.

Edition 2 of this report presents both undistorted and distorted modeling scenarios and uses HEC-RAS Version 4.0. Regular HEC-RAS models were created using standard modeling procedures from the HEC-RAS User's and Hydraulic Manuals (Computer Program Documentation (CPD) 68 and 69). Modified HEC-RAS models were developed based on a review of the original report (Edition 1) by Mr. Gary W. Brunner (GWB), Senior Technical Hydraulic Engineer, Hydrologic Engineering Center (HEC) and subsequent correspondence with him. In fact, he revised the HEC-RAS models for the Type 1, Type 2 and Type 3 experiments and improved the agreement between laboratory and HEC-RAS results. Mr. Brunner found a coding error in the Type

2 and Type 3 models of the Edition 1 HEC-RAS models that consisted of a 0.02 feet gap in the bridge embankments. While fixing this error did not result in large differences it did allow for high flow for the Type 2 experiments to be modeled correctly as pressure/weir flow. He also had concerns regarding cross section spacing, ineffective flow, contraction/expansion ratios and distorted modeling that were addressed in the HEC-RAS models presented in Edition 2. In response to his concerns regarding distorted modeling, equivalent distorted and undistorted HEC-RAS models were developed and compared. They agreed very well.

CHAPTER 2 - LABORATORY MODEL

Figure 2.1 shows the plan view and the test reach cross section of the laboratory flume. The flume was constructed of wood and was 39-feet long and 6.33-feet wide. The test section was 24-feet long. Water was supplied from the constant-head system of the Hydraulics Laboratory. An 8-inch diameter PVC pipe carried the flow to a head basin in the flume. The water issued vertically downward in the head basin then passed over a fixed, horizontal weir. An adjustable flap weir was used to control the depth of flow in the flume. After overtopping the flap weir, the water was returned to the laboratory sump system.



A valve in the inflow pipe was used to control the discharge. One piezometer was installed in the head tank and another was placed upstream from three 90-degree bends in the pipe supply line. The head difference between the two piezometers was measured using a differential manometer. The calibration curve shown in Figure 2.2 was then developed to express discharge versus head loss between the two piezometers.

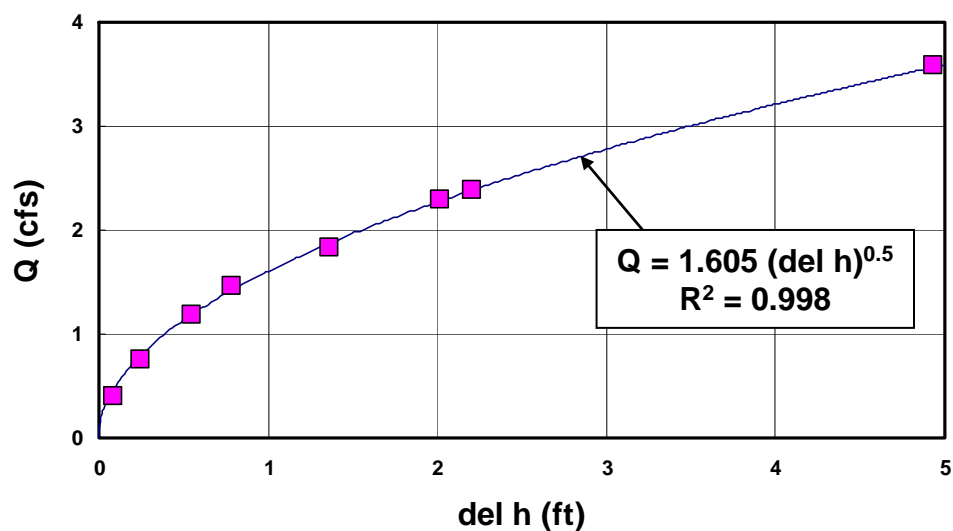
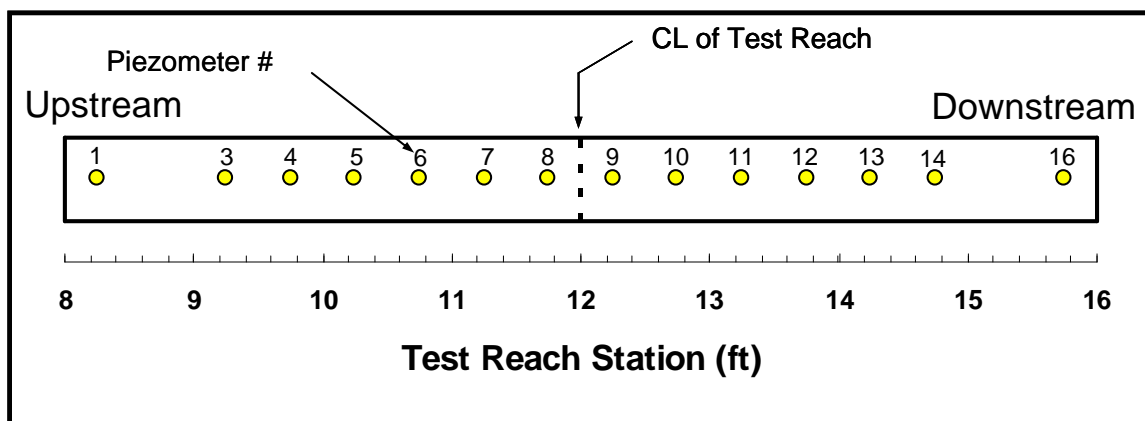


Figure 2.2: Calibration Curve for Flume Inflow Pipe

Water surface profiles were measured 3.75 feet upstream and 3.75 feet downstream of the centerline of the test reach by piezometers installed in the left overbank sidewall of the main channel. The piezometers were spaced at 6-inch intervals as shown in Figure 2.3 below. The next to the last piezometers on each end were not used. These would have been piezometers 2 and 15. Tubing was attached to each of the piezometers and extended under the flume as shown in Figure 2.4 to the manometer bank in Figure 2.5. The HGL elevations were easily read from the manometer bank and used to determine the water depths at each piezometer station. A

vacuum pump was connected to all of the manometers so the water surface elevation could be raised to a readable height. This was necessary since the flume was essentially on the ground. The water surface elevations were recorded for each manometer then the values were adjusted to match a physical depth measurement in the flume at either the upstream or downstream piezometers station. Some experimental runs with low downstream tailwater elevations were not conducive to this type of measurement since the pressure distribution was clearly not hydrostatic for the entire test reach. These runs were not analyzed.



**Figure 2.3: Locations of Piezometers in Test Reach
(Piezometers 2 and 15 Inoperable)**

The three types of experiments performed in this study are listed below.

- Type 1. General Bridge Modeling.
- Type 2. Combination Bridge/Weir Flow.
- Type 3. Skewed Bridge.

Each of the experimental types had different physical bridge models. They are described in the following sections.

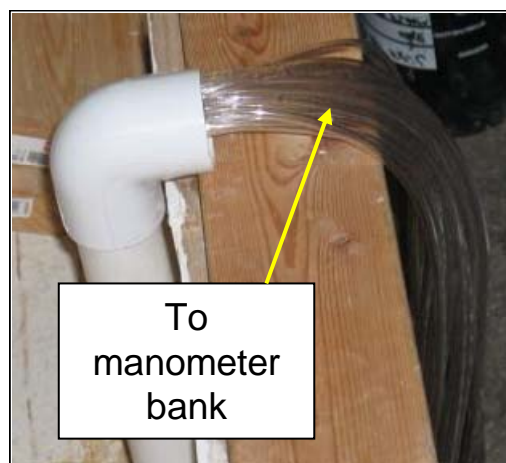
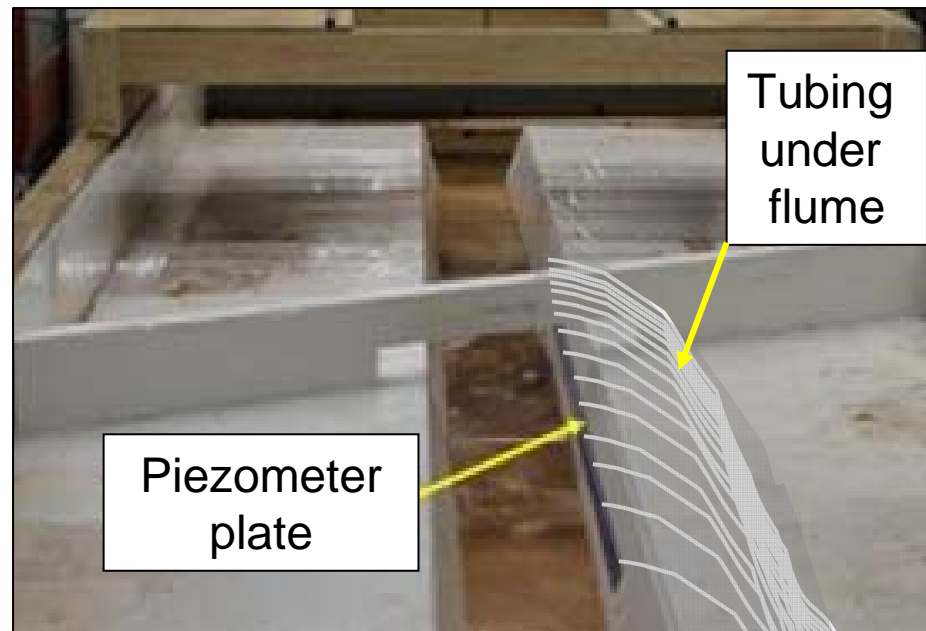


Figure 2.4: Piezometer Bank Location and Construction

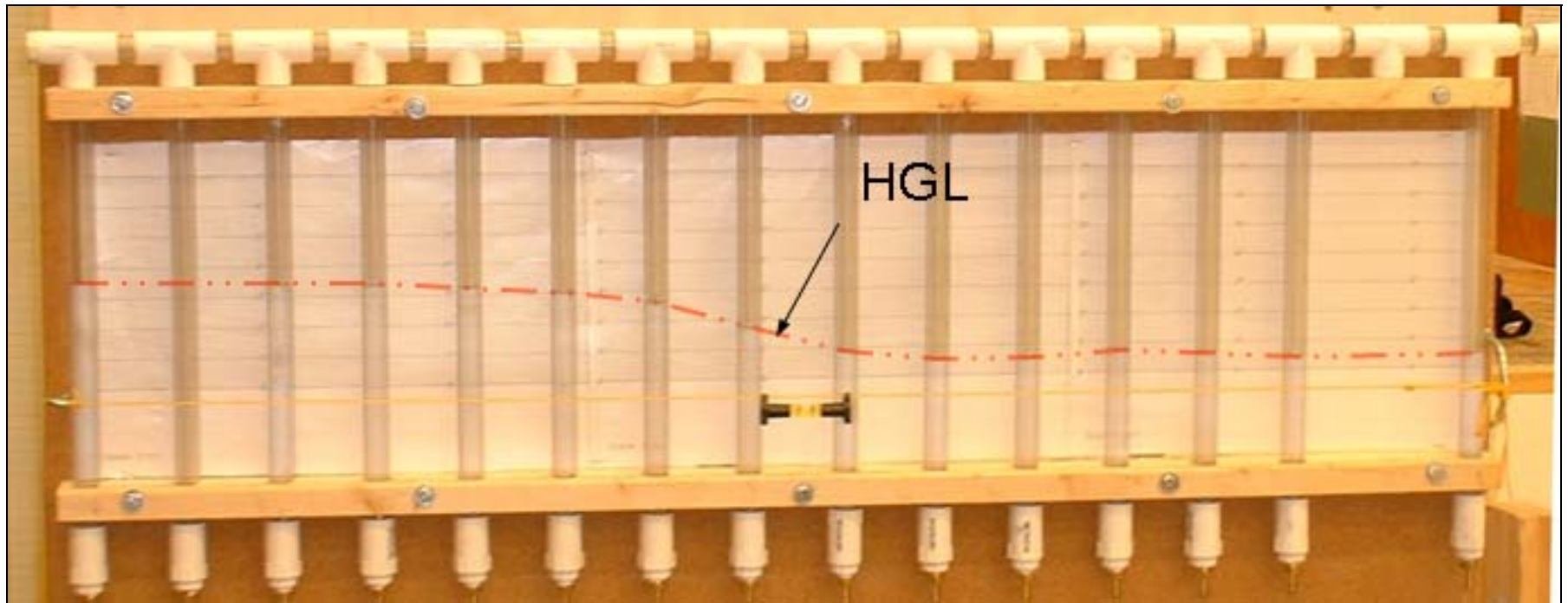


Figure 2.5: Manometer Bank for a Typical Experiment

CHAPTER 3 - MODELING CRITERIA

New HEC-RAS models in Edition 2 of this report were developed for the assumption of both distorted and undistorted laboratory models. The original study assumed that the laboratory model was distorted with a horizontal scale ($X_r = X_{\text{prototype}} / X_{\text{model}} = X_p / X_m$) of 100:1 and a vertical scale ($Y_r = Y_{\text{prototype}} / Y_{\text{model}} = Y_p / Y_m$) of 20:1. The n-value modeling criteria for the distorted model have been changed in Edition 2 to account for differences in overbank and main channel n-values. The undistorted model assumes a 20:1 prototype to model scale for all dimensions.

Froude Number similarity dictates the following for undistorted and distorted models. (pp 494-496, Henderson, 1966)

Undistorted ($L_r = X_r = Y_r = 20$)

$$Q_r = \frac{Q_p}{Q_m} = L_r^{5/2} \rightarrow Q_p = L_r^{5/2} Q_m = (20)^{5/2} Q_m = 1789 Q_m \quad \text{Equation 4.1}$$

$$n_r = \frac{n_p}{n_m} = L_r^{1/6} \rightarrow n_p = L_r^{1/6} n_m = (20)^{1/6} n_m = 1.648 n_m \quad \text{Equation 4.2}$$

Distorted ($X_r = 100; Y_r = 20$)

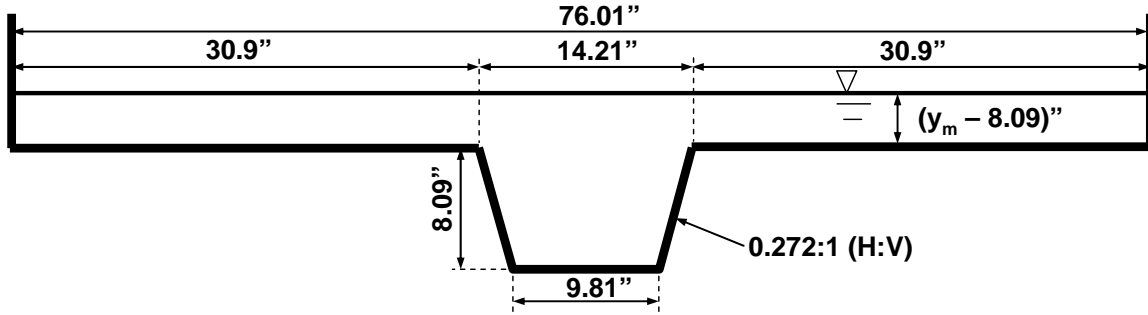
$$Q_r = \frac{Q_p}{Q_m} = X_r Y_r^{3/2} \rightarrow Q_p = X_r Y_r^{3/2} Q_m = 100(20)^{3/2} Q_m = 8944 Q_m \quad \text{Equation 4.3}$$

$$n_r = \frac{n_p}{n_m} = \frac{R_r^{2/3}}{X_r^{1/2}} \rightarrow n_p = \frac{R_r^{2/3}}{X_r^{1/2}} n_m = \frac{R_r^{2/3}}{(100)^{1/2}} n_m = 0.1 R_r^{2/3} n_m \quad \text{Equation 4.4}$$

The measured n-value for the laboratory model was 0.0141. The corresponding prototype n-value for the undistorted HEC-RAS model Equation 2 gives the following for the prototype. This value applied to the main channel and the overbanks.

$$n_p = 1.648(0.0141) = 0.0233 \text{ (Undistorted Model)}$$

Our initial distorted HEC-RAS models used 0.0135 for overbanks and the main channel. In the revised distorted models, different n-values are used for the main channel and the overbank regions based on the following analysis. The equations in Figure 3.1 show that for a laboratory model n-value of 0.0141, the appropriate prototype main channel n-value is 0.0150. Figure 3.2 shows that the overbank n-values should be 0.0104 when the effective flow does not come in contact with the banks due to the ineffective flow area option. When the effective overbank flow contacts the banks, the overbank n-value is given in the table of Figure 3.2 as a function of the model depth, y_m , in inches. Using the functional relationship would involve trial and error between the equation and HEC-RAS in addition to requiring separate plans for each HEC-RAS profile. Consequently, an overbank n-value of 0.0110 was used for all cross sections for which the effective overbank flow contacts the banks. The n-values round to 0.011 for prototype depths ranging from 15 to 23.5 feet which covers most of the experimental data.



Main Channel (X_r = horizontal scale; Y_r = vertical scale)

$$R_r = \frac{R_p}{R_m} = \left(\frac{A_p}{P_{w,p}} \right) / \left(\frac{A_m}{P_{w,m}} \right) = \left[\frac{P_{w,m}}{P_{w,p}} \right] \left[\frac{A_p}{A_m} \right] = \left[\frac{P_{w,m}}{P_{w,p}} \right] [A_r] = \left[\frac{P_{w,m}}{P_{w,p}} \right] [X_r Y_r]$$

$$R_r = \frac{\left[9.81 + 2\sqrt{8.09^2 + ((14.21 - 9.81)/2)^2} \right]}{\left[[X_r] 9.81 + 2\sqrt{[Y_r] 8.09^2 + [X_r] (14.21 - 9.81)/2^2} \right]} [X_r Y_r]$$

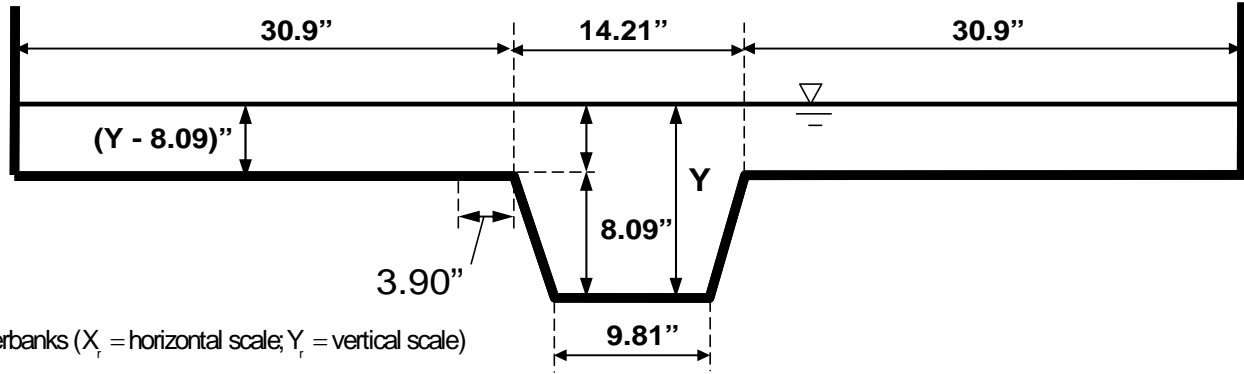
$$R_r = \frac{\left[9.81 + 2\sqrt{8.09^2 + ((14.21 - 9.81)/2)^2} \right]}{\left[[100] 9.81 + 2\sqrt{[20] 8.09^2 + [100] (14.21 - 9.81)/2^2} \right]} [(100)(20)]$$

$$R_r = \left[\frac{2.214}{127.3} \right] [2000] = 34.8$$

$$\eta_r = \frac{R_r^{2/3}}{X_r^{1/2}} = \frac{34.8^{2/3}}{100^{1/2}} = 1.067$$

$$\eta_{p,mc} = 1.067 \eta_{m,mc} = 1.067 (0.0141) = \boxed{0.0150}$$

Figure 3.1: Derivation of Equation for the Prototype Main Channel n-value in Terms of the n-value from the Laboratory Model – Distorted Model



Overbanks (X_r = horizontal scale; Y_r = vertical scale)

Y_m = model depth in ft; Y_p = prototype depth in feet

$$y_m = \frac{12Y_p}{20} = (0.6Y_p) = \text{model depth in inches}$$

With bank contact in overbanks

$$R_r = \left[\frac{(A_p / P_{w,p})}{(A_m / P_{w,m})} \right] = \left[\frac{P_{w,m}}{P_{w,p}} \right] \left[\frac{A_p}{A_m} \right] = \left[\frac{P_{w,m}}{P_{w,p}} \right] A_r = \left[\frac{P_{w,m}}{P_{w,p}} \right] [X_r Y_r]$$

$$R_r = \frac{[(y_m - 8.09) + 30.9]}{[[Y_r][y_m - 8.09] + [X_r]30.9]} [X_r Y_r] = \frac{[(Y_p - 8.09) + 30.9]}{[[Y_r][Y_p - 8.09] + [X_r]30.9]} [X_r Y_r]$$

$$R_r = \frac{[(0.6Y_p - 8.09) + 30.9]}{[[20][0.6Y_p - 8.09] + [100]30.9]} [(100)(20)] = \frac{[(0.6Y_p - 8.09) + 30.9]}{[(12Y_p - 161.9) + 3090]} [X_r Y_r]$$

$$n_r = R_r^{2/3} X_r^{-1/2} = \left(\frac{[(0.6Y_p - 8.09) + 30.9]}{[(12Y_p - 161.9) + 3090]} \right)^{2/3} (100)^{2/3} (20)^{2/3} (100)^{-1/2} = 15.87 \left(\frac{[(0.6Y_p - 8.09) + 30.9]}{[(12Y_p - 161.9) + 3090]} \right)^{2/3}$$

$$n_p = 15.87 \left(\frac{[(0.6Y_p - 8.09) + 30.9]}{[(12Y_p - 161.9) + 3090]} \right)^{2/3} n_m = 15.87 \left(\frac{[(y_m - 8.09) + 30.9]}{[(20y_m - 161.9) + 3090]} \right)^{2/3} n_m$$

$$n_{p,lab} = n_{p,rob} = \left[0.224 \left(\frac{[(y_m - 8.09) + 30.9]}{[(20y_m - 161.9) + 3090]} \right)^{2/3} \right]$$

Without bank contact in overbanks

$$R_r = R_r = \left[\frac{P_{w'm}}{P_{w'p}} \right] [X_r Y_r] = \frac{(L)}{([X_r]L)} [X_r Y_r] = Y_r$$

$$n_r = \frac{R_r^{2/3}}{X_r^{1/2}} = \frac{Y_r^{2/3}}{X_r^{1/2}} = \frac{20^{2/3}}{100^{1/2}} = 0.737$$

$$n_{p,lab} = n_{p,rob} = 0.737 n_{m,lab} = 0.737(0.0141) = \boxed{0.0104}$$

Flow Contacts Overbanks

y_m (in)	Y_p (ft)	n_p
8.1	13.50	0.0104
8.4	14.00	0.0105
8.7	14.50	0.0105
9	15.00	0.0106
9.3	15.50	0.0106
9.6	16.00	0.0107
9.9	16.50	0.0107
10.2	17.00	0.0108
10.5	17.50	0.0108
10.8	18.00	0.0109
11.1	18.50	0.0109
11.4	19.00	0.0110
11.7	19.50	0.0110
12	20.00	0.0111
12.3	20.50	0.0111
12.6	21.00	0.0112
12.9	21.50	0.0112
13.2	22.00	0.0113
13.5	22.50	0.0113
13.8	23.00	0.0114
14.1	23.50	0.0114
14.4	24.00	0.0115

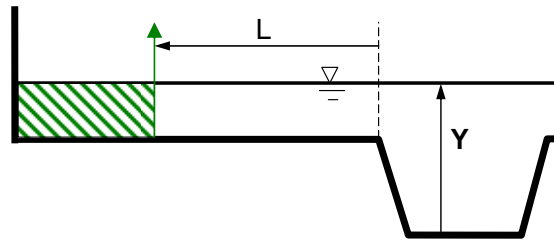


Figure 3.2: Derivation of Equations for Prototype Overbank n-values in Terms of the n-value from the Laboratory Model – Distorted Model

CHAPTER 4 - TYPE 1 EXPERIMENTS – STANDARD BRIDGE

FLOW

This experimental set-up was designed to simulate a typical “real-world” bridge. It included roadway embankments, bridge deck, guard rails and piers. Figure 4.1 shows the cross section of the roadway embankment for the model, undistorted and distorted conditions. Figure 4.2 shows the bridge model with units in inches and the undistorted 20-scale prototype dimensions in feet. These undistorted prototype dimensions were determined by multiplying the model dimensions by $(20/12 = 1.667)$. The model bridge was centered in the 24-foot test reach of the flume. Figure 4.3 shows a prototype sketch of the distorted bridge model for 1:100 horizontal and 1:20 vertical scales. These “prototype” dimensions were used to create the HEC-RAS model of Type 1 Experiments.

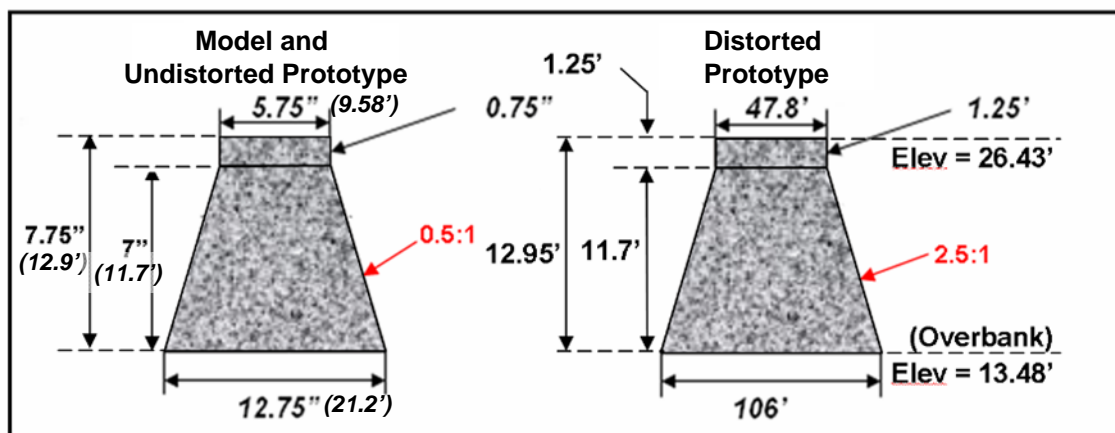
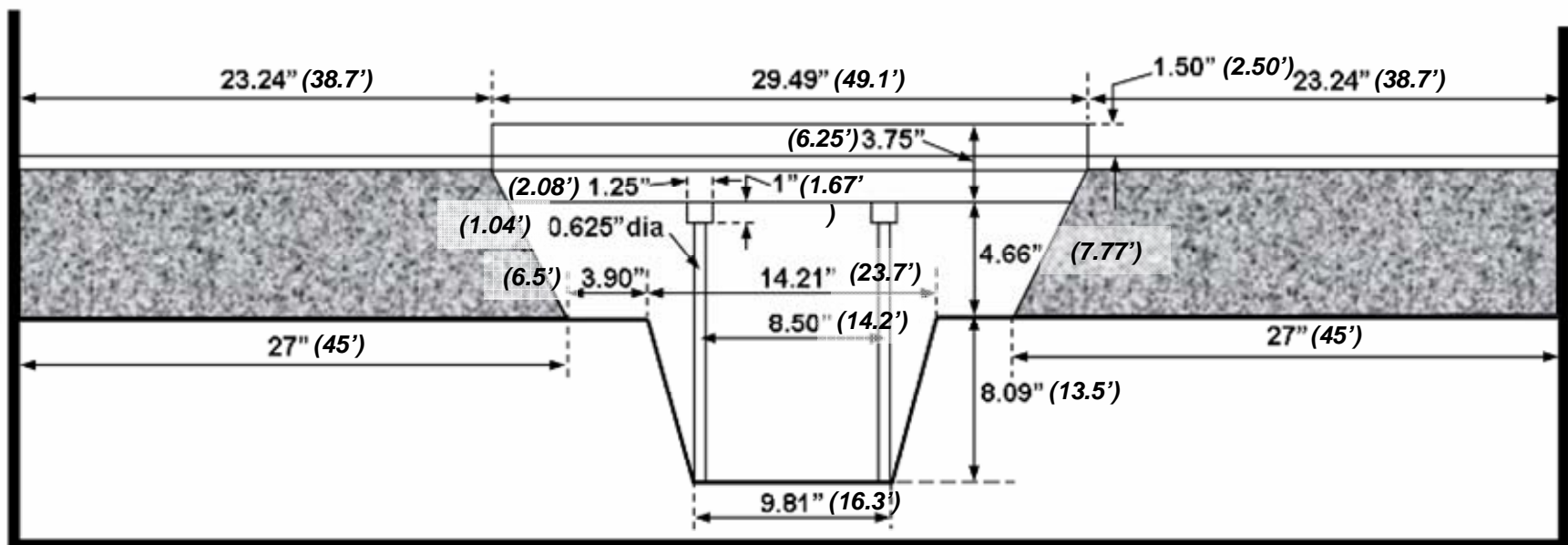


Figure 4.1: Model and Prototype Roadway Embankments for Type 1 Experiments



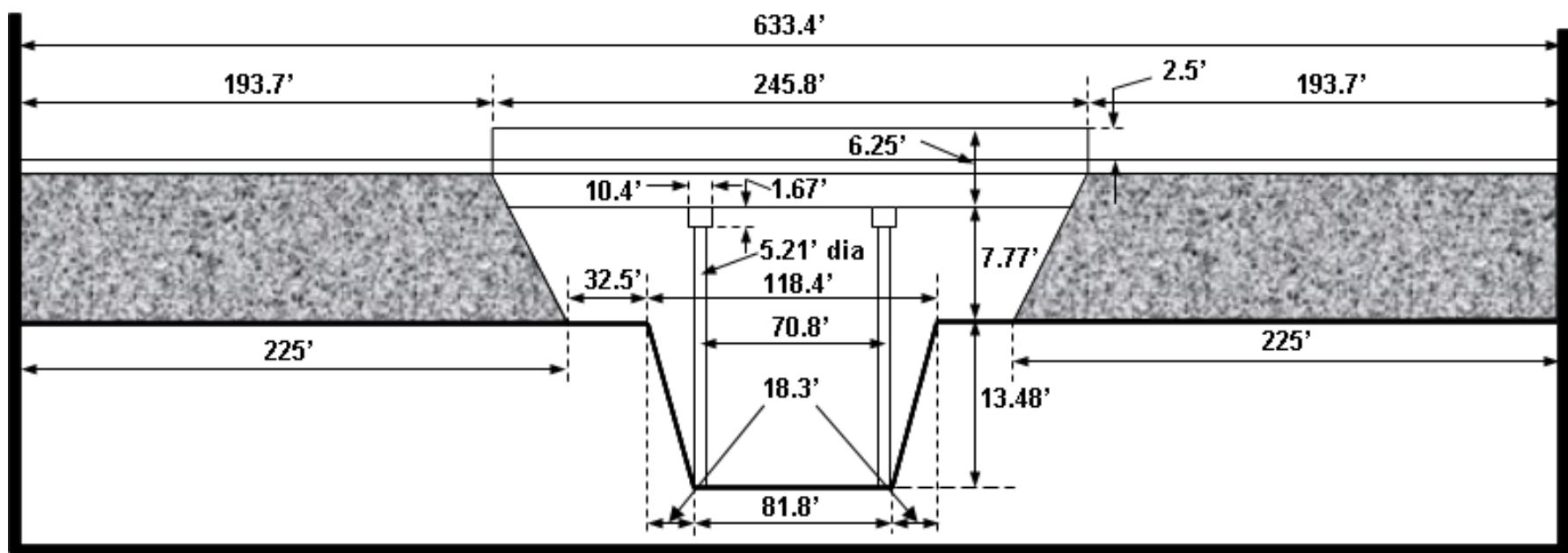


Figure 4.3: Distorted Prototype Dimensions of Bridge for Type 1 Experiments

Type 1 laboratory experiments were performed for 3 different discharges - 2.02, 2.46 and 3.13 cfs. Three trials with different tailwater elevations were performed for each discharge. The nine experiments performed in the laboratory for Type 1 Experiments are shown in Table 4.1 along with laboratory and prototype dimensions. Figure 4.4 shows the upstream and downstream views of flow through the Type 1 Bridge for one of the experiments.

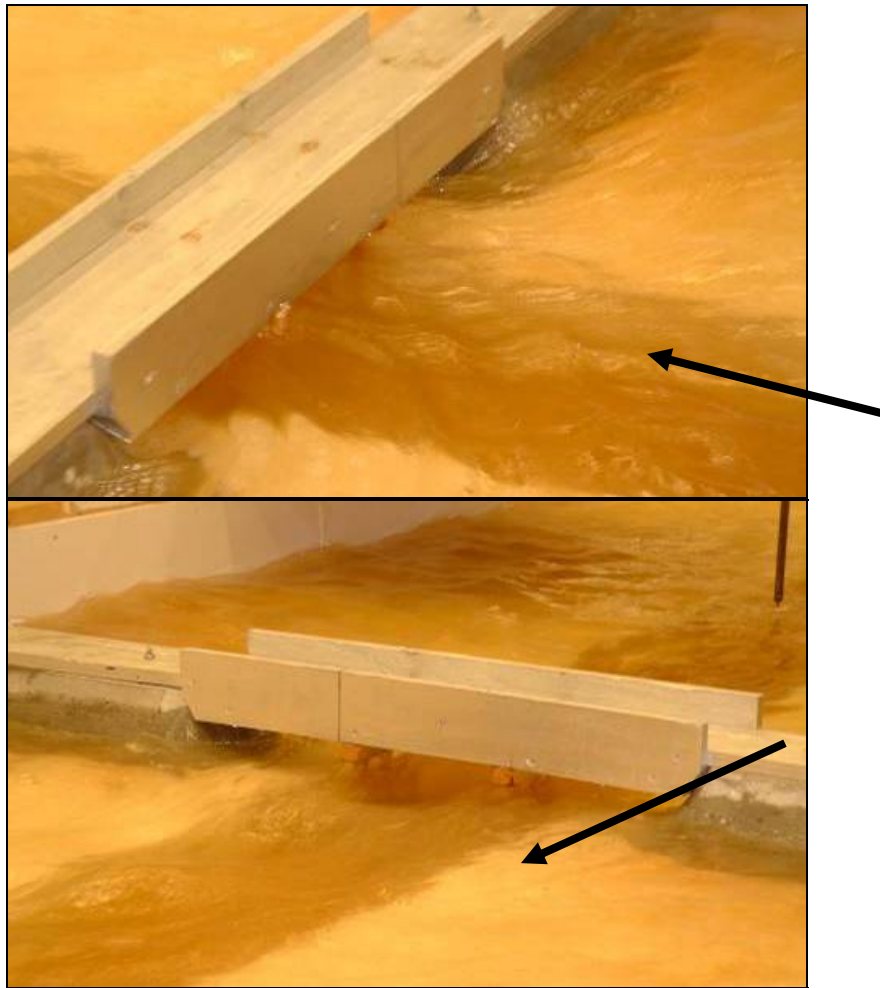


Figure 4.4: Upstream and Downstream Views of a Type 1 Experiment

Table 4.1: Parameters for Type 1 Experiments

Profile No.	Tailwater (RS 0) (ft)	Discharge		
		Laboratory Model (cfs)	Prototype Distorted (cfs)	Prototype Undistorted (cfs)
1	2	3	4	5
1	18.83	2.02	18100	3620
2	17.86	2.02	18100	3620
3	16.09	2.02	18100	3620
4	16.90	2.46	22000	4400
5	15.43	2.46	22000	4400
6	13.58	2.46	22000	4400
7	19.08	3.13	28000	5600
8	18.50	3.13	28000	5600
9	16.03	3.13	28000	5600

4.1 Regular Undistorted Type 1 HEC-RAS Models

Figure 4.5 shows screen captures of the cross section layout and the upstream bridge section for the Regular Undistorted Type 1 HEC-RAS Model. The HEC-RAS cross section spacings were irregular as per HEC-RAS modeling procedures. The lab piezometer spacings in distorted prototype dimensions were 10 feet except for the first two and the last two operating piezometers (See Figure 2.3). The energy method was used with a contraction ratio C_c of 1 and an expansion ratio C_e of 2 as recommended by Gary Brunner. The Manning n -values were 0.0233 throughout.

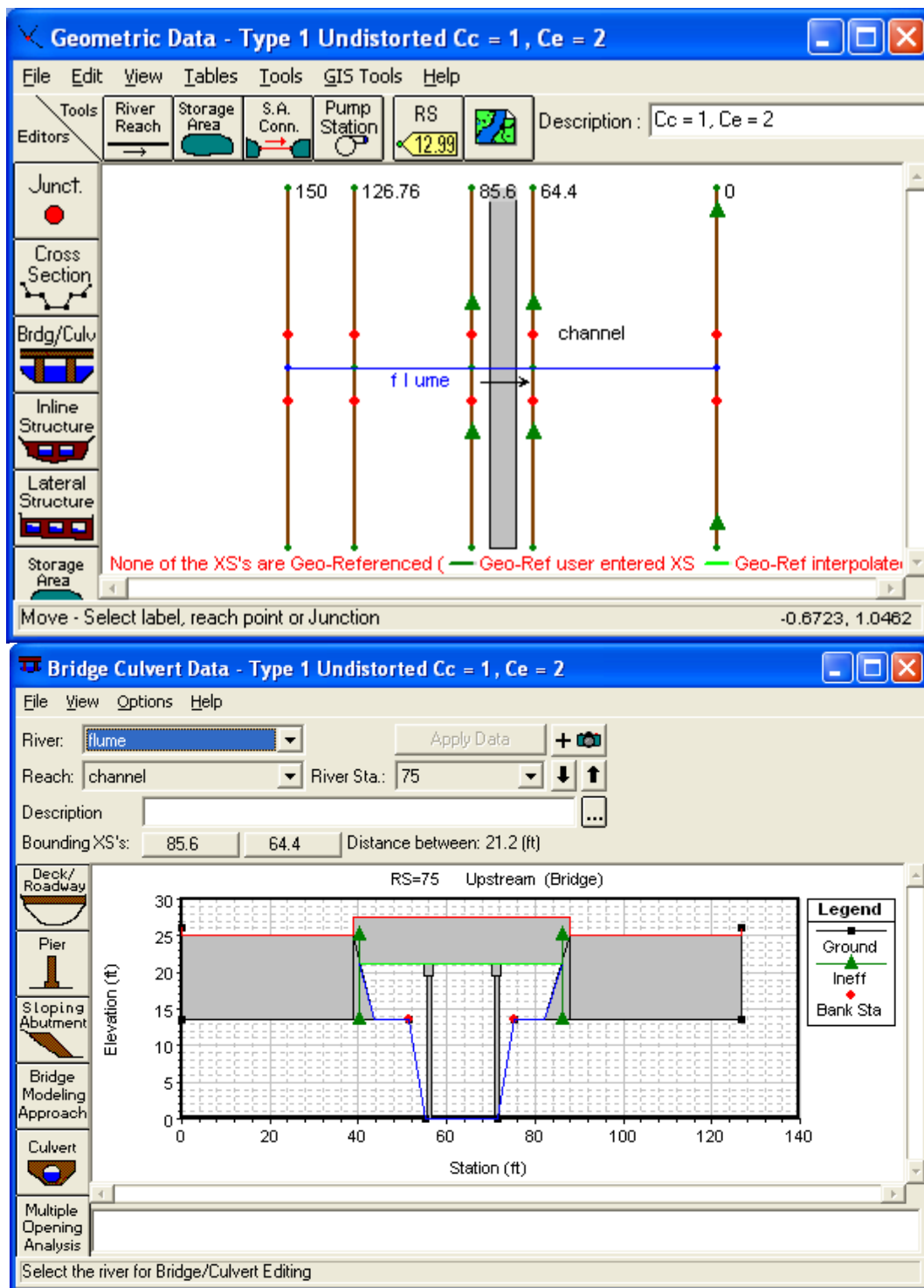


Figure 4.5: Screen Captures of the Regular Distorted HEC-RAS Model for Type 1 Experiments

The laboratory results are expressed in prototype depths in Table 4.2. (This is the depth in inches multiplied by (20/12).) Table 4.3 shows laboratory values from Table 4.2 for the HEC-RAS stations. Linear interpolation was used to obtain the values in the gray cells. The Regular Distorted Type 1 HEC-RAS model results are presented in Table 4.4. The differences between the Table 4.4 and Table 4.3 values are given in Table 4.5.

Table 4.2: Type 1 Laboratory Water Surface Profiles Expressed in Prototype Dimensions

River Station (ft) 1	Laboratory Results								
	Prof 1 (ft) 2	Prof 2 (ft) 3	Prof 3 (ft) 4	Prof 4 (ft) 5	Prof 5 (ft) 6	Prof 6 (ft) 7	Prof 7 (ft) 8	Prof 8 (ft) 9	Prof 9 (ft) 10
150	20.08	19.36	18.18	19.49	18.77	17.91	21.33	21.00	19.45
130	20.08	19.36	18.18	19.49	18.77	17.91	21.24	20.91	19.37
120	20.08	19.27	18.09	19.40	18.60	17.83	21.16	20.83	19.28
110	20.00	19.19	18.01	19.32	18.52	17.66	20.99	20.75	19.20
100	19.91	19.11	17.84	19.24	18.27	17.41	20.83	20.50	18.87
90	19.66	18.86	17.51	18.82	17.77	16.66	20.49	20.16	18.45
80	19.33	18.52	16.93	17.99	16.77	15.41	19.83	19.33	17.45
70	19.00	18.11	16.34	17.32	15.93	14.16	19.33	18.75	16.53
60	18.91	18.02	16.34	17.24	15.85	13.91	19.16	18.66	16.45
50	18.83	17.94	16.18	17.07	15.77	13.91	18.99	18.50	16.28
40	18.83	17.86	16.18	17.07	15.60	13.75	18.99	18.50	16.20
30	18.83	17.86	16.18	17.07	15.68	13.58	19.08	18.58	16.20
20	18.83	17.86	16.18	17.02	15.60	13.75	19.08	18.58	16.28
0	18.83	17.86	16.09	16.90	15.43	13.58	19.08	18.50	16.03

Table 4.3: Laboratory Results for Regular Undistorted HEC-RAS Stations

Laboratory Undistorted RS (ft) 1	Low Q			Middle Q			High Q		
	Prof 1 (ft) 2	Prof 2 (ft) 3	Prof 3 (ft) 4	Prof 4 (ft) 5	Prof 5 (ft) 6	Prof 6 (ft) 7	Prof 7 (ft) 8	Prof 8 (ft) 9	Prof 9 (ft) 10
150	20.08	19.36	18.18	19.49	18.77	17.91	21.33	21.00	19.45
126.76	20.135	19.330	18.149	19.461	18.656	17.943	21.271	20.887	19.338
85.6	19.515	18.710	17.253	18.455	17.326	16.111	20.199	19.797	18.009
64.4	18.949	18.060	16.343	17.275	15.886	14.023	19.232	18.701	16.485
0	18.83	17.86	16.09	16.90	15.43	13.58	19.08	18.50	16.03

 Interpolated Values

Table 4.4: Regular Undistorted HEC-RAS Model Results

Regular Undistorted RS (ft) 1	Low Q			Middle Q			High Q		
	Prof 1 (ft) 2	Prof 2 (ft) 3	Prof 3 (ft) 4	Prof 4 (ft) 5	Prof 5 (ft) 6	Prof 6 (ft) 7	Prof 7 (ft) 8	Prof 8 (ft) 9	Prof 9 (ft) 10
150	19.68	18.93	17.9	19.23	19.32	19.32	21.42	21.25	21.34
126.76	19.68	18.92	17.89	19.22	19.31	19.31	21.41	21.24	21.33
85.6	18.88	17.98	16.64	17.66	17.8	17.8	19.65	19.39	19.53
64.4	18.59	17.59	15.81	16.43	15.05	15.23	18.45	17.8	15.64
0	18.83	17.86	16.09	16.9	15.43	14	19.08	18.5	16.03

Table 4.5: Differences in Water Surface Elevations between HEC-RAS and Laboratory for the Regular Undistorted HEC-RAS Model (HR – Lab)

Regular Undistorted RS (ft) 1	Low Q			Middle Q			High Q		
	Prof 1 (ft) 2	Prof 2 (ft) 3	Prof 3 (ft) 4	Prof 4 (ft) 5	Prof 5 (ft) 6	Prof 6 (ft) 7	Prof 7 (ft) 8	Prof 8 (ft) 9	Prof 9 (ft) 10
150	-0.40	-0.43	-0.28	-0.26	0.55	1.41	0.09	0.25	1.89
126.76	-0.46	-0.41	-0.26	-0.24	0.65	1.37	0.14	0.35	1.99
85.6	-0.64	-0.73	-0.61	-0.79	0.47	1.69	-0.55	-0.41	1.52
64.4	-0.36	-0.47	-0.53	-0.84	-0.84	1.21	-0.78	-0.90	-0.85
0	0.00	0.00	0.00	0.00	0.00	0.42	0.00	0.00	0.00

Figure 4.6 shows plots of the laboratory and HEC-RAS results for the Regular, Undistorted Type 1 HEC-RAS model. The HEC-RAS results agree with the laboratory measurements very well for the low flow conditions. The headwater for the HEC-RAS model does not appear to be affected by the tailwater for the middle and high flows, however, even though a clear effect is seen for the corresponding laboratory results.

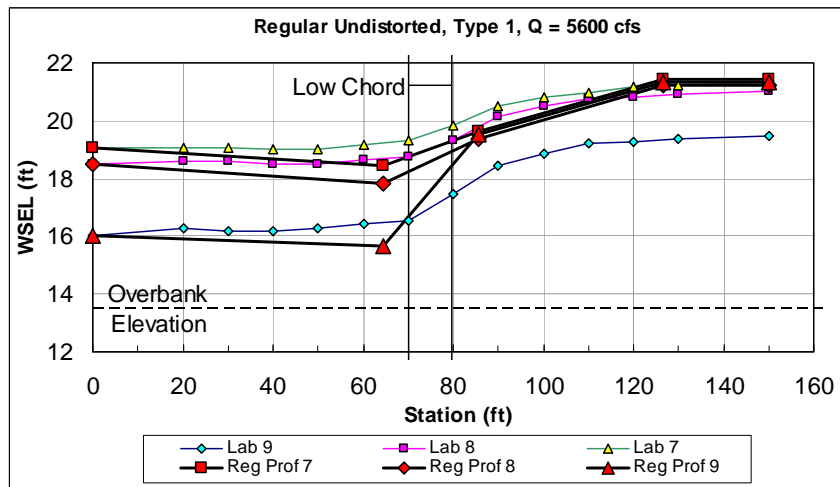
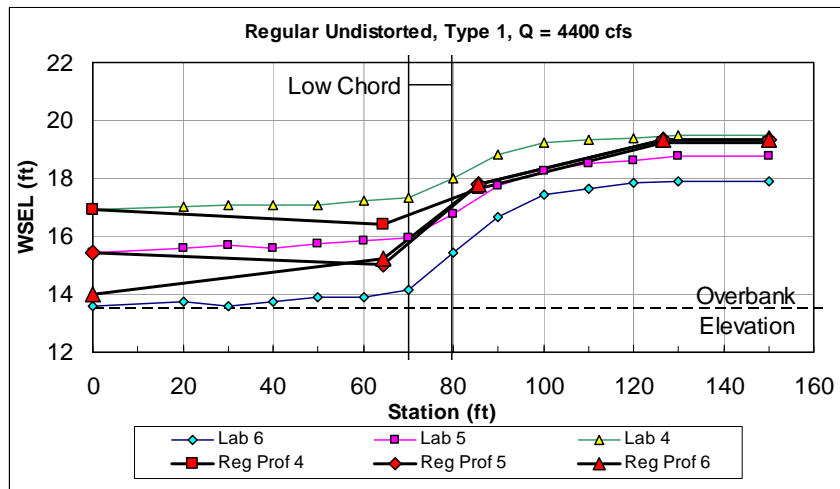
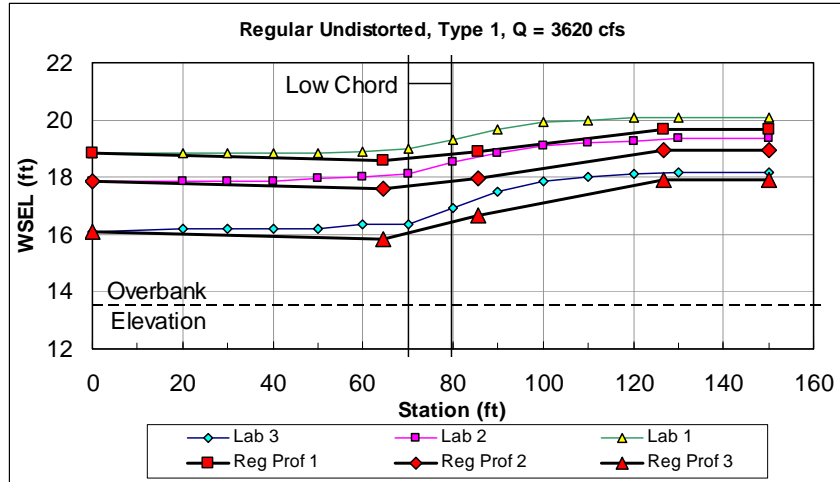


Figure 4.6: Laboratory and Regular Distorted HEC-RAS Results for Type1 Experiments

4.2 Modified Undistorted Type 1 HEC-RAS Models

The Modified Undistorted Type 1 HEC-RAS model layout is shown by the screen capture in Figure 4.8 together with the n-value table. This model was created by Gary Brunner and supplemented with the n-values from the previous section. The text below was transmitted in an e-mail from Mr. Brunner to us. It explains his revisions to the Type 1 model.

Type 1 Model:

1. I interpolated a few cross sections on the upstream side of the model. In my previous comments about the appropriate contraction and expansion reach lengths, I think you misunderstood me, in that you can still have intermediate cross sections, but you must estimate the ineffective flow areas appropriately.
2. I added ineffective flow areas to the interpolated cross sections, but I did not use a linear transition for the ineffective flow areas. In general, for a contraction upstream of a bridge, the flow will start to contract very slowly, and then the rate of contraction will increase as it gets closer to the bridge. Flow contractions are very non-linear.
3. I raised the starting water surface on profile 6 from 13.58 to 14. This profile is fairly problematic. The lab data had the water surface just above the main channel. By placing the water surface at that elevation, the program was computing a starting energy, actually greater than profile 5, which had a higher tailwater. This tremendously high energy right from the start is causing the bad profile computations. Since the program can only

add energy, it already has too much energy by the time it gets to the bridge, so the water surface goes way up. We need to discuss this. I have concerns about how the water surface elevations were measured in the flume, versus what is being applied and used in RAS. **(Parr: See Figure 4.10)**

4. After these changes, all of the water surfaces were closer to the observed. They are not perfect, but they look pretty good.

The main difference between the Modified model and the Regular model discussed above is that the boundary of the effective flow region upstream from the bridge is not linear but rather follows the nonlinear “typical flow transition pattern” shown in Figure 5-1 of the *HEC-RAS River Analysis System Hydraulic Reference Manual Report No. CPD 69* (Brunner, 2008). This pattern or one similar to it is what is actually seen in the laboratory and in the field. This is illustrated by the dye streakline in Figure 4.7 below from the Type 1 lab set up with the bridge deck removed. He also raised the tailwater elevation at RS 0 for Profile 6 from 13.58 feet to 14 feet to get better model conversion.



Figure 4.7: Dye Streakline Showing Nonlinear Flow Pattern

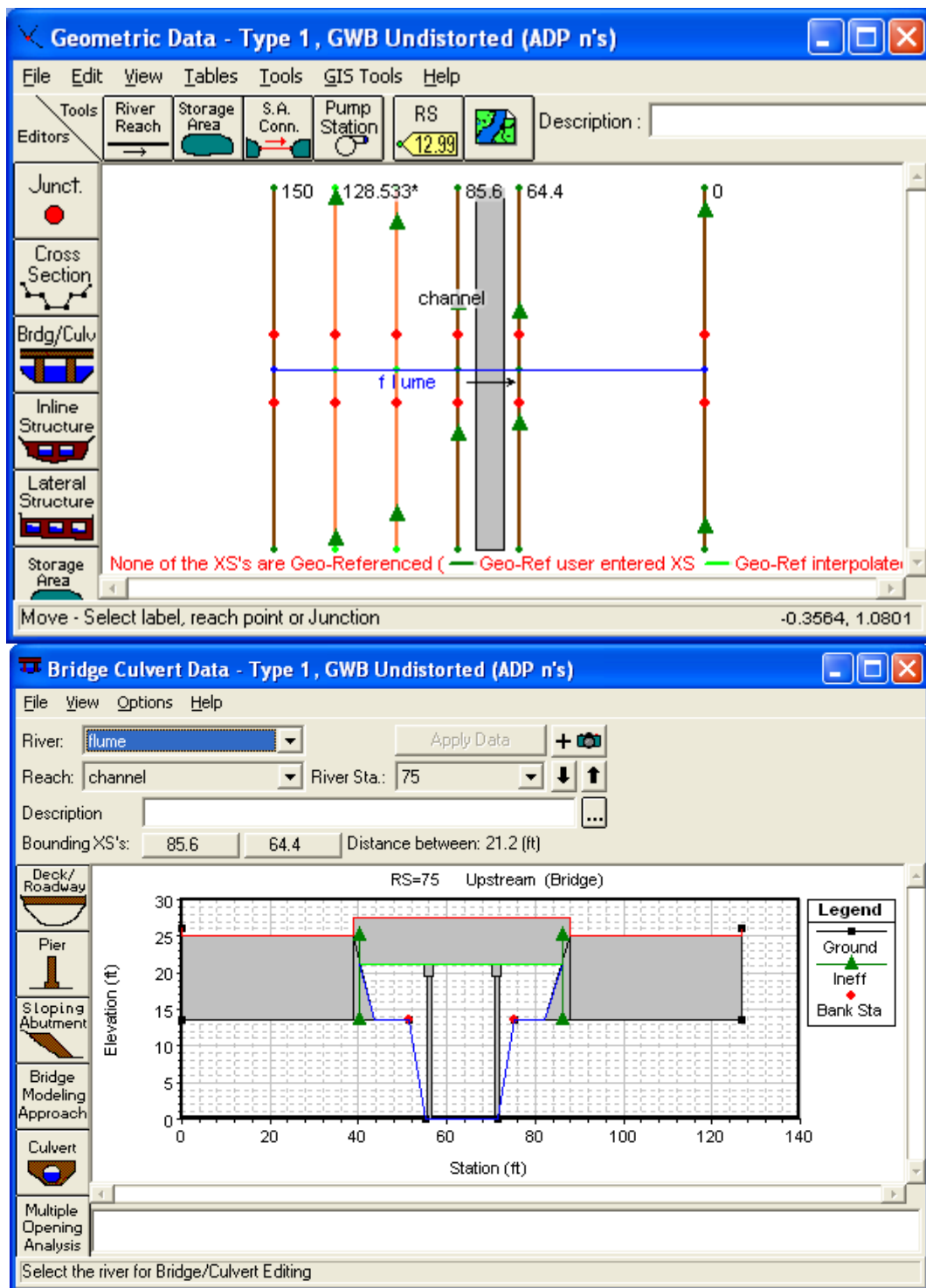


Figure 4.8: Plan, Bridge and n-value Table for Modified GWB HEC-RAS Model

The results for the Modified Distorted HEC-RAS model are shown in Table 4.6. Table 4.7 shows the measured and interpolated laboratory results from Table 4.2. The differences between the Modified HEC-RAS model and the laboratory values in Table 4.7 are presented in Table 4.8. Table 4.5 for the Regular model is also included under Table 4.8 for comparison.

Table 4.6: Modified Undistorted HEC-RAS Model Results

Modified Distorted RS (ft) <i>1</i>	Low Q			Middle Q			High Q		
	Prof 1 (ft) <i>2</i>	Prof 2 (ft) <i>3</i>	Prof 3 (ft) <i>4</i>	Prof 4 (ft) <i>5</i>	Prof 5 (ft) <i>6</i>	Prof 6 (ft) <i>7</i>	Prof 7 (ft) <i>8</i>	Prof 8 (ft) <i>9</i>	Prof 9 (ft) <i>10</i>
150	19.78	18.98	17.89	19.24	19.29	19.29	21.65	21.41	21.4
128.5332	19.76	18.96	17.86	19.2	19.25	19.25	21.61	21.37	21.37
107.0666	19.68	18.86	17.71	19.06	19.11	19.11	21.48	21.23	21.23
85.6	19	18.05	16.63	17.68	17.76	17.76	19.99	19.63	19.63
64.4	18.53	17.53	15.75	16.33	14.98	14.29	18.27	17.61	15.35
0	18.83	17.86	16.09	16.9	15.43	14	19.08	18.5	16.03

Table 4.7: Laboratory Results for Modified Distorted HEC-RAS Stations

Laboratory Undistorted RS (ft) <i>1</i>	Low Q			Middle Q			High Q		
	Prof 1 (ft) <i>2</i>	Prof 2 (ft) <i>3</i>	Prof 3 (ft) <i>4</i>	Prof 4 (ft) <i>5</i>	Prof 5 (ft) <i>6</i>	Prof 6 (ft) <i>7</i>	Prof 7 (ft) <i>8</i>	Prof 8 (ft) <i>9</i>	Prof 9 (ft) <i>10</i>
150	20.08	19.36	18.18	19.49	18.77	17.91	21.33	21.00	19.45
128.53	20.079	19.345	18.164	19.476	18.742	17.901	21.230	20.902	19.353
107.07	19.971	19.166	17.960	19.297	18.443	17.590	20.943	20.674	19.101
85.60	19.515	18.710	17.253	18.455	17.326	16.111	20.199	19.797	18.009
64.40	18.949	18.060	16.343	17.275	15.886	14.023	19.232	18.701	16.485
0.00	18.83	17.86	16.09	16.90	15.43	13.58	19.08	18.50	16.03

 Interpolated Values

Table 4.8: Differences in Water Surface Elevations between HEC-RAS and Laboratory for the Modified Undistorted HEC-RAS Model (HR – Lab)

Modified Undistorted RS (ft) 1	Low Q			Middle Q			High Q		
	Prof 1 (ft) 2	Prof 2 (ft) 3	Prof 3 (ft) 4	Prof 4 (ft) 5	Prof 5 (ft) 6	Prof 6 (ft) 7	Prof 7 (ft) 8	Prof 8 (ft) 9	Prof 9 (ft) 10
150	-0.30	-0.38	-0.29	-0.25	0.52	1.38	0.32	0.41	1.95
128.53	-0.32	-0.38	-0.30	-0.28	0.51	1.35	0.38	0.47	2.02
107.07	-0.29	-0.31	-0.25	-0.24	0.67	1.52	0.54	0.56	2.13
85.60	-0.52	-0.66	-0.62	-0.77	0.43	1.65	-0.21	-0.17	1.62
64.40	-0.42	-0.53	-0.59	-0.94	-0.91	0.27	-0.96	-1.09	-1.14
0.00	0.00	0.00	0.00	0.00	0.00	0.42	0.00	0.00	0.00

Table 4.5: (Repeated) Differences in Water Surface Elevations between HEC-RAS and Laboratory for the Regular Undistorted HEC-RAS Model (HR – Lab)

Regular Undistorted RS (ft) 1	Low Q			Middle Q			High Q		
	Prof 1 (ft) 2	Prof 2 (ft) 3	Prof 3 (ft) 4	Prof 4 (ft) 5	Prof 5 (ft) 6	Prof 6 (ft) 7	Prof 7 (ft) 8	Prof 8 (ft) 9	Prof 9 (ft) 10
150	-0.40	-0.43	-0.28	-0.26	0.55	1.41	0.09	0.25	1.89
126.76	-0.46	-0.41	-0.26	-0.24	0.65	1.37	0.14	0.35	1.99
85.6	-0.64	-0.73	-0.61	-0.79	0.47	1.69	-0.55	-0.41	1.52
64.4	-0.36	-0.47	-0.53	-0.84	-0.84	1.21	-0.78	-0.90	-0.85
0	0.00	0.00	0.00	0.00	0.00	0.42	0.00	0.00	0.00

The water surface profile plots for the Modified Distorted HEC-RAS model are shown together with the laboratory data in Figures 4.9, 4.10 and 4.11 for the low, middle and high flows, respectively. Plots of the Regular Distorted HEC-RAS model are also shown for comparison. The results for the Modified model are somewhat better than for the Regular model. They were significantly better than our original HEC-RAS results presented in Edition 1 of this report.

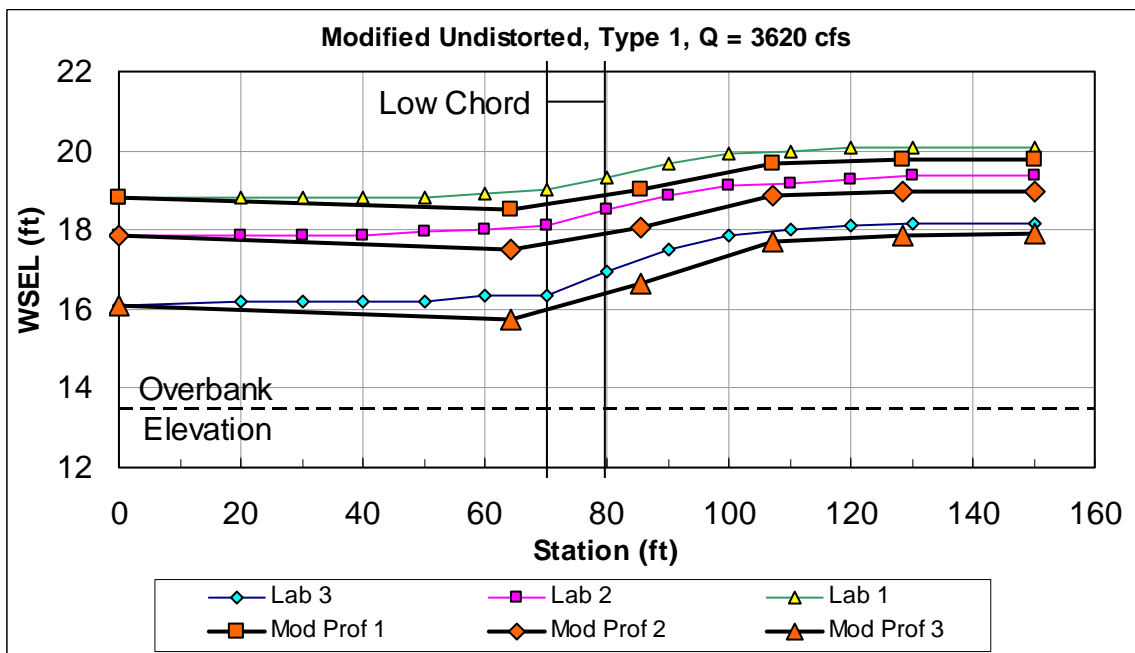
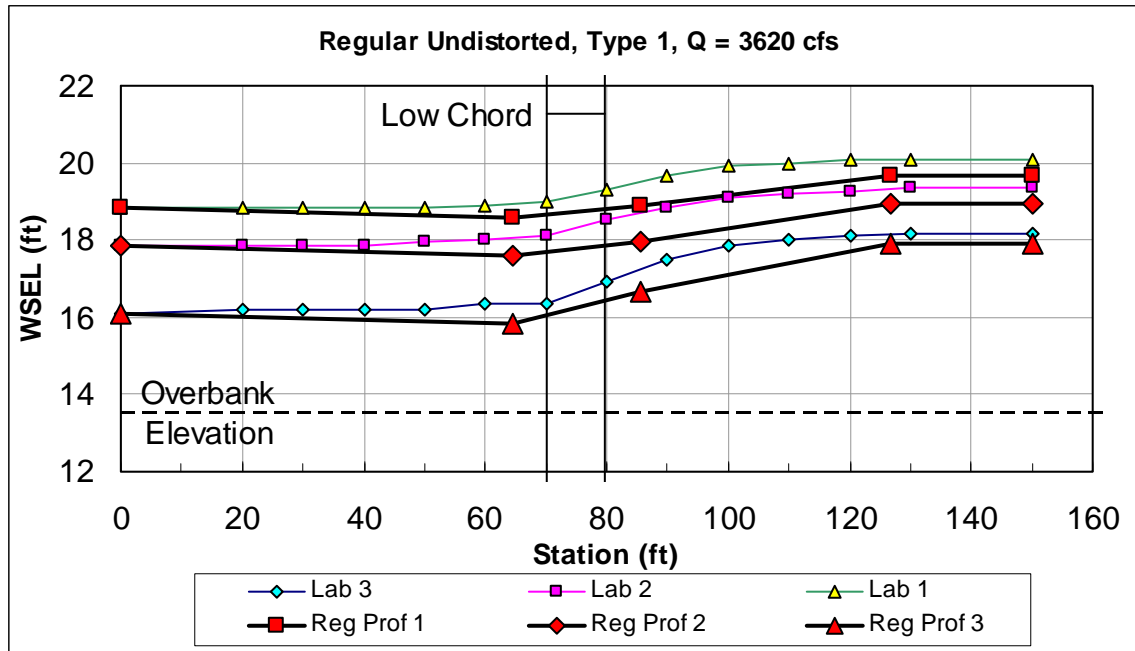


Figure 4.9: Water Surface Profiles for the Laboratory, Regular Distorted HEC-RAS model and Modified Distorted HEC-RAS model – Low Flow

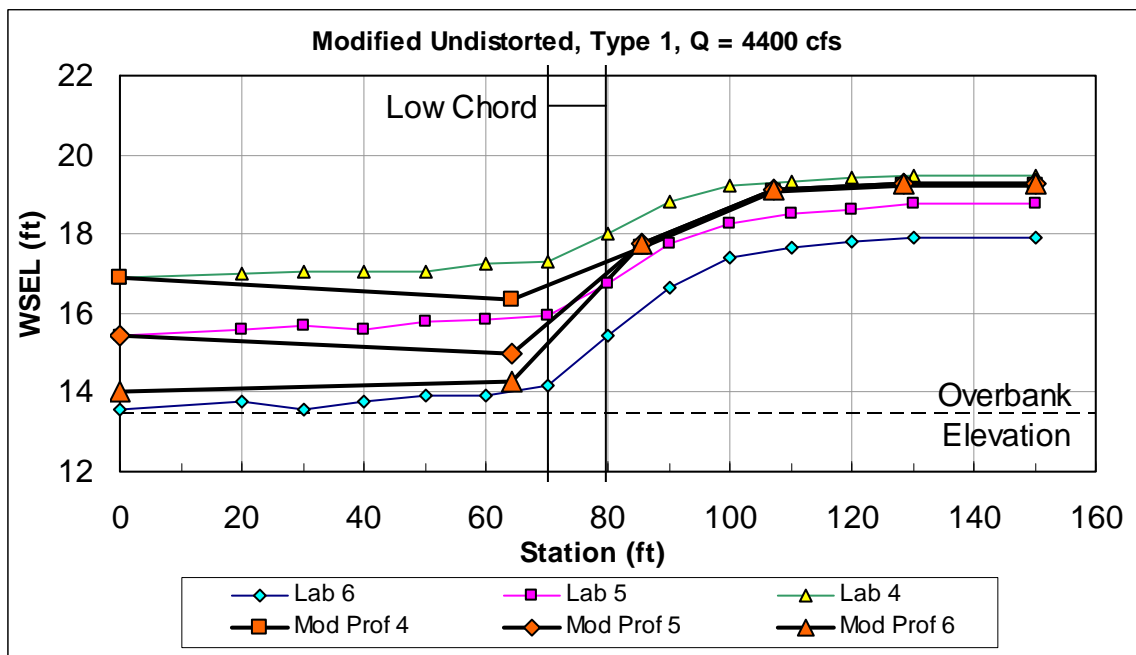
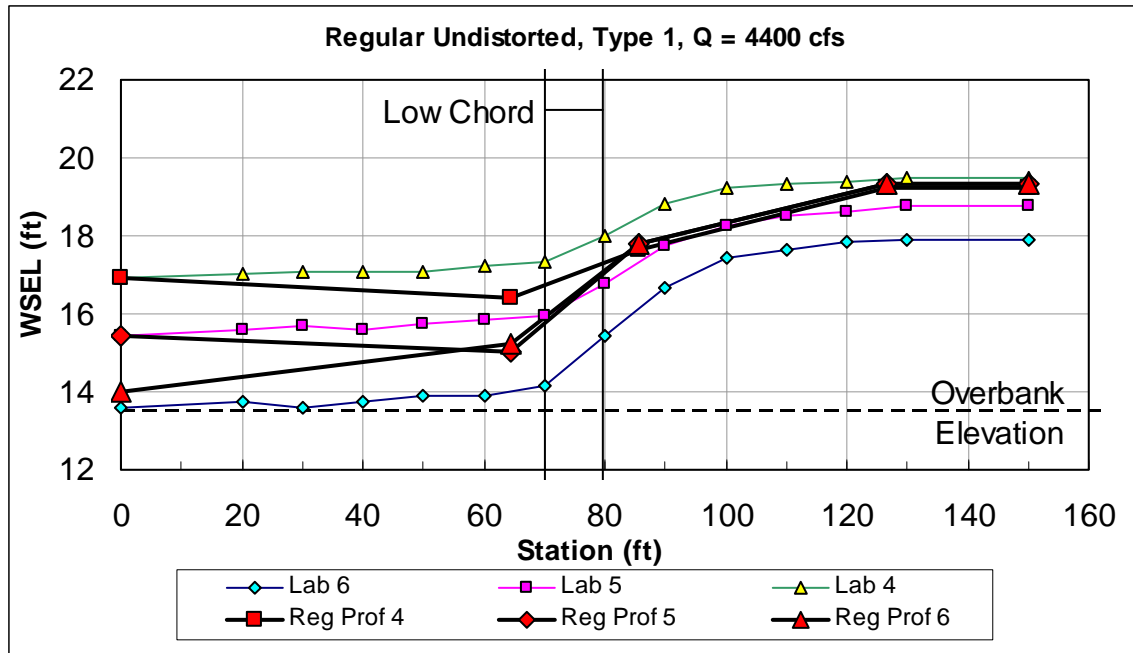


Figure 4.10: Water Surface Profiles for the Laboratory, Regular Distorted HEC-RAS model and Modified Distorted HEC-RAS model – Middle Flow

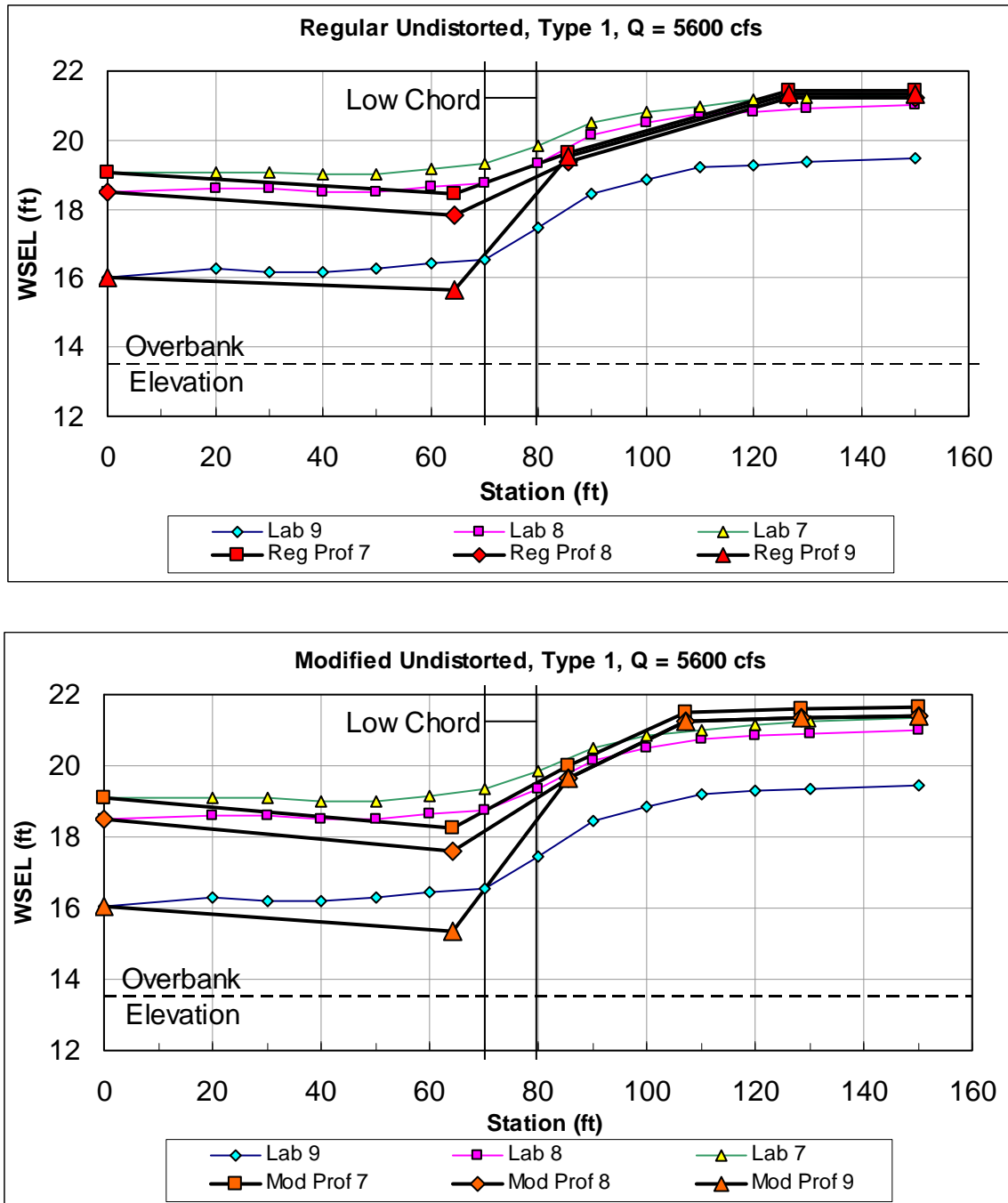


Figure 4.11: Water Surface Profiles for the Laboratory, Regular Distorted HEC-RAS model and Modified Distorted HEC-RAS model – High Flow

4.3 Distorted Type 1 HEC-RAS Models

The prototype distorted model with $X_r = 100$ and $Y_r = 20$ was created from the prototype undistorted model with $L_r = X_r = Y_r = 20$ was obtained by the following steps.

1. Multiply the following by 5.
 - a. Discharges,
 - b. River station names,
 - c. Cross section stations,
 - d. Reach lengths,
 - e. Deck/roadway stations,
 - f. Abutment stations,
 - g. Distance and width parameters in the Deck/Roadway data editor,
 - h. U.S. and D.S. Embankment SS,
 - i. Pier width and stations,
 - j. Ineffective flow stations.
2. Change n-values to 0.0104 in the overbanks where the effective flow does not contact the overbank sidewalls.
3. Change n-values to 0.0110 in the overbanks where the effective flow contacts the overbank sidewalls.
4. Change the main channel n-values to 0.0150.

Tables 4.9 and 4.10 show the computed water surface elevations for the distorted and undistorted HEC-RAS models. The agreement is very good. Note the improvement in Prof 6 at RS 322 achieved by GWB by changing the downstream boundary condition from 13.58 to 14 feet. Table 4.11 shows differences in the computed

and the critical water surface elevations and the ratio of several parameters for the Modified Undistorted and Distorted HEC-RAS models. Note that at stations and profiles with the larger discrepancies in water surface elevations, the flow parameters and the Froude numbers also differ.

Table 4.9: Results for Undistorted and Distorted Regular Type 1 HEC-RAS Models

Regular HEC-RAS Undistorted Model									
Undistorted RS (ft)	Water Surface Elevation (ft)								
	Low Q			Mid Q			High Q		
	PF 1	PF 2	PF 3	PF 4	PF 5	PF 6	PF7	PF 8	PF 9
150	19.68	18.93	17.9	19.23	19.32	19.32	21.42	21.25	21.34
126.76	19.68	18.92	17.89	19.22	19.31	19.31	21.41	21.24	21.33
85.6	18.88	17.98	16.64	17.66	17.8	17.8	19.65	19.39	19.53
64.4	18.59	17.59	15.81	16.43	15.05	15.23	18.45	17.8	15.64
0	18.83	17.86	16.09	16.9	15.43	14	19.08	18.5	16.03

Regular HEC-RAS Distorted Model									
Distorted RS (ft)	Water Surface Elevation (ft)								
	Low Q			Mid Q			High Q		
	PF 1	PF 2	PF 3	PF 4	PF 5	PF 6	PF7	PF 8	PF 9
750	19.66	18.92	17.92	19.28	19.42	19.42	21.4	21.28	21.4
633.8	19.66	18.91	17.9	19.27	19.41	19.41	21.39	21.28	21.4
428	18.86	17.97	16.66	17.74	17.95	17.95	19.61	19.43	19.62
322	18.59	17.59	15.81	16.43	15.04	15.2	18.45	17.8	15.64
0	18.83	17.86	16.09	16.9	15.43	14	19.08	18.5	16.03

Differences for Regular HEC-RAS Undistorted and Distorted Models										
Distorted RS (ft)	Undistorted RS (ft)	Undistorted - Distorted (ft)								
		Low Q			Mid Q			High Q		
		PF 1	PF 2	PF 3	PF 4	PF 5	PF 6	PF7	PF 8	PF 9
750	150	0.02	0.01	-0.02	-0.05	-0.1	-0.1	0.02	-0.03	-0.06
633.8	126.76	0.02	0.01	-0.01	-0.05	-0.1	-0.1	0.02	-0.04	-0.07
428	85.6	0.02	0.01	-0.02	-0.08	-0.15	-0.15	0.04	-0.04	-0.09
322	64.4	0	0	0	0	0.01	0.03	0	0	0
0	0	0	0	0	0	0	0	0	0	0

Table 4.10: Results for Undistorted and Distorted Modified GWB Type 1 HEC-RAS Models

Modified GWB HEC-RAS Undistorted Model									
Undistorted RS (ft)	Water Surface Elevation (ft) - Undistorted								
	Low Q			Mid Q			High Q		
	PF 1	PF 2	PF 3	PF 4	PF 5	PF 6	PF7	PF 8	PF 9
150	19.78	18.98	17.89	19.24	19.29	19.29	21.65	21.41	21.4
128.533*	19.76	18.96	17.86	19.2	19.25	19.25	21.61	21.37	21.37
107.067*	19.68	18.86	17.71	19.06	19.11	19.11	21.48	21.23	21.23
85.6	19	18.05	16.63	17.68	17.76	17.76	19.99	19.63	19.63
64.4	18.53	17.53	15.75	16.33	14.98	14.29	18.27	17.61	15.35
0	18.83	17.86	16.09	16.9	15.43	14	19.08	18.5	16.03

Modified GWB HEC-RAS Distorted Model									
Distorted RS (ft)	Water Surface Elevation (ft) - Distorted								
	Low Q			Mid Q			High Q		
	PF 1	PF 2	PF 3	PF 4	PF 5	PF 6	PF7	PF 8	PF 9
750	19.71	18.95	17.92	19.29	19.41	19.41	21.51	21.35	21.46
642.666*	19.68	18.93	17.89	19.26	19.38	19.38	21.47	21.31	21.42
535.333*	19.6	18.83	17.74	19.12	19.24	19.24	21.33	21.17	21.28
428	18.91	18.01	16.67	17.77	17.94	17.94	19.77	19.55	19.71
322	18.53	17.52	15.75	16.33	14.97	14.28	18.27	17.61	15.35
0	18.83	17.86	16.09	16.9	15.43	14	19.08	18.5	16.03

Differences for Modified GWB HEC-RAS Undistorted and Distorted Models										
Distorted RS (ft)	Undistorted RS (ft)	Undistorted - Distorted (ft)								
		Low Q			Mid Q			High Q		
		PF 1	PF 2	PF 3	PF 4	PF 5	PF 6	PF7	PF 8	PF 9
750	150	0.07	0.03	-0.03	-0.05	-0.12	-0.12	0.14	0.06	-0.06
642.666*	128.533*	0.08	0.03	-0.03	-0.06	-0.13	-0.13	0.14	0.06	-0.05
535.333*	107.067*	0.08	0.03	-0.03	-0.06	-0.13	-0.13	0.15	0.06	-0.05
428	85.6	0.09	0.04	-0.04	-0.09	-0.18	-0.18	0.22	0.08	-0.08
322	64.4	0	0.01	0	0	0.01	0.01	0	0	0
0	0	0	0	0	0	0	0	0	0	0

Table 4.11: Parameters for the Modified Undistorted and Distorted HEC-RAS Models

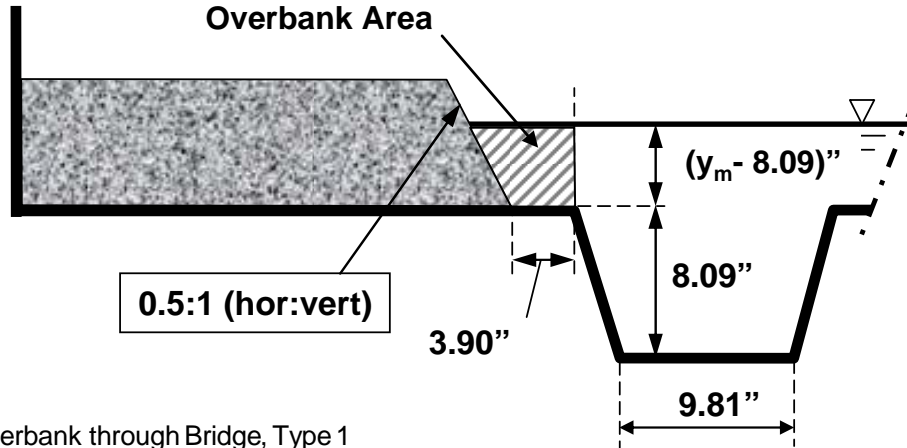
River Sta Undistorted	River Sta Distorted	Profile	W.S. Elev Und-Dist (ft)	Crit W.S. Und-Dist (ft)	Vel Total Und/Dist (ft/s)	Hydr Depth Und/Dist (ft)	Fr # XS Und/Dist	Fr # XS Undistorted	Fr # XS Distorted
1	2	3	4	5	6	7	8	9	10
150	750	1	0.07	0	0.99	1.01	1.00	0.21	0.21
150	750	2	0.03	0	0.99	1.00	1.00	0.24	0.24
150	750	3	-0.03	0	1.00	1.00	1.00	0.30	0.30
150	750	4	-0.05	0	1.01	0.99	1.04	0.28	0.27
150	750	5	-0.12	0	1.02	0.99	1.00	0.27	0.27
150	750	6	-0.12	0	1.02	0.99	1.00	0.27	0.27
150	750	7	0.14	0	0.99	1.01	1.00	0.24	0.24
150	750	8	0.06	0	1.00	1.00	0.96	0.24	0.25
150	750	9	-0.06	0	1.01	0.99	1.00	0.24	0.4
128.533*	642.666*	1	0.08	0	0.99	1.01	0.95	0.21	0.22
128.533*	642.666*	2	0.03	0	0.99	1.00	1.00	0.25	0.25
128.533*	642.666*	3	-0.03	0	1.00	1.00	1.00	0.31	0.31
128.533*	642.666*	4	-0.06	0	1.01	0.99	1.00	0.29	0.29
128.533*	642.666*	5	-0.13	0	1.02	0.99	1.04	0.29	0.28
128.533*	642.666*	6	-0.13	0	1.02	0.99	1.04	0.29	0.28
128.533*	642.666*	7	0.14	-0.01	0.99	1.01	1.00	0.25	0.25
128.533*	642.666*	8	0.06	-0.01	1.00	1.00	1.00	0.26	0.26
128.533*	642.666*	9	-0.05	-0.01	1.01	0.99	1.04	0.26	0.25
107.067*	535.333*	1	0.08	0	0.99	1.01	1.00	0.24	0.24
107.067*	535.333*	2	0.08	0	1.00	1.01	1.00	0.28	0.28
107.067*	535.333*	3	-0.03	0	1.00	1.00	1.03	0.35	0.34
107.067*	535.333*	4	-0.06	0	1.01	0.99	1.00	0.32	0.32
107.067*	535.333*	5	-0.13	0	1.02	0.98	1.03	0.32	0.31
107.067*	535.333*	6	-0.13	0	1.02	0.98	1.03	0.32	0.31
107.067*	535.333*	7	0.15	-0.01	0.99	1.01	1.00	0.28	0.28
107.067*	535.333*	8	0.06	-0.01	0.99	1.00	1.00	0.29	0.29
107.067*	535.333*	9	-0.05	-0.01	1.01	0.99	1.00	0.29	0.29
85.6	428	1	0.09	0	0.99	1.01	0.97	0.36	0.37
85.6	428	2	0.04	0	1.00	1.00	1.00	0.41	0.41
85.6	428	3	-0.04	0	1.00	1.00	1.00	0.51	0.51
85.6	428	4	-0.09	0	1.01	0.99	1.02	0.53	0.52
85.6	428	5	-0.18	0	1.02	0.98	1.02	0.52	0.51
85.6	428	6	-0.18	0	1.02	0.98	1.02	0.52	0.51
85.6	428	7	0.22	0	0.98	1.02	0.96	0.49	0.51
85.6	428	8	0.08	0	0.99	1.01	1.00	0.52	0.52
85.6	428	9	-0.08	0	1.01	0.99	1.02	0.52	0.51
75	375					Bridge			
64.4	322	1	0	0	1.00	1.00	1.00	0.40	0.40
64.4	322	2	0.01	0	1.00	1.00	1.00	0.45	0.45
64.4	322	3	0	0	1.00	1.00	1.00	0.59	0.59
64.4	322	4	0	0	1.00	1.00	1.00	0.65	0.65
64.4	322	5	0.01	0	1.00	1.00	1.00	0.81	0.81
64.4	322	6	0.01	0	1.00	1.00	1.00	0.93	0.93
64.4	322	7	0	0	1.00	1.00	1.00	0.63	0.63
64.4	322	8	0	0	1.00	1.00	1.00	0.69	0.69
64.4	322	9	0	0	1.00	1.00	1.00	0.97	0.97
0	0	1	0	0	1.00	1.00	1.00	0.27	0.27
0	0	2	0	0	1.00	1.00	1.00	0.32	0.32
0	0	3	0	0	1.00	1.00	1.00	0.51	0.51
0	0	4	0	0.01	1.00	1.00	1.00	0.49	0.49
0	0	5	0	0.01	1.00	1.00	1.00	0.76	0.76
0	0	6	0	0.01	1.00	1.00	1.00	1.38	1.38
0	0	7	0	0	1.00	1.00	1.00	0.39	0.39
0	0	8	0	0	1.00	1.00	1.00	0.44	0.44
0	0	9	0	0	1.00	1.00	1.00	0.80	0.80

4.4 Adjusting n-Values through the Bridge Opening

Although the differences upstream from the bridge are small, they may be due to the fact that the n-values through the bridge should be adjusted separately from the standard channel cross sections. The overbank wetted perimeter through the bridge should not be constant but should vary with depth for the Type 1 (and Type 3) experiments. It would be possible to input specific overbank n-values through the bridge using the Internal Bridge Cross Sections editor in HEC-RAS. Figures 4.12 and 4.13 show the appropriate overbank bridge opening n-values as functions of the prototype depth y_p for the Types 1 and Type 3 experiments.

The Type 2 experiments do not have overbank flow through the bridge opening. However, the n-value for the bridge opening for Type 2 should probably also be expressed as a function of y_p since the wetted perimeter varies with depth. Figure 4.14 shows the adjusted n-values that could be used through the Type 2 bridge opening via the *Internal Bridge Cross Sections* editor.

The equations discussed above were not tested. Since the equations express the overbanks and main channel n-values as functions of depth, each profile would need to be run separately in an iterative manner.



Overbank through Bridge, Type 1

Overbanks (X_r = horizontal scale; Y_r = vertical scale)

Y_m = model depth in ft; Y_p = prototype depth in feet

$$y_m = \frac{12Y_p}{20} = (0.6Y_p) = \text{model depth in inches}$$

$$R_r = \left[\frac{P_{w,m}}{P_{w,p}} \right] [X_r Y_r] = \frac{\left[\sqrt{(y_m - 8.09)^2 + (.5(y_m - 8.09))^2 + 3.9} \right]}{\left[\sqrt{\{[Y_r](y_m - 8.09)\}^2 + \{[X_r](.5(y_m - 8.09))\}^2 + [X_r]3.9} \right]} [X_r Y_r]$$

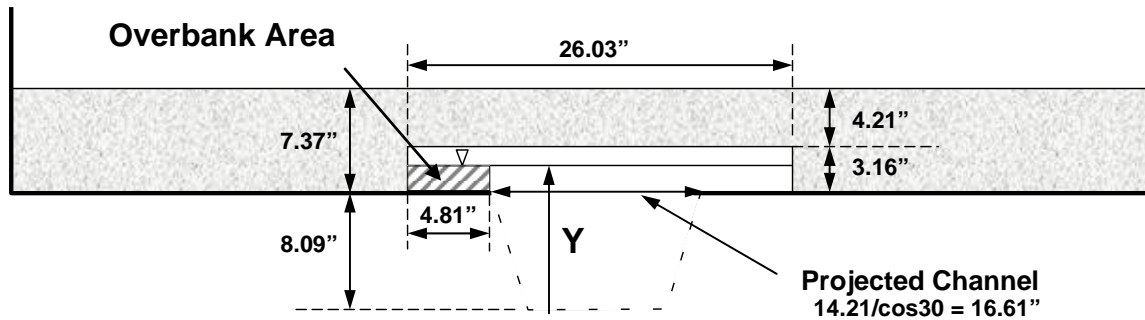
$$R_r = \frac{\left[\sqrt{(y_m - 8.09)^2 + (.5(y_m - 8.09))^2 + 3.9} \right]}{\left[\sqrt{\{[20](y_m - 8.09)\}^2 + \{[100](.5(y_m - 8.09))\}^2 + [100]3.9} \right]} [(100)(20)]$$

$$n_{r,ob} = \frac{R_r^{2/3}}{X_r^{1/2}} = \frac{R_r^{2/3}}{100^{1/2}} = \frac{R_r^{2/3}}{10}$$

Type 1 Experiments $n_{m,brob} = 0.0141$

y_m (in.)	Y_p (ft)	R_r (ft)	$n_{r,brob}$	$n_{p,brob}$
8.1	13.5	20.03	0.738	0.0104
8.4	14	20.88	0.758	0.0107
8.7	14.5	21.67	0.777	0.0110
9	15	22.40	0.795	0.0112
9.3	15.5	23.08	0.811	0.0114
9.6	16	23.71	0.825	0.0116
9.9	16.5	24.30	0.839	0.0118
10.2	17	24.86	0.852	0.0120
10.5	17.5	25.37	0.863	0.0122
10.8	18	25.86	0.875	0.0123
11.1	18.5	26.32	0.885	0.0125
11.4	19	26.75	0.894	0.0126
11.7	19.5	27.16	0.904	0.0127
12	20	27.55	0.912	0.0129
12.3	20.5	27.91	0.920	0.0130
12.6	21	28.26	0.928	0.0131

Figure 4.12: Derivation of Equations for Type 1 Bridge Overbank n-values in Terms of the n-value from the Laboratory Model



Overbank through Bridge, Type 3

Overbanks (X_r = horizontal scale; Y_r = vertical scale)

Y_m = model depth in ft; Y_p = prototype depth in feet

$$y_m = \frac{12 Y_p}{20} = (0.6 Y_p) = \text{model depth in inches}$$

$$R_r = \left[\frac{P_{w,m}}{P_{w,p}} \right] [X_r Y_r] = \frac{[(y_m - 8.09) + (4.81)]}{\{[Y_r](y_m - 8.09) + [X_r](4.81)\}} [X_r Y_r]$$

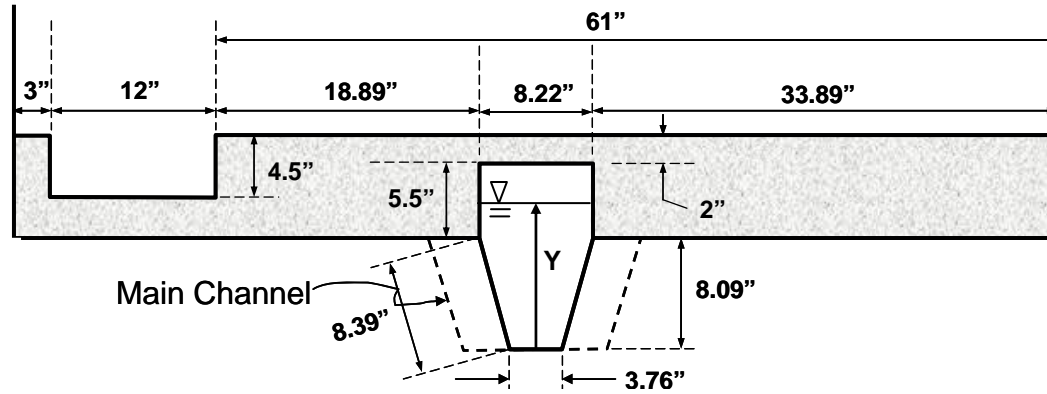
$$R_r = \frac{\{[y_m - 8.09] + (4.81)\}}{\{[20][y_m - 8.09] + [100](4.81)\}} [2000]$$

$$n_{r,ob} = \frac{R_r^{2/3}}{X_r^{1/2}} = \frac{R_r^{2/3}}{100^{1/2}} = \frac{R_r^{2/3}}{10}$$

Type 3 Experiments $n_{m,brob} = 0.0141$

y_m (in.)	Y_p (ft)	R_r (ft)	$n_{r,brob}$	$n_{p,brob}$
8.1	13.5	20.0	0.738	0.0104
8.4	14	21.0	0.762	0.0107
8.7	14.5	22.0	0.785	0.0111
9	15	22.9	0.807	0.0114
9.3	15.5	23.8	0.828	0.0117
9.6	16	24.7	0.849	0.0120
9.9	16.5	25.6	0.869	0.0122
10.2	17	26.5	0.888	0.0125
10.5	17.5	27.3	0.906	0.0128
10.8	18	28.1	0.924	0.0130
11.1	18.5	28.9	0.942	0.0133
11.4	19	29.7	0.959	0.0135

Figure 4.13: Derivation of Equations for Type 3 Bridge Overbank n-values in Terms of the n-value from the Laboratory Model



Main Channel (X_r = horizontal scale; Y_r = vertical scale)

Y_m = model depth in ft; Y_p = prototype depth in feet

$$y_m = \frac{12Y_p}{20} = (0.6Y_p) = \text{model depth in inches}$$

$$R_r = \left[\frac{P_{w,m}}{P_{w,p}} \right] [X_r Y_r] = \frac{\left[2(y_m - 8.09) + 3.76 + 2\sqrt{8.09^2 + (0.5(8.22 - 3.76))^2} \right]}{\left[Y_r 2(y_m - 8.09) + X_r 3.76 + 2\sqrt{[Y_r 8.09]^2 + (0.5[X_r](8.22 - 3.76))^2} \right]} [X_r Y_r]$$

$$R_r = \frac{[2y_m + 4.36]}{\left[[20]2(y_m - 8.09) + [100]3.76 + 2\sqrt{[20]8.09^2 + (0.5[100](8.22 - 3.76))^2} \right]} [2000]$$

$$R_r = \frac{2000[2y_m + 4.36]}{[24y_m + 603.4]}$$

$$n_r = \frac{R_r^{2/3}}{X_r^{1/2}} = \frac{R_r^{2/3}}{100^{1/2}} = \frac{R_r^{2/3}}{10}$$

Type 2 Experiments $n_{m,br} = 0.0141$

y_m (in.)	Y_p (ft)	R_r (ft)	$n_{r,br}$	$n_{p,br}$
8.1	13.5	51.5	1.38	0.0195
8.4	14	52.6	1.40	0.0198
8.7	14.5	53.6	1.42	0.0200
9	15	54.6	1.44	0.0203
9.3	15.5	55.6	1.46	0.0205
9.6	16	56.5	1.47	0.0208
9.9	16.5	57.5	1.49	0.0210
10.2	17	58.4	1.50	0.0212
10.5	17.5	59.3	1.52	0.0214
10.8	18	60.2	1.54	0.0217
11.1	18.5	61.1	1.55	0.0219
11.4	19	61.9	1.57	0.0221
11.7	19.5	62.8	1.58	0.0223
12	20	63.6	1.59	0.0225
12.3	20.5	64.5	1.61	0.0227
12.6	21	65.3	1.62	0.0229
12.9	21.5	66.1	1.63	0.0230
13.2	22	66.9	1.65	0.0232
13.5	22.5	67.6	1.66	0.0234
13.8	23	68.4	1.67	0.0236

Figure 4.14: Derivation of Equations for Type 2 Main Channel n-values in Terms of the n-value from the Laboratory Model

CHAPTER 5 - TYPE 2 EXPERIMENTS – COMBINATION

BRIDGE/WEIR FLOW

These experiments test bridge crossings where significant weir flow occurs in low roadway areas in the approaches to the bridge. This is discussed as a perched bridge in Chapter 5 of the *HEC-RAS River Analysis System Hydraulic Reference Manual Report No. CPD 69* (Brunner, 2008). The bridge model for the laboratory is shown in Figure 5.1. Dimensions are in inches for the laboratory model and in feet for the 20-scale undistorted prototype. The channel is the same as shown in Figure 2.1. The bridge was constructed of dimension lumber and is 0.25-feet thick. Figure 5.2 shows the distorted prototype bridge expressed for 100:1 horizontal scaling and 20:1 vertical scaling. The dimensions in this figure were used to create the distorted Type 2 HEC-RAS models.

The weir was constructed in the left overbank region of the channel. Also, note from Figures 5.1 and 5.2 that the bridge openings were smaller on both sides of the main channel by 0.25 feet (thickness of two 2x4's) and 25, respectively, for the model and prototype. This was done to create enough head to cause a significant portion of the flow to pass through the overbank weir.

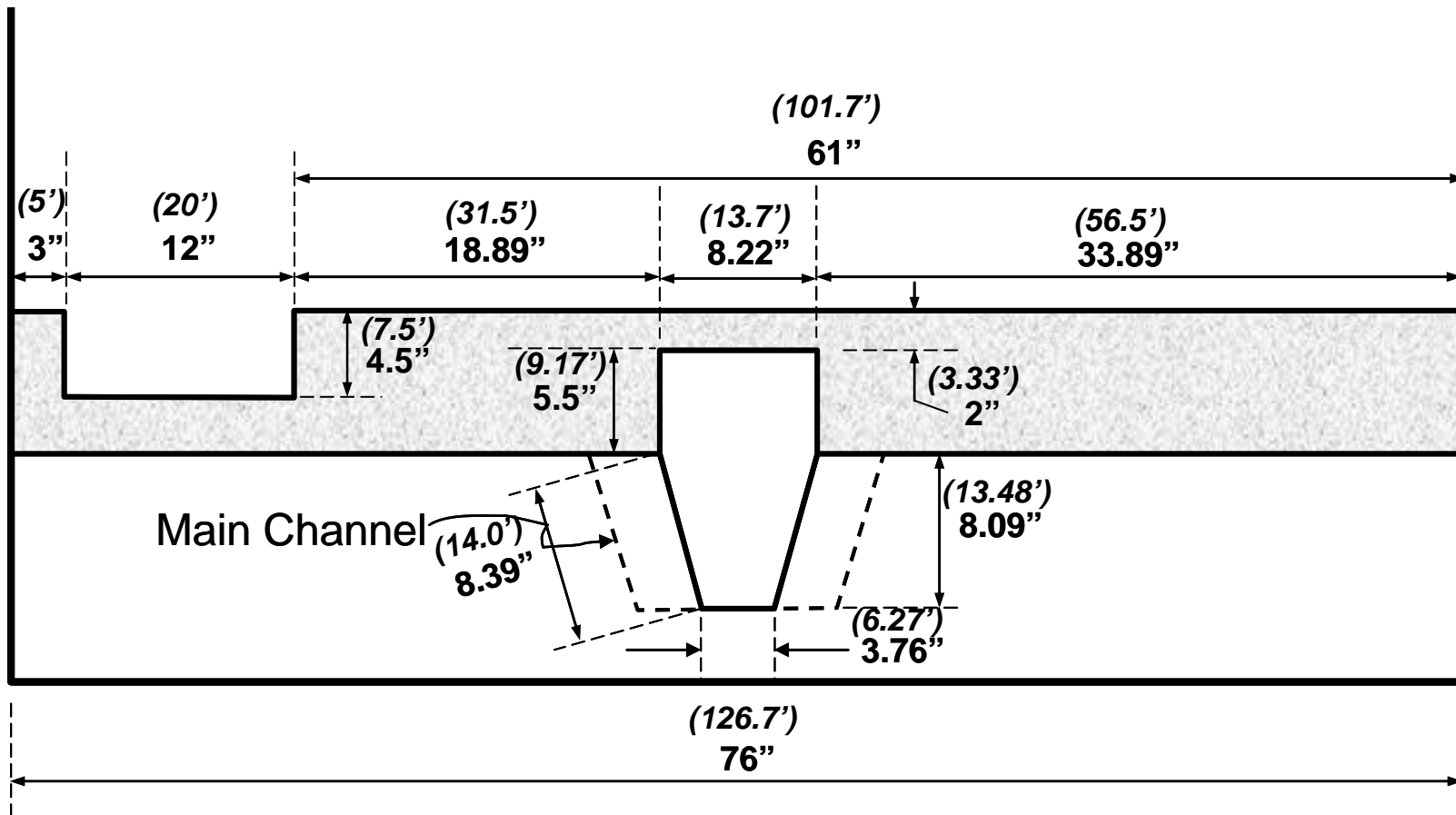


Figure 5.1: Bridge Model for Type 2 Experiments (Lab Model units in inches, Undistorted 20-scale Prototype Dimensions of Bridge in feet)

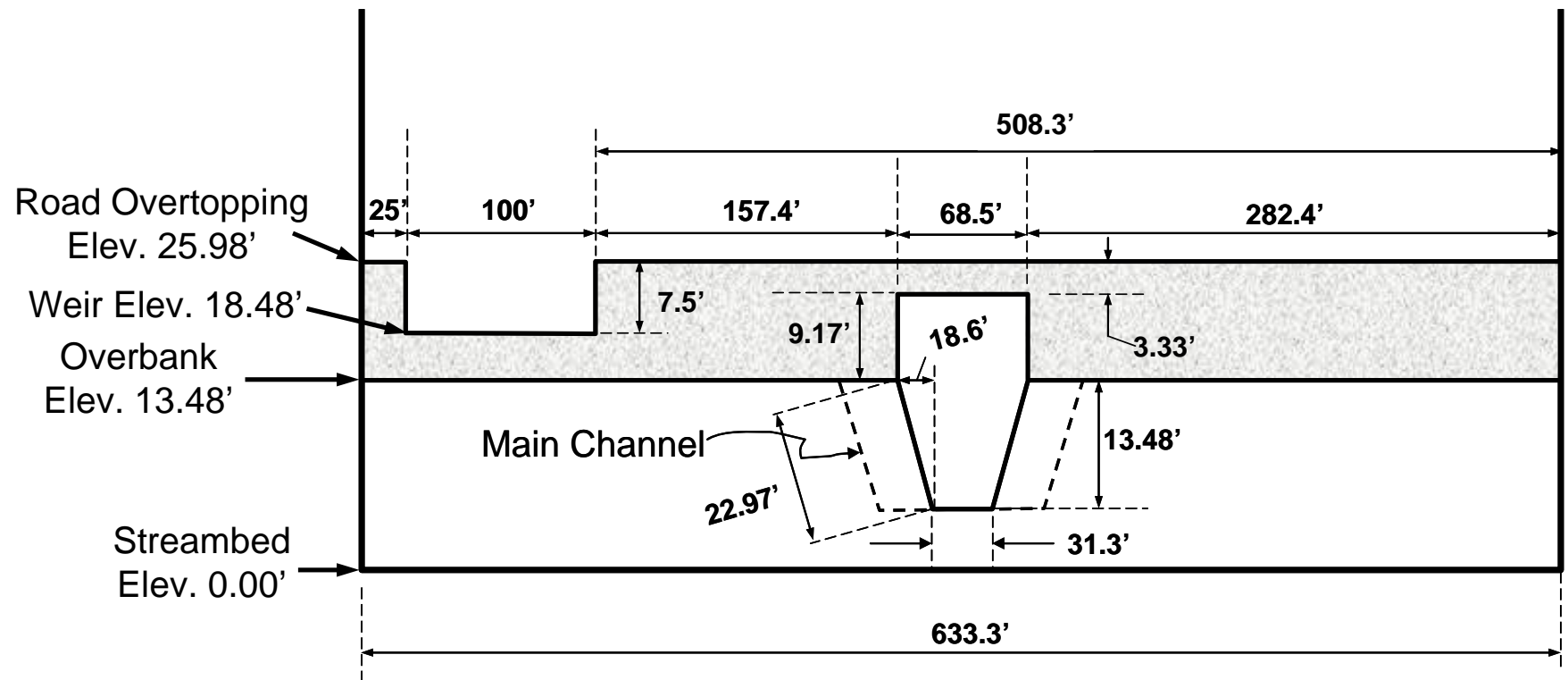


Figure 5.2: Prototype of Bridge Model for Type 2 Experiments (1:100 H, 1:20 V Scales)

The weir was calibrated to obtain a relationship between weir discharge and the head on the weir. (Note: This calibration served only to estimate the portion of the total flow going over the weir. It had nothing to do with the water surface profile measurements.) The weir discharge was measured by capturing the weir overflow in a separate region in the downstream overbank. This is illustrated in Figure 5.3. Weir discharge was the volume captured divided by the capture-time interval. The empirical equation used to determine the weir flow is given below.

$$Q_{\text{weir}} = 0.0987h^{1.5}$$

where Q_{weir} is in cfs and h is the height of the water surface over the weir in inches. Note that this height is not the distance between the upstream energy grade line and the weir crest. It is just a fixed point over the weir crest we used for calibration purposes. Figure 5.4 shows the weir and bridge opening in operation for one of the experiments. Note the pointer in the upper picture. It was used to measure the water surface height on the weir. Figure 5.4a shows the system used to measure the head over the weir.

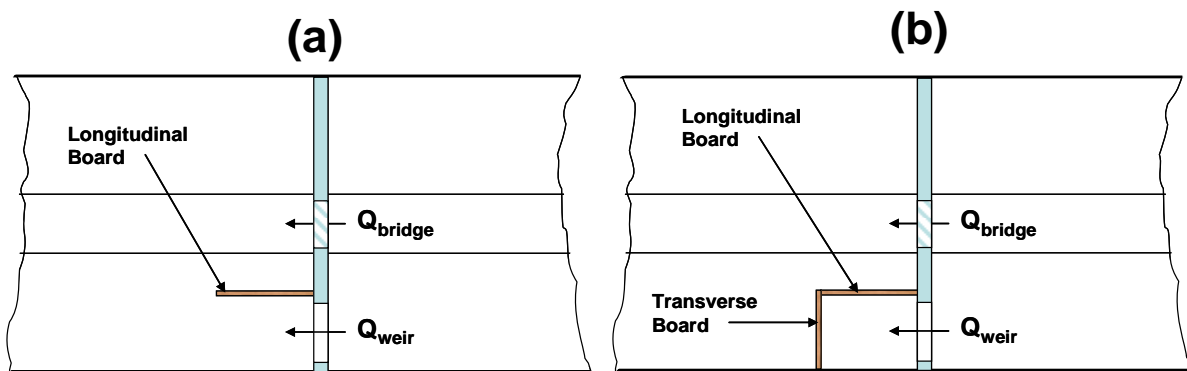


Figure 5.3: Illustration of Containment Region for Measuring the Weir Discharge
(a) Before Q_{weir} Measurement (b) During Q_{weir} measurement.



**Figure 5.4: Weir (a) and Bridge (b) for a Type 2 Experiment
(1:100 H, 1:20 V Scales)**

Type 2 laboratory experiments were performed for 3 different discharges - 2.21, 2.56 and 2.89 cfs. Three trials with different tailwater elevations were performed for each discharge. The nine 9 experiments performed in the laboratory for Type 2 Experiments are shown in Table 5.1 along with laboratory and prototype discharges and tailwater elevations expressed in the prototype scale. Table 5.2 presents the laboratory results for undistorted prototype stations. Figure 5.5 shows a Type 2 experiment.

Table 5.1: Parameters for Type 2 Experiments

Profile No.	Tailwater (RS 0) (ft)	Discharge		
		Laboratory Model (cfs)	Prototype Distorted (cfs)	Prototype Undistorted (cfs)
1	2	3	4	5
1	17.14	2.21	19800	3960
2	18.17	2.21	19800	3960
3	19.06	2.21	19800	3960
4	19.11	2.56	22900	4580
5	18.68	2.56	22900	4580
6	17.79	2.56	22900	4580
7	16.74	2.89	25900	5180
8	15.55	2.89	25900	5180
9	14.90	2.89	25900	5180

Table 5.2: Laboratory Results for Type 2 Experiments

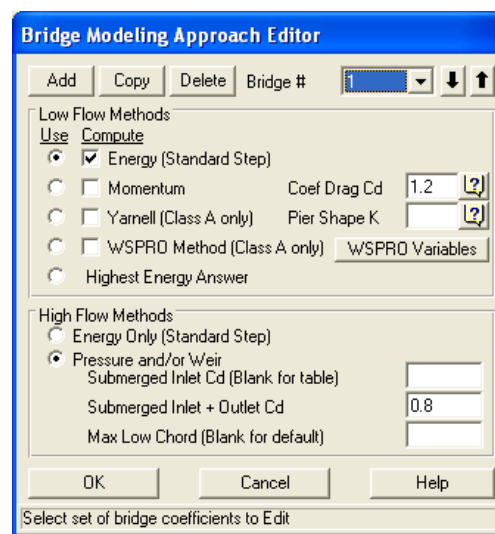
River Station (ft)	Laboratory Results								
	Prof 1 (ft)	Prof 2 (ft)	Prof 3 (ft)	Prof 4 (ft)	Prof 5 (ft)	Prof 6 (ft)	Prof 7 (ft)	Prof 8 (ft)	Prof 9 (ft)
1	2	3	4	5	6	7	8	9	10
150	22.31	22.83	23.23	24.28	24.02	23.62	24.41	23.88	24.15
130	22.31	22.83	23.23	24.28	24.02	23.62	24.41	23.72	24.15
120	22.23	22.83	23.23	24.28	24.02	23.62	24.41	23.72	24.15
110	22.23	22.75	22.98	24.19	23.93	23.54	24.33	23.72	24.06
100	22.23	22.58	22.90	24.11	23.85	23.46	24.16	23.55	23.81
90	21.89	22.42	22.81	23.86	23.68	23.21	24.08	21.63	23.56
80	21.89	22.42	22.73	23.86	23.60	23.21	23.91	21.63	23.48
70	16.39	17.67	18.48	18.61	17.93	16.96	15.83	14.05	12.31
60	17.23	18.25	19.06	19.53	19.02	17.87	17.16	16.13	15.65
50	17.23	18.42	19.31	19.94	19.18	18.04	17.24	15.63	13.32
40	16.89	18.00	18.90	19.28	18.60	17.37	16.41	14.97	13.31
30	16.89	17.92	18.73	18.94	18.35	17.37	16.33	14.88	13.31
20	16.98	18.00	18.73	18.94	18.35	17.54	16.49	15.13	14.31
0	17.14	18.17	19.06	19.11	18.68	17.79	16.74	15.55	14.90



Figure 5.5: Type 2 Experiment

5.1 Regular Undistorted Type 2 HEC-RAS Models

Figure 5.6 shows screen captures of the cross section layout, bridge and n-value table for the Regular Distorted HEC-RAS Type 2 Model. Typical modeling methods were used to create this model. The pressure/weir method of high flow modeling was used. Note that the right overbank ineffective flow area elevation is at the top of the roadway and the left ineffective flow area elevation is at the weir crest elevation. The elevation of the top of the roadway in the laboratory model corresponded to 26 feet. This had to be set to 28 feet in HEC-RAS to avoid overtopping of the roadway for the higher flows. Contraction and expansion ratios of 1:1 and 4:1, respectively, were used to set the ineffective flow locations for the Regular Type 2 HEC-RAS models. Expansion and contraction coefficients of 0.3 and 0.5, respectively, were used 2 cross sections upstream and 1 cross section downstream from the bridge. Also, the weir coefficient was 2.6. The Pressure and/or Weir Submerged Inlet Cd in the Bridge Modeling Approach Editor was left blank as shown below.



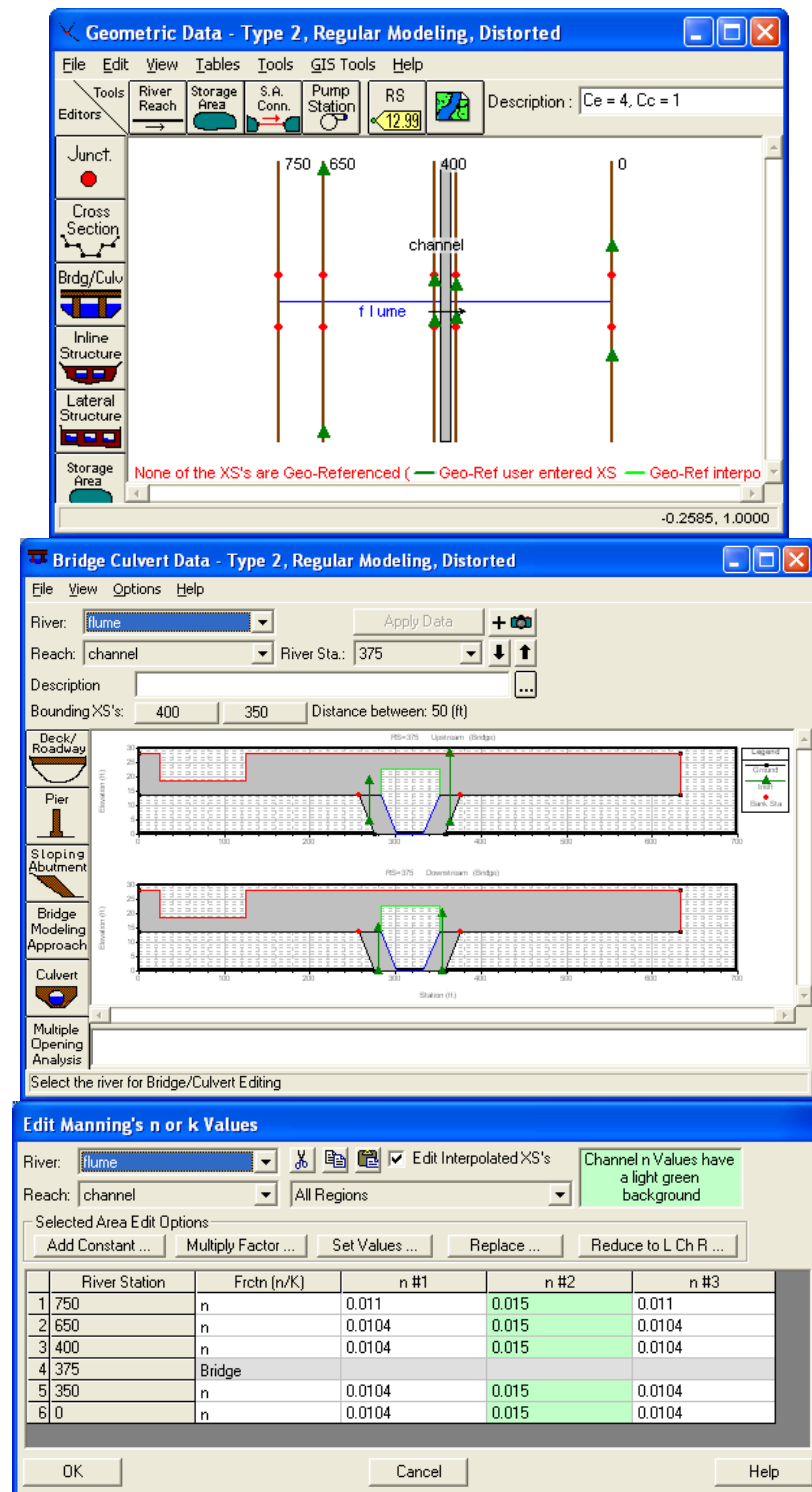


Figure 5.6: Plan, Bridge and n-value Table for Regular Distorted Type 2 HEC-RAS Model

The water surface profiles for the Regular Distorted Type 2 HEC-RAS model is given in Table 5.3. Table 5.4 gives the laboratory values for the HEC-RAS stations. Table 5.5 shows the differences in the values in Table 5.4 and 5.3 for the HEC-RAS stations (HEC-RAS – Lab). Plots of the profiles will be presented later with the GWB Modified HEC-RAS Models.

Table 5.3: Water Surface Profiles for the Regular Undistorted HEC-RAS Type 2 Experiments

Regular Undistorted RS (ft) 1	Low Q			Middle Q			High Q		
	Prof 1 (ft) 2	Prof 2 (ft) 3	Prof 3 (ft) 4	Prof 4 (ft) 5	Prof 5 (ft) 6	Prof 6 (ft) 7	Prof 7 (ft) 8	Prof 8 (ft) 9	Prof 9 (ft) 10
150	25.47	25.47	25.47	26.58	26.58	26.58	27.77	27.77	27.77
130	25.47	25.47	25.47	26.57	26.57	26.57	27.76	27.76	27.76
80	25.3	25.3	25.3	26.38	26.38	26.38	27.55	27.55	27.55
70	16.95	18.03	18.95	18.96	18.51	17.56	16.32	16.32	16.32
0	17.14	18.17	19.06	19.11	18.68	17.79	16.74	15.7	15.7

Table 5.4: Lab Results for Type 2 Experiments at Undistorted HEC-RAS Stations

Laboratory Distorted RS (ft) 1	Low Q			Middle Q			High Q		
	Prof 1 (ft) 2	Prof 2 (ft) 3	Prof 3 (ft) 4	Prof 4 (ft) 5	Prof 5 (ft) 6	Prof 6 (ft) 7	Prof 7 (ft) 8	Prof 8 (ft) 9	Prof 9 (ft) 10
750	22.31	22.83	23.23	24.28	24.02	23.62	24.41	23.88	24.15
650	22.31	22.83	23.23	24.28	24.02	23.62	24.41	23.72	24.15
400	21.89	22.42	22.73	23.86	23.60	23.21	23.91	21.63	23.48
350	16.39	17.67	18.48	18.61	17.93	16.96	15.83	14.05	12.31
0	17.14	18.17	19.06	19.11	18.68	17.79	16.74	15.55	14.90

Table 5.5: Differences (HEC-RAS - Lab) for Regular Undistorted Model

Regular Undistorted RS (ft) 1	Low Q			Middle Q			High Q		
	Prof 1 (ft) 2	Prof 2 (ft) 3	Prof 3 (ft) 4	Prof 4 (ft) 5	Prof 5 (ft) 6	Prof 6 (ft) 7	Prof 7 (ft) 8	Prof 8 (ft) 9	Prof 9 (ft) 10
150	3.16	2.64	2.24	2.30	2.56	2.96	3.36	3.89	3.62
130	3.16	2.64	2.24	2.29	2.55	2.95	3.35	4.04	3.61
80	3.41	2.88	2.57	2.52	2.78	3.17	3.64	5.92	4.07
70	0.56	0.36	0.47	0.35	0.58	0.60	0.49	2.27	4.01
0	0.00	0.00	0.00	0.00	0.00	0.00	0.00	0.15	0.80

5.2 Modified Distorted Type 2 HEC-RAS Models

Mr. Gary Brunner developed the model presented in this section. Via e-mail he sent the text below describing this model.

Type 2 model:

1. I changed the weir coefficient on the deck and roadway editor from 2.6 to 3.2. Your bridge for this experiment is only a board. The length to depth ratio for flow over the weir is not very high, so I would say it is not acting like a broad crested weir, more like a sharp crested weir. So a value of 3.2 is more appropriate for a sharp crested weir. This lowered the water surface quite a bit by itself.
2. I modified the ineffective flow areas at the cross section just upstream and downstream of the bridge. I changed from what we call "Normal" Ineffective flow areas to "Blocked" Ineffective flow areas. This allowed me to capture the stagnant flow areas between the weir and the bridge opening, as well as just left of the weir opening. So the active flow areas are limited to just upstream and downstream of the weir and the bridge opening only. This also improved the water surface calculation downstream as well as upstream of the bridge.
3. I used a 2:1 expansion ratio, instead of a 4:1 for setting the ineffective flow areas at cross section 0.0.
4. For the low flow rate the program is using low flow energy through the bridge and then weir flow for the flow over the weir. We call this an Energy/Weir solution in the bridge output. For the mid and high flow rates,

the program is using pressure flow and weir flow. Since the downstream end of the bridge is unsubmerged, the program uses a Sluice gate type of equation for the pressure flow through the bridge. Since most of the flow is going through the bridge, the coefficient selected for this type of flow will control the answer upstream. The default in RAS is to leave this coefficient blank and a look up table will be used. This works ok, if there is a very large head on the bridge opening. In your case there is not, so Instead of using the default coefficient, I put in a value of 0.5, which is a common value for this coefficient for the form of the equation being used. This is probably an area that we need further experimentation to see what values are appropriate. The default curve is from an older FHWA publication with not too much data to support it.

5. I changed the top elevation of the road back to 26 feet. Not sure why you changed it to 28 feet. **(Parr: HEC-RAS models over top the roadway at 26 feet where lab model did not.)**

The Plan View and the bridge are shown in Figure 5.7 for the Modified Undistorted Type 2 HEC-RAS Model. The differences between the Modified and the Regular models are

- Changed from Normal to Multiple Block Ineffective Flow Areas,
- Used an expansion ratio C_e of approximately 2.8 downstream from the bridge,
- Changed the weir coefficient from 2.6 to 3.2,
- Changed the Pressure and/or Weir Submerged Inlet C_d from blank to 0.5.

These changes dramatically improved the agreement with the laboratory data. The change that had the most dramatic effect was the Pressure and/or Weir Submerged Inlet C_d -value. In addition to those changes by GWB, we changed the Manning n -values to 0.0104, 0.0110 for the overbanks and 0.0150 for the main channel as per the discussion in Chapter 2.

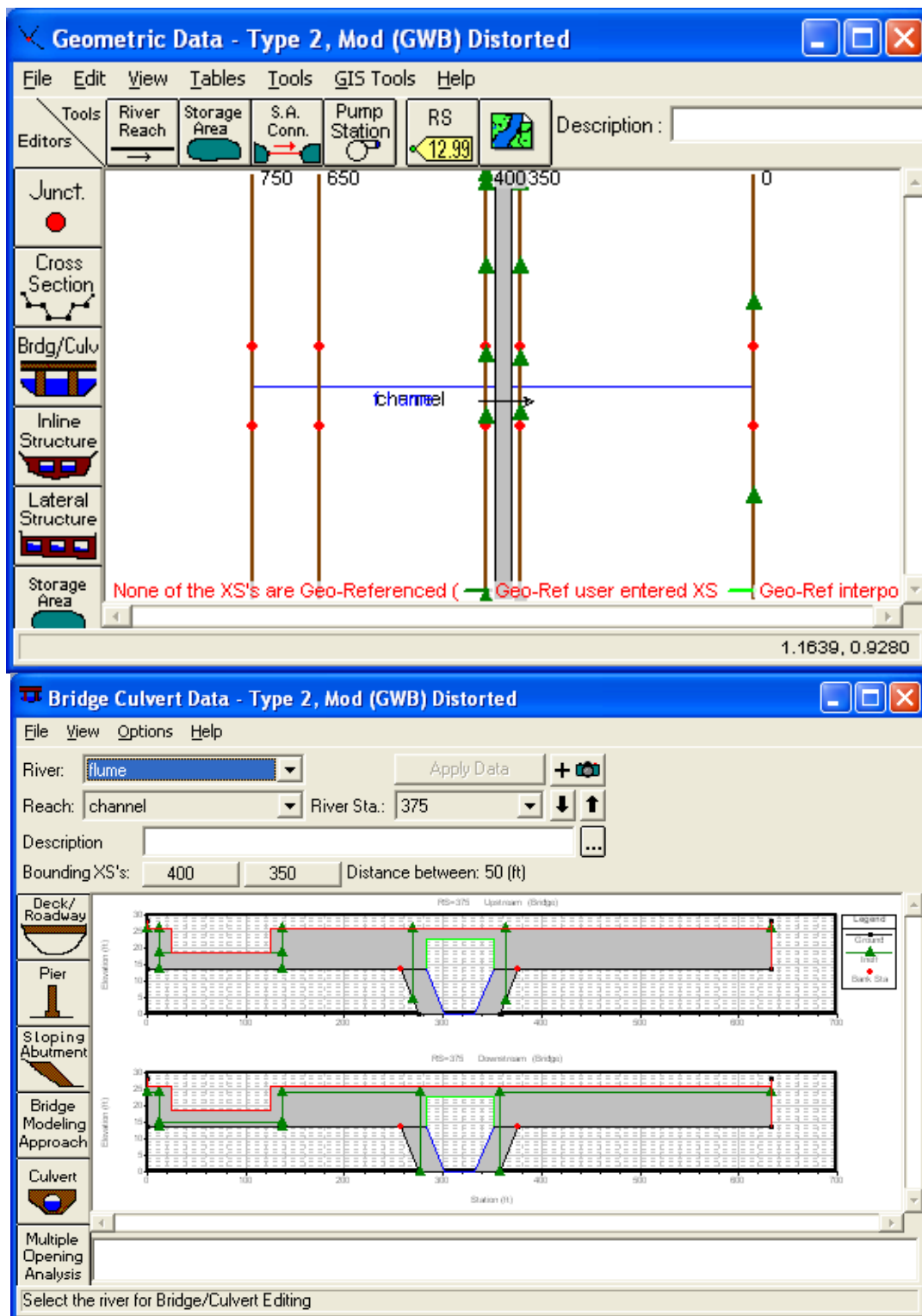


Figure 5.7: Plan View and Bridge for Regular Distorted HEC-RAS Type 2 Model

The results for the Modified Undistorted Type 2 HEC-RAS model are presented in Table 5.6. The differences between these values and the laboratory values of Table 5.4 are shown in Table 5.7. Note that these values are much improved over the values for the Regular Model presented in Table 5.5 which is repeated just below Table 5.7 for easy comparison.

Table 5.6: Water Surface Profiles for the Modified (GWB) Distorted HEC-RAS Type 2 Experiments

Modified Undistorted RS (ft) 1	Low Q			Middle Q			High Q		
	Prof 1 (ft) 2	Prof 2 (ft) 3	Prof 3 (ft) 4	Prof 4 (ft) 5	Prof 5 (ft) 6	Prof 6 (ft) 7	Prof 7 (ft) 8	Prof 8 (ft) 9	Prof 9 (ft) 10
150	23.49	23.49	23.4	24.88	24.88	24.88	26.1	26.1	26.1
130	23.48	23.48	23.4	24.88	24.88	24.88	26.1	26.1	26.1
80	22.81	22.81	22.72	24.13	24.13	24.13	26.1	26.1	26.1
70	16.15	17.4	18.43	18.2	17.67	16.49	16.62	16.62	16.62
0	17.14	18.17	19.06	19.11	18.68	17.79	16.74	15.71	15.71

Table 5.7: Differences (HEC-RAS - Lab) for Modified Undistorted Model

Modified Undistorted RS (ft) 1	Low Q			Middle Q			High Q		
	Prof 1 (ft) 2	Prof 2 (ft) 3	Prof 3 (ft) 4	Prof 4 (ft) 5	Prof 5 (ft) 6	Prof 6 (ft) 7	Prof 7 (ft) 8	Prof 8 (ft) 9	Prof 9 (ft) 10
150	1.18	0.66	0.17	0.60	0.86	1.26	1.69	2.22	1.95
130	1.17	0.65	0.17	0.60	0.86	1.26	1.69	2.38	1.95
80	0.92	0.39	-0.01	0.27	0.53	0.92	2.19	4.47	2.62
70	-0.24	-0.27	-0.05	-0.41	-0.26	-0.47	0.79	2.57	4.31
0	0.00	0.00	0.00	0.00	0.00	0.00	0.00	0.16	0.81

(Repeated) Table 5.5: Differences (HEC-RAS - Lab) for Regular Undistorted Model

Regular Undistorted RS (ft) 1	Low Q			Middle Q			High Q		
	Prof 1 (ft) 2	Prof 2 (ft) 3	Prof 3 (ft) 4	Prof 4 (ft) 5	Prof 5 (ft) 6	Prof 6 (ft) 7	Prof 7 (ft) 8	Prof 8 (ft) 9	Prof 9 (ft) 10
150	3.16	2.64	2.24	2.30	2.56	2.96	3.36	3.89	3.62
130	3.16	2.64	2.24	2.29	2.55	2.95	3.35	4.04	3.61
80	3.41	2.88	2.57	2.52	2.78	3.17	3.64	5.92	4.07
70	0.56	0.36	0.47	0.35	0.58	0.60	0.49	2.27	4.01
0	0.00	0.00	0.00	0.00	0.00	0.00	0.00	0.15	0.80

Table 5.8 shows the difference in water surface elevations between the Modified and Regular Type 2 Undistorted HEC-RAS models.

Table 5.8: Differences between Modified and Regular Undistorted Type 2 HEC-RAS Models (Mod – Reg)

Undistorted RS (ft) 1	Low Q			Middle Q			High Q		
	Prof 1 (ft) 2	Prof 2 (ft) 3	Prof 3 (ft) 4	Prof 4 (ft) 5	Prof 5 (ft) 6	Prof 6 (ft) 7	Prof 7 (ft) 8	Prof 8 (ft) 9	Prof 9 (ft) 10
750	-1.98	-1.98	-2.07	-1.7	-1.7	-1.7	-1.67	-1.67	-1.67
650	-1.99	-1.99	-2.07	-1.69	-1.69	-1.69	-1.66	-1.66	-1.66
400	-2.49	-2.49	-2.58	-2.25	-2.25	-2.25	-1.45	-1.45	-1.45
350	-0.8	-0.63	-0.52	-0.76	-0.84	-1.07	0.3	0.3	0.3
0	0	0	0	0	0	0	0	0.01	0.01

Plots of the profiles for the Regular and Modified Undistorted Type 2 HEC-RAS models are presented together with the laboratory data in Figures 5.8, 5.9 and 5.10. The dramatic improvement is apparent for the Gary Brunner model. Figures 5.11, 5.12, and 5.13 show the Regular and Modified Undisorted Type 2 HEC-RAS model profiles with the Cd value set at 0.5 for the Regular model. This alone brings the Regular and the Modified profiles much closer. However, the Modified model is still the better one.

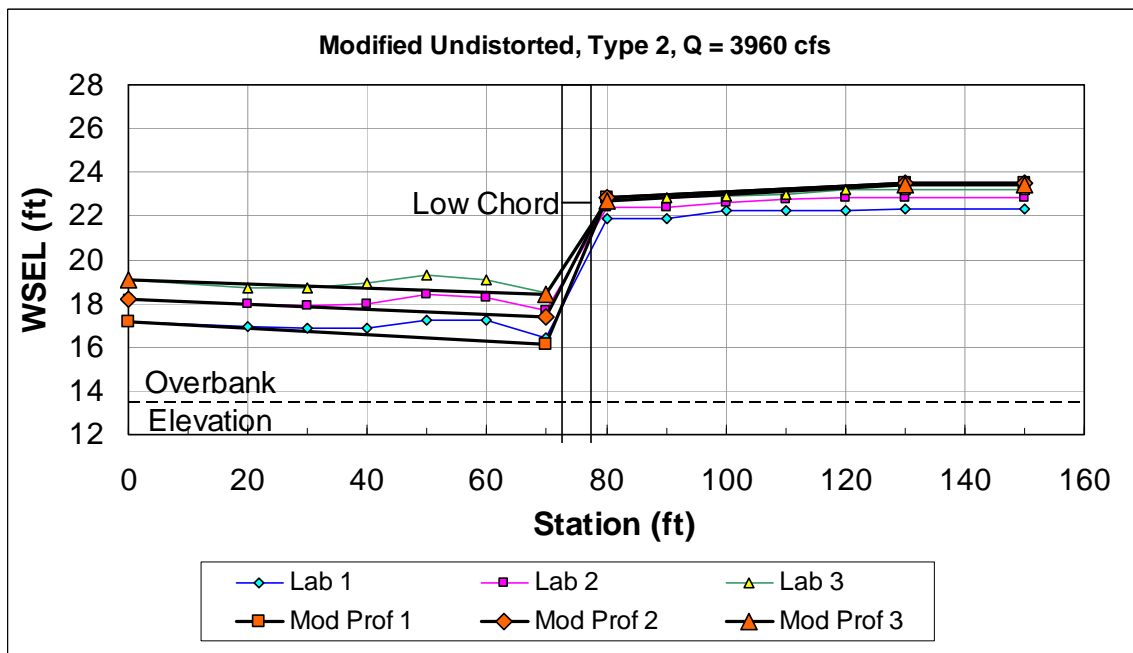
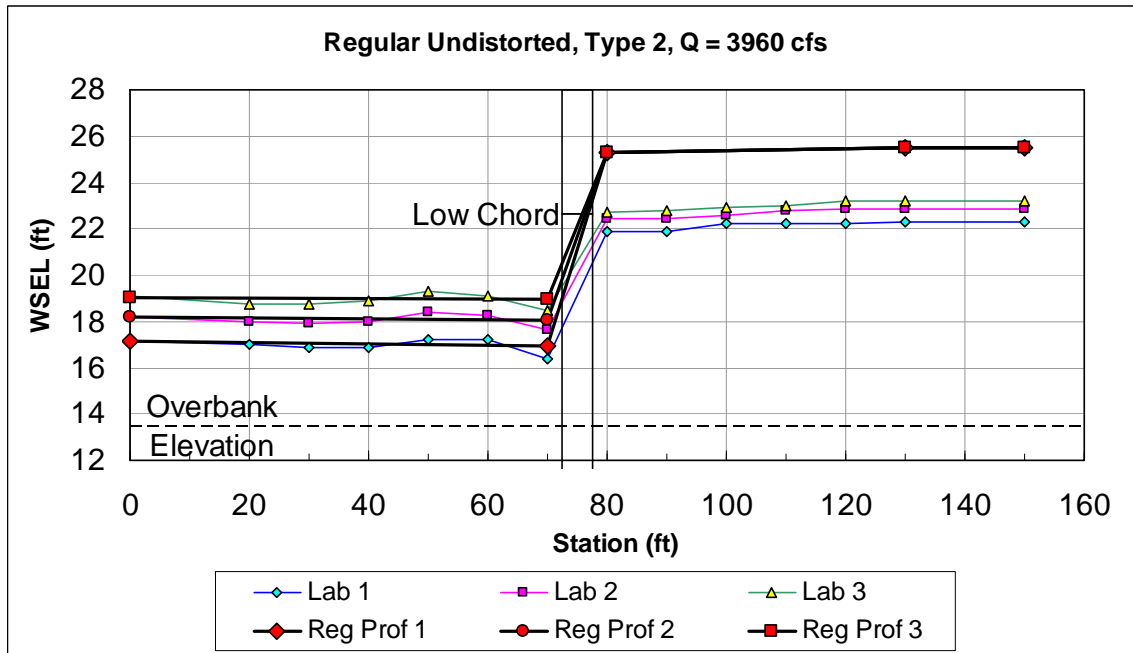


Figure 5.8: Lab and Undistorted Regular and Modified HEC-RAS Results for Type 2 Experiments - Low Flow

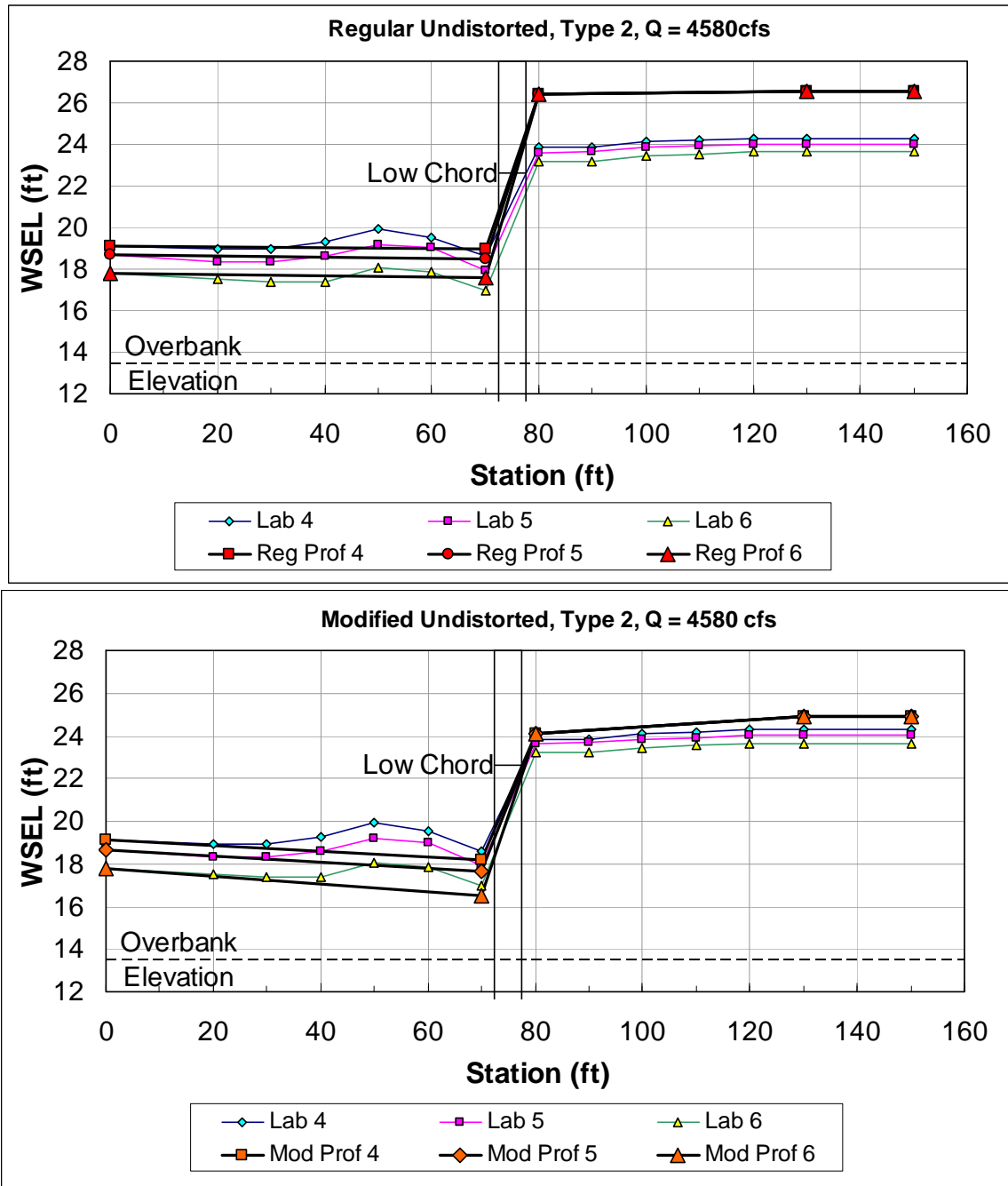


Figure 5.9: Lab and Undistorted Regular and Modified HEC-RAS Results for Type 2 Experiments - Middle Flow

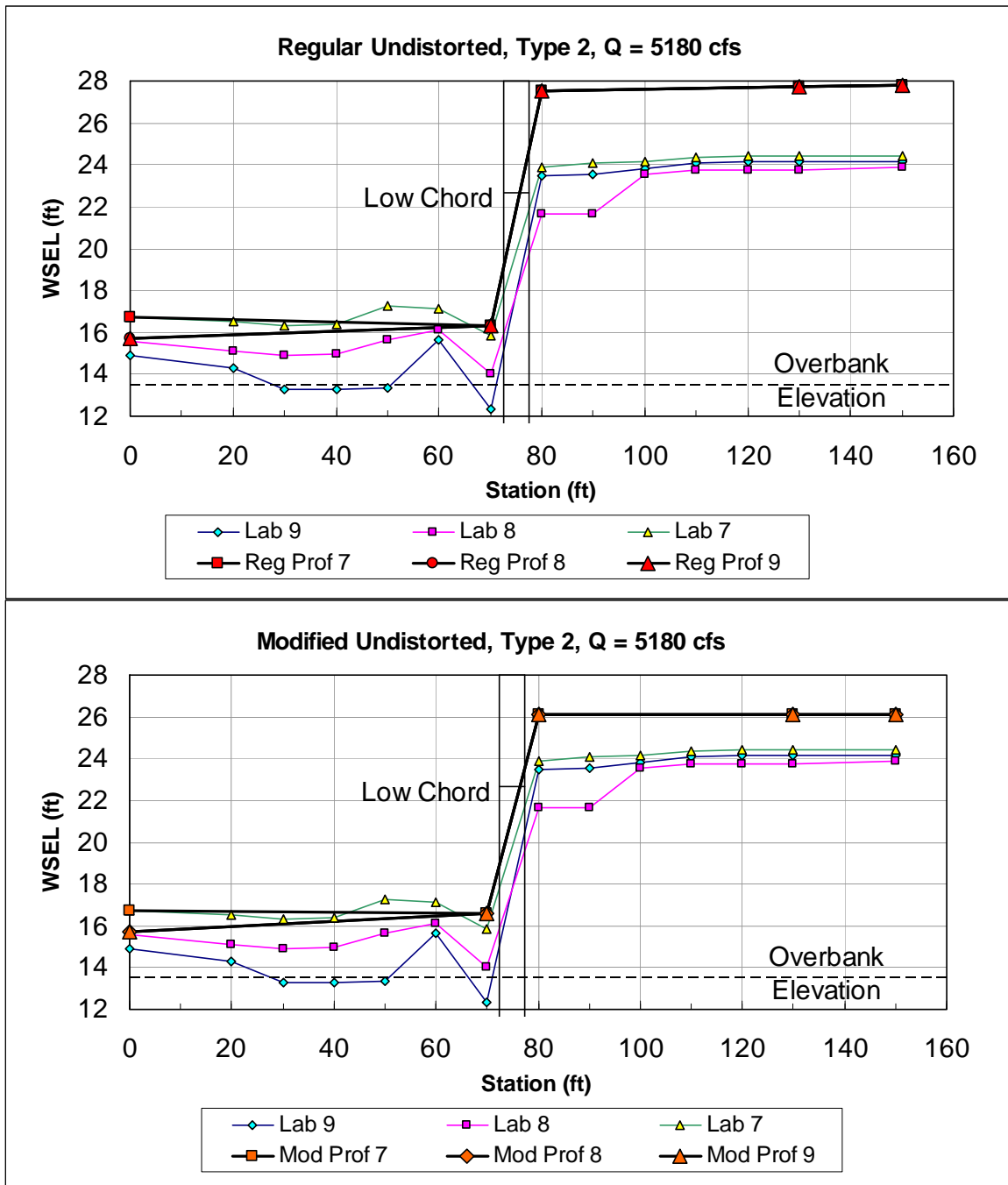


Figure 5.10: Lab and Undistorted Regular and Modified HEC-RAS Results for Type 2 Experiments - High Flow

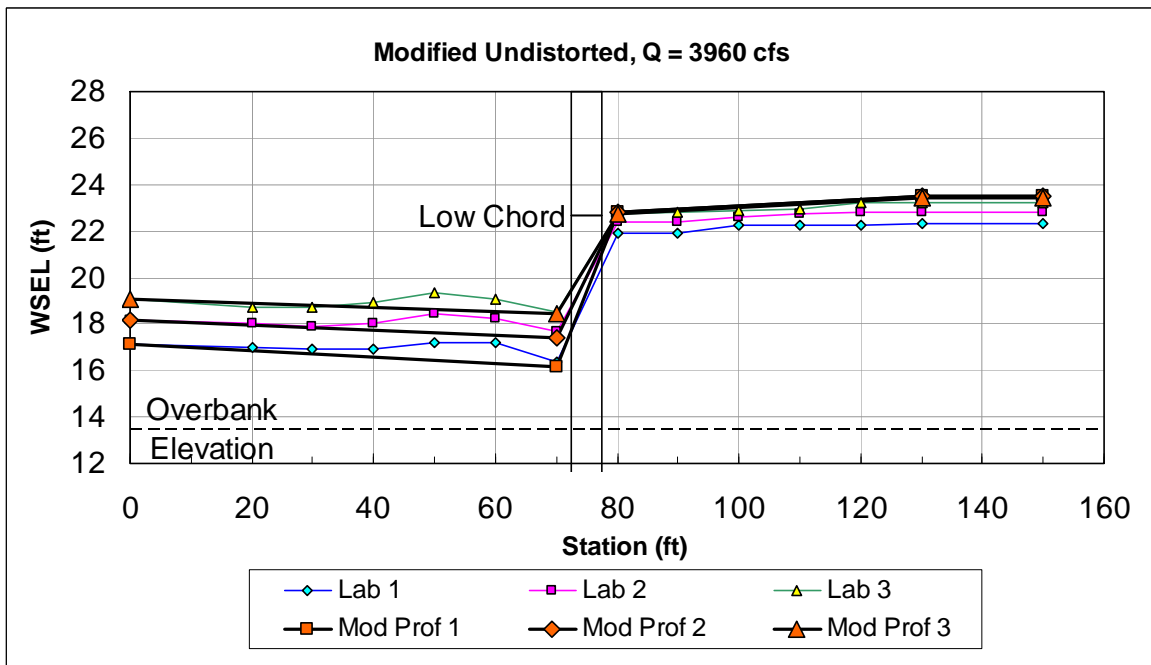
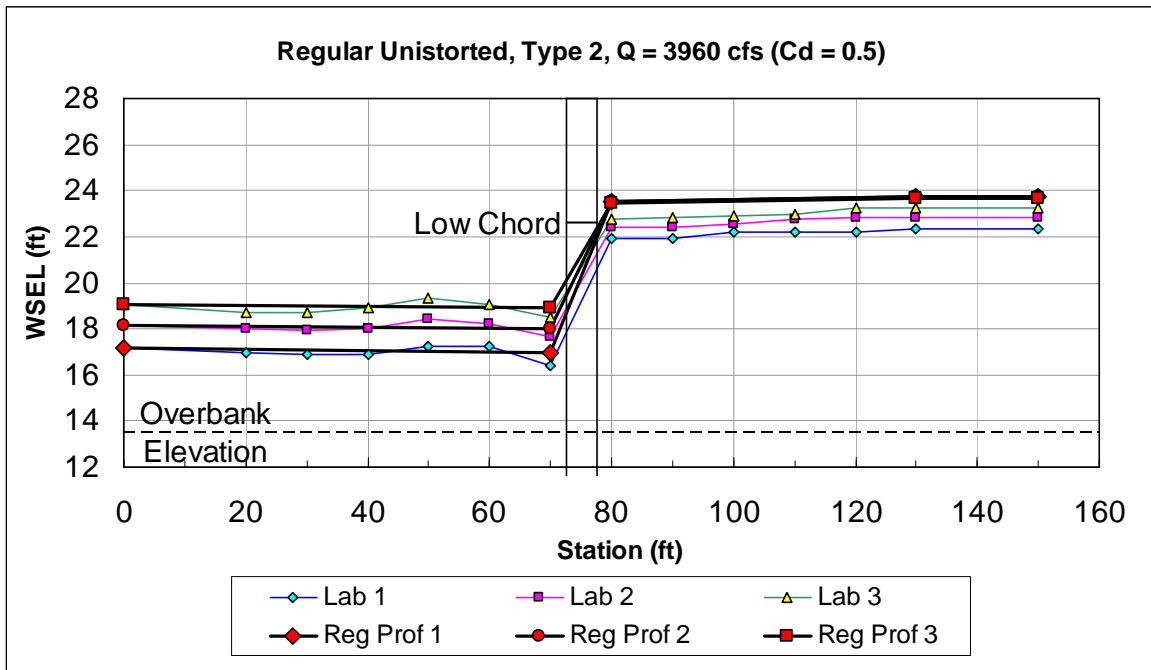


Figure 5.11: Lab and Undistorted Regular and Modified HEC-RAS Results for Type 2 Experiments - Low Flow (*Regular Model with Cd = 0.5*)

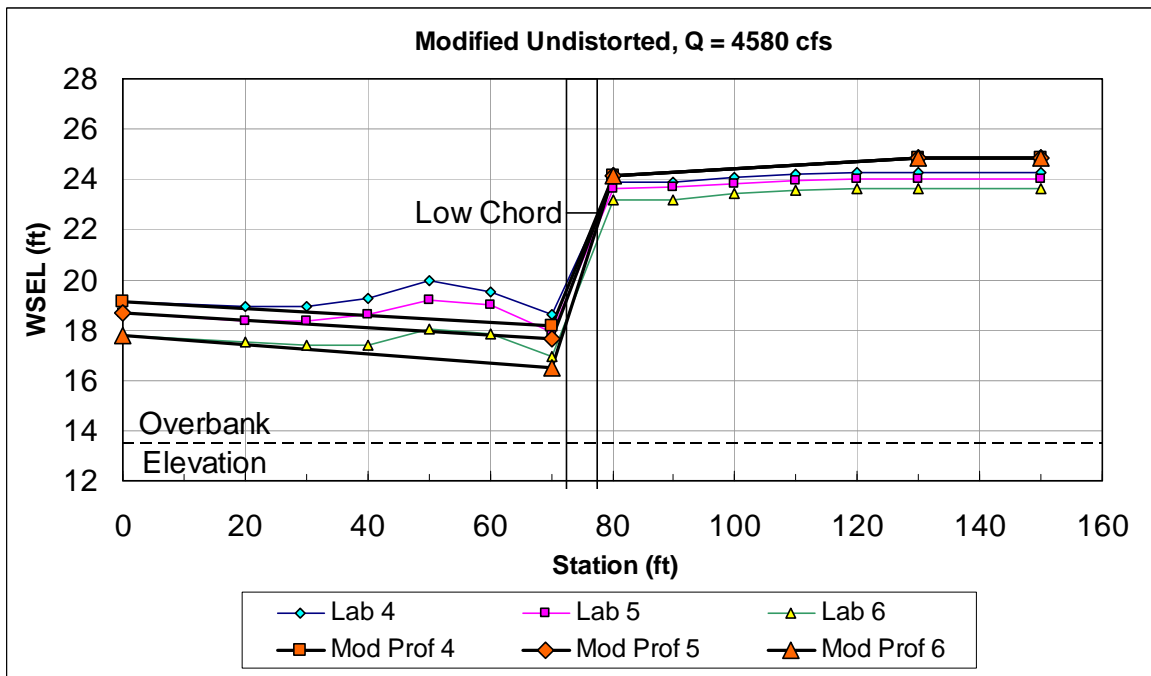
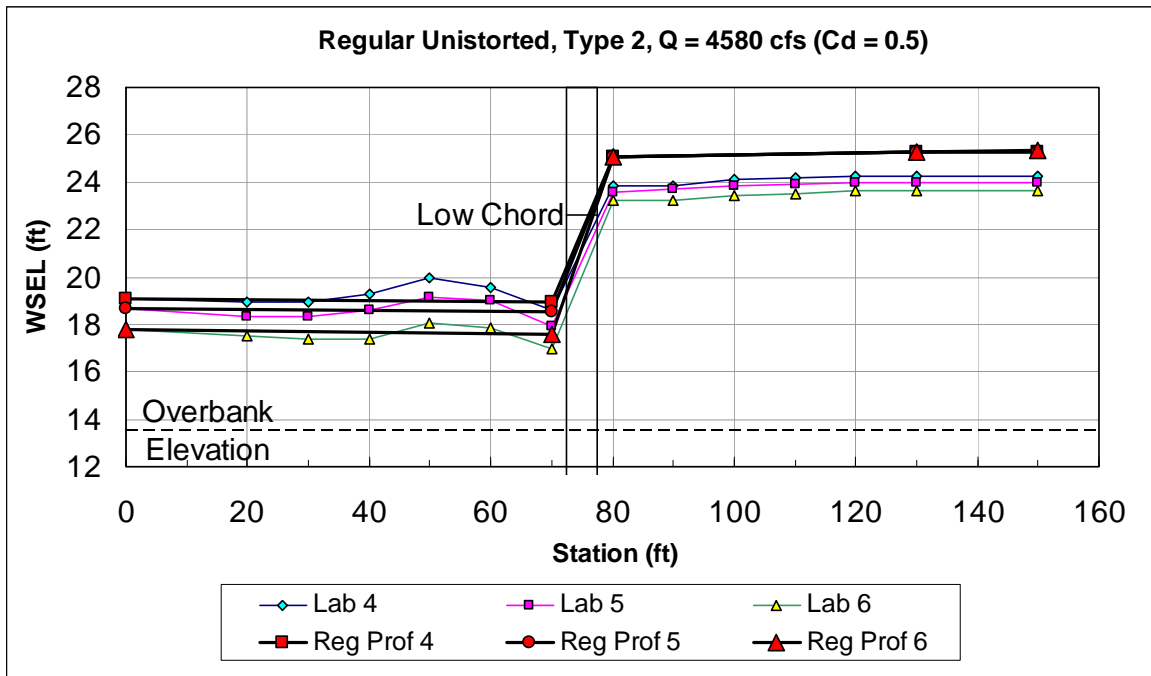


Figure 5.12: Lab and Undistorted Regular and Modified HEC-RAS Results for Type 2 Experiments - Middle Flow (*Regular Model with $C_d = 0.5$*)

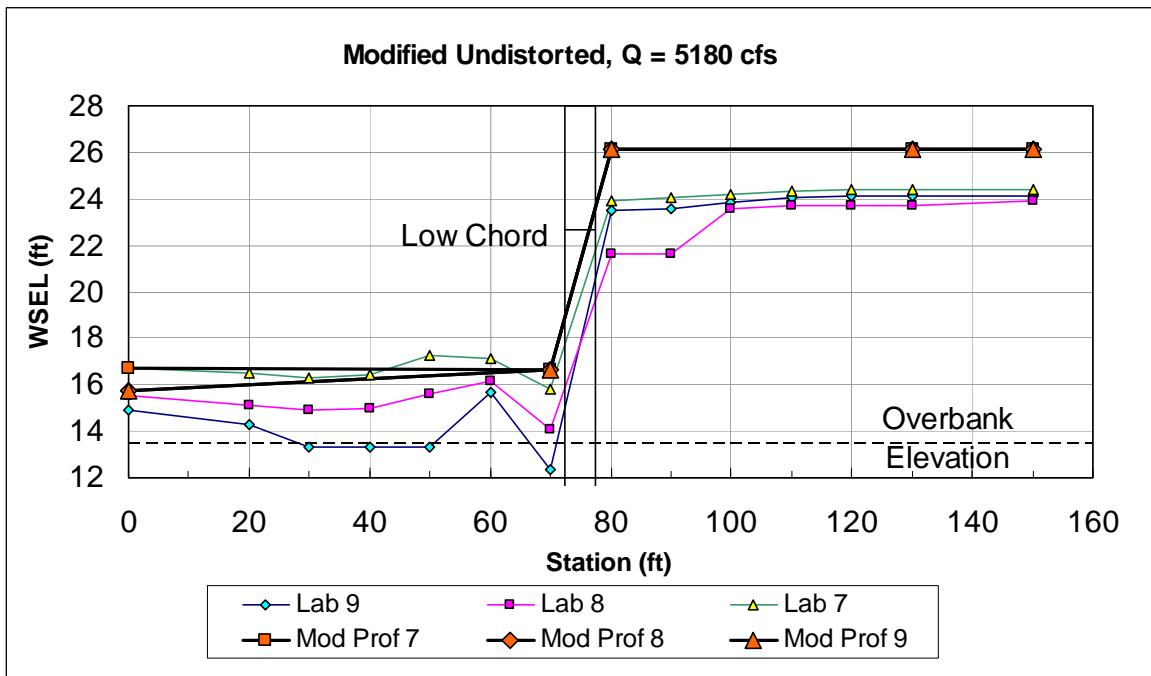
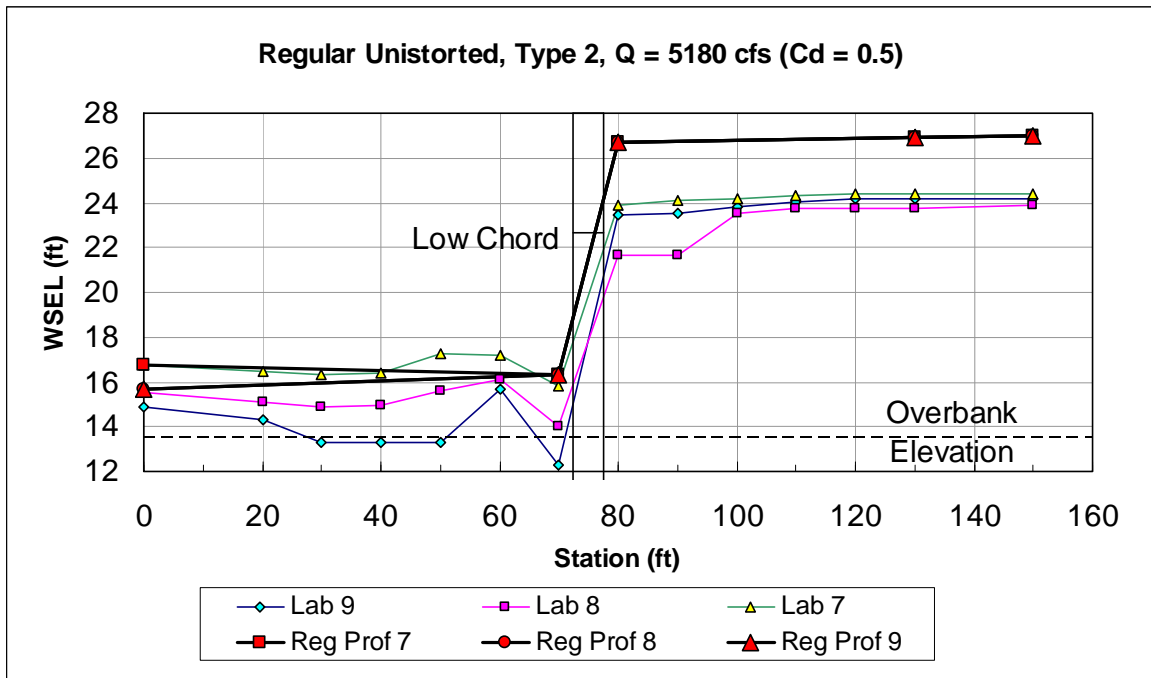


Figure 5.13: Lab and Undistorted Regular and Modified HEC-RAS Results for Type 2 Experiments - High Flow (*Regular Model with Cd = 0.5*)

5.3 Distorted Type 2 HEC-RAS Models

The prototype distorted model with $X_r = 100$ and $Y_r = 20$ was created from the prototype undistorted model with $L_r = X_r = Y_r = 20$ by the steps presented in Chapter 4, Section C. Tables 5.9 and 5.10 show the computed water surface elevations for the distorted and undistorted HEC-RAS models. The agreement is very good. The discrepancies for the distorted model may be due to differences in the Froude number and velocities. Table 5.11 shows the parameters for the Undistorted and Distorted Modified Type 2 HEC-RAS models obtained from the Profile Output tables. The last column is the ratio of the Froude number for the undistorted and distorted models. It is interesting to look at the parameters for undistorted RS 70 and distorted RS 350 where the largest discrepancies in water surface elevations and the flow conditions are near critical.

Table 5.9: Results for Undistorted and Distorted Regular GWB Type 2 HEC-RAS Models

Regular HEC-RAS Undistorted Model									
Undistorted RS (ft)	Water Surface Elevation (ft) - Undistorted								
	Low Q			Mid Q			High Q		
	PF 1	PF 2	PF 3	PF 4	PF 5	PF 6	PF 7	PF 8	PF 9
150	25.47	25.47	25.47	26.58	26.58	26.58	27.77	27.77	27.77
130	25.47	25.47	25.47	26.57	26.57	26.57	27.76	27.76	27.76
80	25.3	25.3	25.3	26.38	26.38	26.38	27.55	27.55	27.55
70	16.95	18.03	18.95	18.96	18.51	17.56	16.32	16.32	16.32
0	17.14	18.17	19.06	19.11	18.68	17.79	16.74	15.7	15.7

Regular HEC-RAS Distorted Model									
Distorted RS (ft)	Water Surface Elevation (ft) - Distorted								
	Low Q			Mid Q			High Q		
	PF 1	PF 2	PF 3	PF 4	PF 5	PF 6	PF 7	PF 8	PF 9
750	25.46	25.46	25.46	26.56	26.56	26.57	27.76	27.76	27.76
650	25.45	25.45	25.45	26.55	26.55	26.55	27.74	27.74	27.74
400	25.3	25.3	25.3	26.38	26.38	26.38	27.55	27.55	27.55
350	17	18.07	18.98	19	18.56	17.63	16.39	16.3	16.3
0	17.14	18.17	19.06	19.11	18.68	17.79	16.74	15.71	15.71

Difference for Regular HEC-RAS Undistorted and Distorted Models										
Distorted RS (ft)	Undistorted RS (ft)	Undistorted - Distorted (ft)								
		Low Q			Mid Q			High Q		
		PF 1	PF 2	PF 3	PF 4	PF 5	PF 6	PF 7	PF 8	PF 9
750	150	0.01	0.01	0.01	0.02	0.02	0.01	0.01	0.01	0.01
650	130	0.02	0.02	0.02	0.02	0.02	0.02	0.02	0.02	0.02
400	80	0	0	0	0	0	0	0	0	0
350	70	-0.05	-0.04	-0.03	-0.04	-0.05	-0.07	-0.07	0.02	0.02
0	0	0	0	0	0	0	0	0	-0.01	-0.01

Table 5.10: Results for Undistorted and Distorted Modified GWB Type 2 HEC-RAS Models

Modified GWB HEC-RAS Undistorted Model									
Undistorted RS (ft)	Water Surface Elevation (ft) - Undistorted								
	Low Q			Mid Q			High Q		
	PF 1	PF 2	PF 3	PF 4	PF 5	PF 6	PF 7	PF 8	PF 9
150	23.49	23.49	23.4	24.88	24.88	24.88	26.1	26.1	26.1
130	23.48	23.48	23.4	24.88	24.88	24.88	26.1	26.1	26.1
80	22.81	22.81	22.72	24.13	24.13	24.13	26.1	26.1	26.1
70	16.15	17.4	18.43	18.2	17.67	16.49	16.62	16.62	16.62
0	17.14	18.17	19.06	19.11	18.68	17.79	16.74	15.71	15.71

Modified GWB HEC-RAS Distorted Model									
Distorted RS (ft)	Water Surface Elevation (ft) - Distorted								
	Low Q			Mid Q			High Q		
	PF 1	PF 2	PF 3	PF 4	PF 5	PF 6	PF 7	PF 8	PF 9
750	23.47	23.47	23.39	24.86	24.88	24.88	26.1	26.1	26.1
650	23.47	23.47	23.39	24.86	24.88	24.88	26.1	26.1	26.1
400	22.85	22.85	22.76	24.15	24.18	24.18	26.1	26.1	26.1
350	16.34	17.56	18.56	18.41	17.89	16.77	16.7	16.7	16.7
0	17.14	18.17	19.06	19.11	18.68	17.79	16.74	15.72	15.72

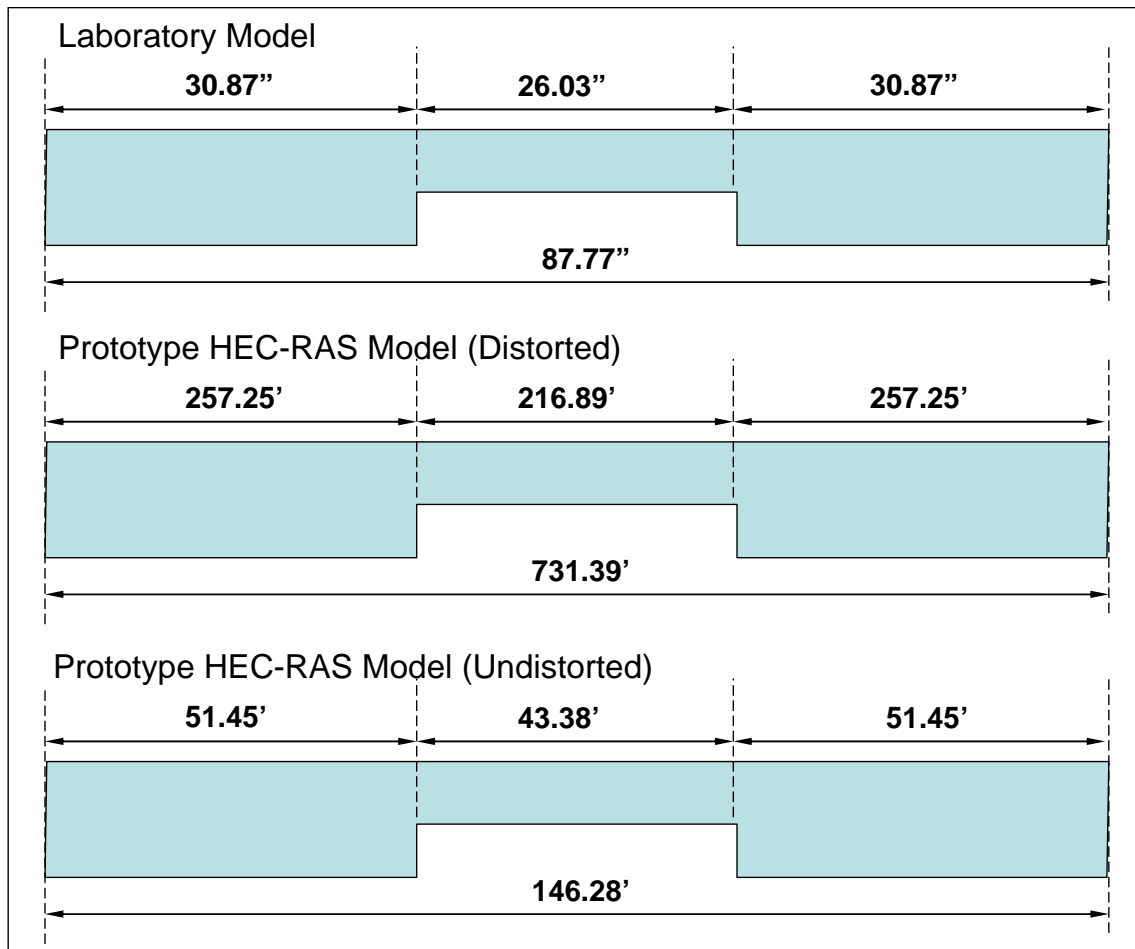
Difference for Modified HEC-RAS Undistorted and Distorted Models										
Distorted RS (ft)	Undistorted RS (ft)	Undistorted - Distorted (ft)								
		Low Q			Mid Q			High Q		
		PF 1	PF 2	PF 3	PF 4	PF 5	PF 6	PF 7	PF 8	PF 9
750	150	0.02	0.02	0.01	0.02	0	0	0	0	0
650	130	0.01	0.01	0.01	0.02	0	0	0	0	0
400	80	-0.04	-0.04	-0.04	-0.02	-0.05	-0.05	0	0	0
350	70	-0.19	-0.16	-0.13	-0.21	-0.22	-0.28	-0.08	-0.08	-0.08
0	0	0	0	0	0	0	0	0	-0.01	-0.01

**Table 5.11: HEC-RAS Parameters for Undistorted and Distorted Modified GWB
Type 2 HEC-RAS Models**

Undistorted River Sta	Distorted River Sta	Profile	Und - Dist W.S. Elev (ft)	Und - Dist Crit W.S. (ft)	Und/Dist Vel Total (ft/s)	Und/Dist Hydr Depth (ft)	Und/Dist Fr # XS	Undistorted Fr # XS	Distorted Fr # XS
1	2	3	4	5	6	7	8	9	10
150	750	1	0.02	0	1.00	1.00	1.00	0.13	0.13
150	750	2	0.02	0	1.00	1.00	1.00	0.13	0.13
150	750	3	0.01	0	1.00	1.00	1.00	0.13	0.13
150	750	4	0.02	0	1.00	1.00	1.00	0.13	0.13
150	750	5	0	0	1.00	1.00	1.00	0.13	0.13
150	750	6	0	0	1.00	1.00	1.00	0.13	0.13
150	750	7	0	0	1.00	1.00	1.00	0.13	0.13
150	750	8	0	0	1.00	1.00	1.00	0.13	0.13
150	750	9	0	0	1.00	1.00	1.00	0.13	0.13
130	650	1	0.01	0	1.00	1.00	1.00	0.13	0.13
130	650	2	0.01	0	1.00	1.00	1.00	0.13	0.13
130	650	3	0.01	0	1.00	1.00	1.00	0.13	0.13
130	650	4	0.02	0	1.00	1.00	1.00	0.13	0.13
130	650	5	0	0	1.00	1.00	1.00	0.13	0.13
130	650	6	0	0	1.00	1.00	1.00	0.13	0.13
130	650	7	0	0	1.00	1.00	1.00	0.13	0.13
130	650	8	0	0	1.00	1.00	1.00	0.13	0.13
130	650	9	0	0	1.00	1.00	1.00	0.13	0.13
80	400	1	-0.04	0	1.00	1.00	1.04	0.28	0.27
80	400	2	-0.04	0	1.00	1.00	1.04	0.28	0.27
80	400	3	-0.04	0	1.00	1.00	1.00	0.28	0.28
80	400	4	-0.02	0	1.00	1.00	1.00	0.28	0.28
80	400	5	-0.05	0	1.00	1.00	1.00	0.28	0.28
80	400	6	-0.05	0	1.00	1.00	1.00	0.28	0.28
80	400	7	0	0	1.00	1.00	1.00	0.13	0.13
80	400	8	0	0	1.00	1.00	1.00	0.13	0.13
80	400	9	0	0	1.00	1.00	1.00	0.13	0.13
75	350	Bridge							
70	350	1	-0.19	-0.01	1.02	0.98	1.04	0.76	0.73
70	350	2	-0.16	-0.01	1.02	0.98	1.03	0.61	0.59
70	350	3	-0.13	-0.01	1.01	0.99	1.02	0.52	0.51
70	350	4	-0.21	-0.27	1.02	0.98	1.03	0.62	0.60
70	350	5	-0.22	-0.27	1.02	0.98	1.03	0.67	0.65
70	350	6	-0.28	-0.27	1.03	0.97	1.05	0.82	0.78
70	350	7	-0.08	-0.08	1.01	0.99	1.02	0.91	0.89
70	350	8	-0.08	-0.08	1.01	0.99	1.02	0.91	0.89
70	350	9	-0.08	-0.08	1.01	0.99	1.02	0.91	0.89
0	0	1	0	0	1.00	1.00	1.00	0.44	0.44
0	0	2	0	0	1.00	1.00	1.00	0.35	0.35
0	0	3	0	0	1.00	1.00	1.00	0.3	0.30
0	0	4	0	0	1.00	1.00	1.00	0.34	0.34
0	0	5	0	0	1.00	1.00	1.00	0.37	0.37
0	0	6	0	0	1.00	1.00	1.00	0.44	0.44
0	0	7	0	-0.01	1.00	1.00	1.00	0.63	0.63
0	0	8	-0.01	-0.01	1.00	1.00	1.00	0.84	0.84
0	0	9	-0.01	-0.01	1.00	1.00	1.00	0.84	0.84

CHAPTER 6 - TYPE 3 EXPERIMENTS – SKEWED BRIDGE

These experiments were performed on a simple bridge to determine the effectiveness of HEC-RAS to model a skewed bridge opening. Figure 6.1 shows the bridge geometry used for the experiments in both model and prototype dimensions (distorted and undistorted). This “bridge” was placed over the main flume channel at a 30 degree skew angle as shown in Figure 6.2. The bridge and the roadway were 0.25 feet thick in the flume and thus the roadway width in the prototype is 25 feet perpendicular to the road for the distorted model and 5 feet for the undistorted model. The sides of the bridge opening were aligned with the longitudinal stream centerline. Consequently, the distance through the bridge in the flume was $0.25/\cos 30^\circ$ or 0.2886 feet. The distance along the main channel centerline from the upstream and downstream bounding cross sections is $10/\cos 30^\circ = 11.55$ feet for the Undistorted HR model and 57.75 feet for the undistorted HR model. Figure 6.3 shows the skewed bridge in operation.



**Figure 6.1: Laboratory and Prototype Bridge Geometry for Type 3 Experiments
(100:1 Hor Scale; 20:1 Vertical Scale)**

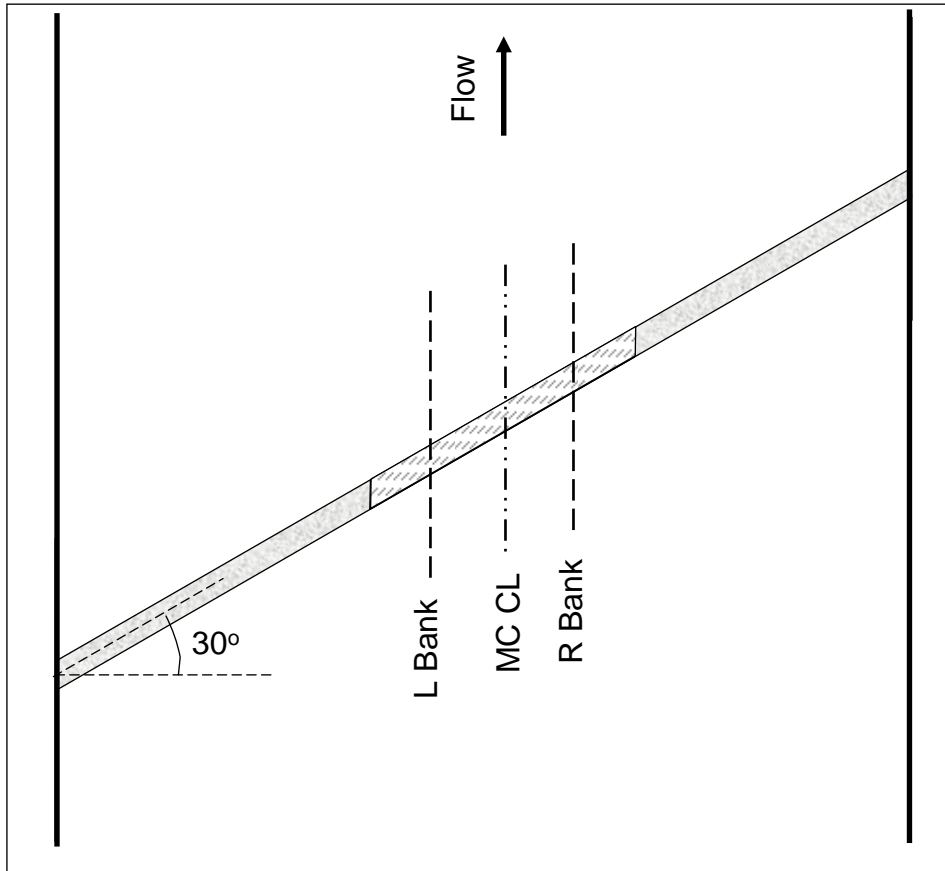


Figure 6.2: Type 3 Laboratory Bridge Model in Flume



Figure 6.3: Upstream View of Skewed Bridge for Type 3 Experiments

6.1 Regular Distorted Type 3 HEC-RAS Models

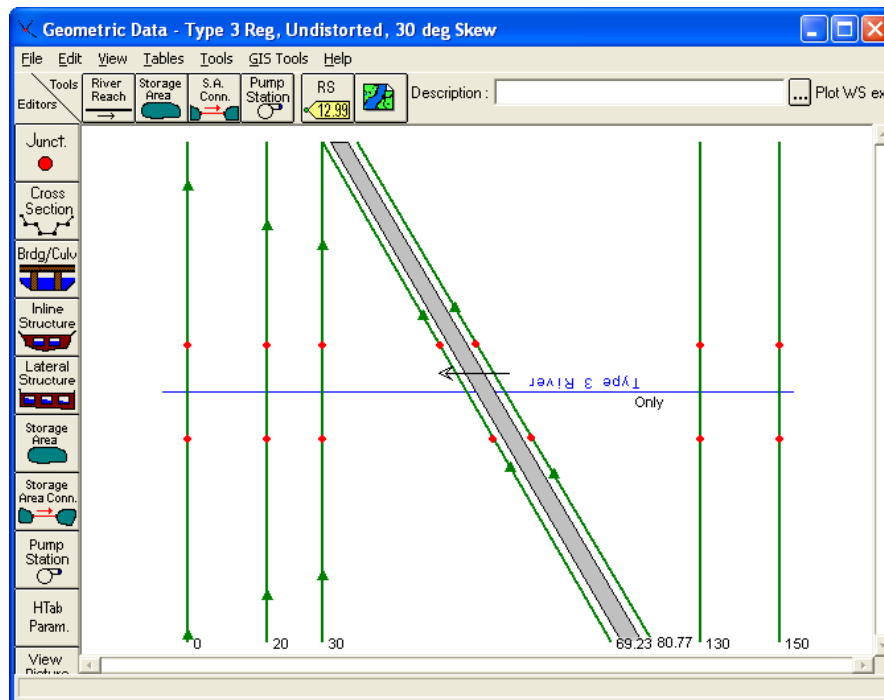
The model cross section plan view for the Regular Undistorted Type 3 HEC-RAS model is shown in Figure 6.4 along with the bounding bridge cross sections RS 69.23 and RS 80.77. The bounding cross sections for the undistorted model were 2.5 feet upstream and downstream from the upstream and downstream bridge faces, respectively, measured perpendicular to the roadway. This data was input with the upstream and downstream bounding cross sections “cut” along the skewed bridge face. This is typically the way it would be done for a real bridge. The other cross sections were “cut” perpendicular to the stream centerline and are the same as they were for regular cross sections in Type 1 and Type 2 models. The values input into the model for the bounding cross sections and for the deck/roadway data are shown under the No Skew columns in Table 6.1 below.

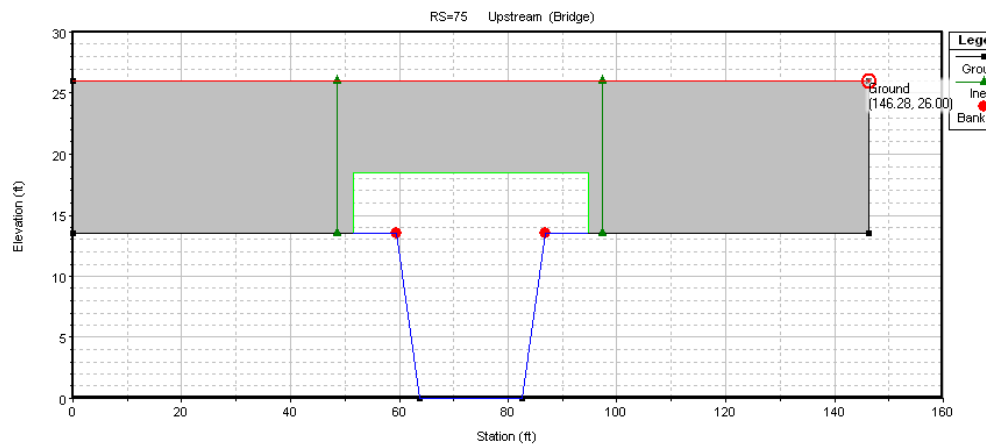
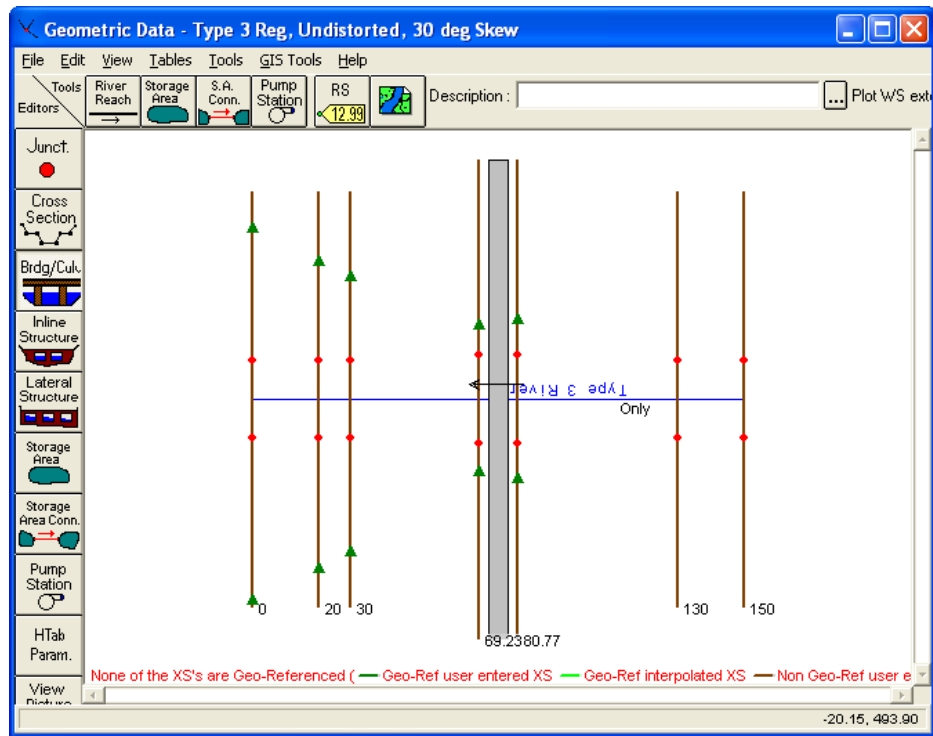
Table 6.1: Bounding Cross Sections and Deck/Roadway Data before and after Invoking the Skew Option in the Bridge Editor

No Skew - Bounding Cross Sections			30° Skew - Bounding Cross Sections		
Station(ft)	Elevation (ft)		Station(ft)	Elevation (ft)	
0.000	26		0	26	
0.000	13.48		0	13.48	
59.467	13.48		51.5	13.48	
63.693	0		55.16	0	
82.584	0		71.52	0	
86.810	13.48		75.18	13.48	
146.277	13.48		126.68	13.48	
146.277	26		126.68	26	

No Skew - Deck/Roadway			30° Skew - Deck/Roadway		
Station(ft)	High Chord (ft)	Low Chord (ft)	Station(ft)	High Chord (ft)	Low Chord (ft)
0	26	13.48	0.00	26	13.48
51.45	26	13.48	44.56	26	13.48
51.45	26	18.5	44.56	26	18.5
94.827	26	18.5	82.12	26	18.5
94.827	26	13.48	82.12	26	13.48
146.277	26	13.48	126.68	26	13.48

The bridge and bounding cross sections (RS 69.23 and RS 80.77) are skewed in the Geometry editor by selecting Brdg/Culv, Options, Skew Bridge/Culvert. This is illustrated in the screen captures shown in Figure 6.5. Note that the bridge and the bounding cross sections are shortened from the non skewed layout in Figure 6.5. Basically, the skew option multiplies the Deck/Roadway and the bounding cross section stationing by the cosine of the skew angle. Note, however, that the Distance and Width values of 2.887 and 5.774, respectively, were not changed by the skew option and should remain at those values. Also, the ineffective flow area locations downstream from the bridge in Figure 6.5 are not symmetrical in the left and right overbanks due to the fact that the actual bridge is skewed as shown below in a pseudo georeferenced version of the model.






Deck/Roadway Data Editor							
Distance			Width		Weir Coef		
2.886			5.774		2.6		
Clear		Del Row		Ins Row		Copy US to DS	
Upstream				Downstream			
	Station	high chord	low chord	Station	high chord	low chord	
2	51.45	26.	13.48	51.45	26.	13.48	
3	51.45	26.	18.5	51.45	26.	18.5	
4	94.827	26.	18.5	94.827	26.	18.5	
5	94.827	26.	13.48	94.827	26.	13.48	
6	146.277	26.	13.48	146.277	26.	13.48	
7							

Figure 6.4: Screen Captures for Regular Undistorted Type 3 HR Model with No Bridge Skew

Bridge/Culvert Skew

In the publication "Hydraulics of Bridge Waterways" (Bradley, 1978) the effect of skew on low flow is discussed. In model testing, skewed crossings with angle up to 20 degrees showed no objectionable flow patterns. For increasing angles, flow efficiency decreased. A graph illustrating the impact of skewness indicates that using the projected length is adequate for angles up to 30 degrees for small flow contractions.

Deck Roadway and abutments skew angle (0-45 deg):

☒ Skew Upstream XS the same amount as the deck
☒ Skew Downstream XS the same amount as the deck

Pier skew angle (0-45 deg):

Deck/Roadway Data Editor

Distance	Width	Weir Coef
2.886	5.774	2.6

Clear Del Row Ins Row Copy US to DS

Upstream			Downstream		
Station	high chord	low chord	Station	high chord	low chord
1 0.	26.	13.48	0.	26.	13.48
2 44.557	26.	13.48	44.557	26.	13.48
3 44.557	26.	18.5	44.557	26.	18.5
4 82.123	26.	18.5	82.123	26.	18.5
5 82.123	26.	13.48	82.123	26.	13.48
6 126.68	26.	13.48	126.68	26.	13.48
7					

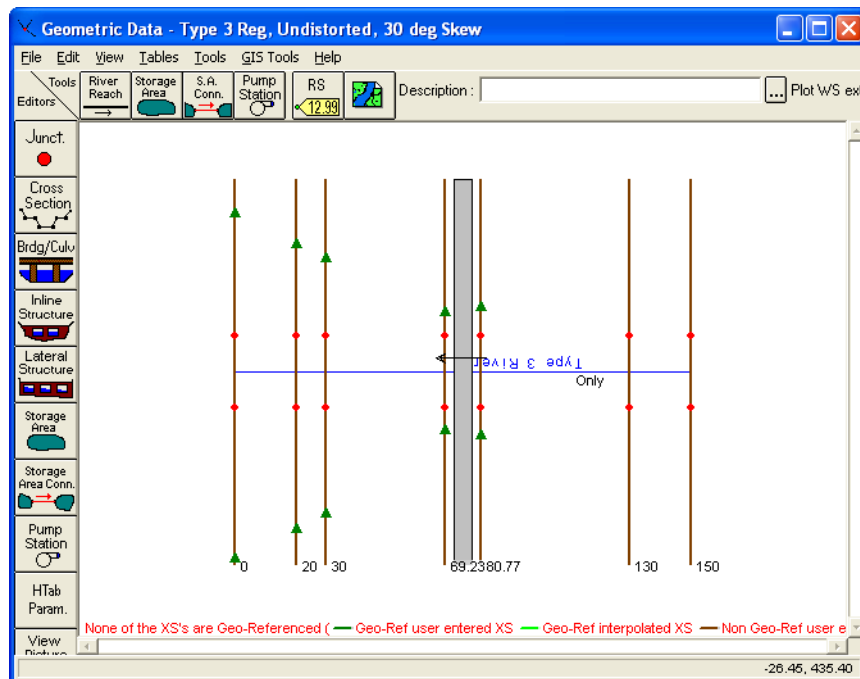
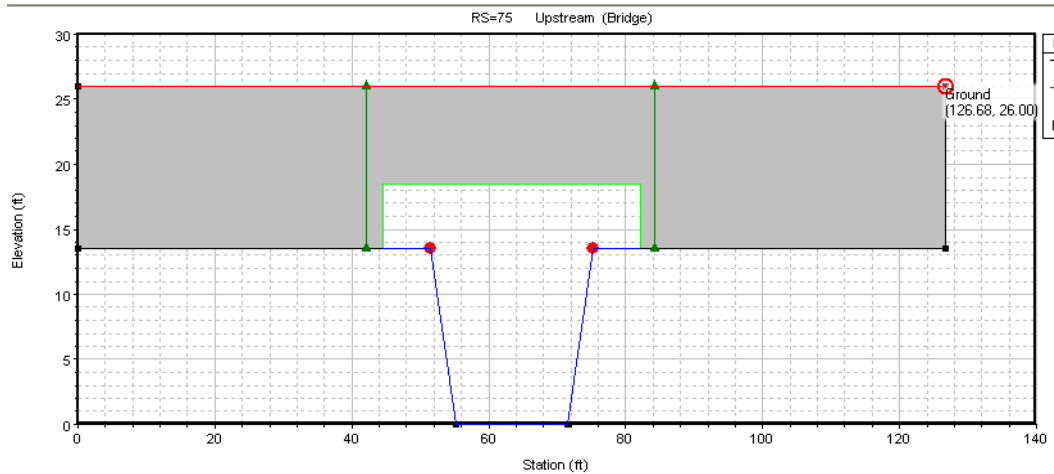


Figure 6.5: Screen Captures for Regular Undistorted Type 3 HR Model with 30° Bridge Skew

The reach lengths for the overbanks should not be equal to the main channel reach length in the reaches downstream and upstream from RS 69.23 and RS 80.77, respectively. The centerline distance from RS 69.23 to RS 30 is 39.23 feet. The LOB and ROB reach lengths will be 17.53 feet and 60.93 feet respectively. The ineffective flow locations were not considered. These values were determined from Figure 6.6 as follows. Similar adjustments were made for the distance from RS 130 to RS 80.77.

$$\text{ROB} = 2.66 + 29.74\sin 30^\circ = 17.53'$$

$$\text{MC} = 2.66 + 73.14\sin 30^\circ = 39.23'$$

$$\text{LOB} = 2.66 + 116.54\sin 30^\circ = 60.93'$$

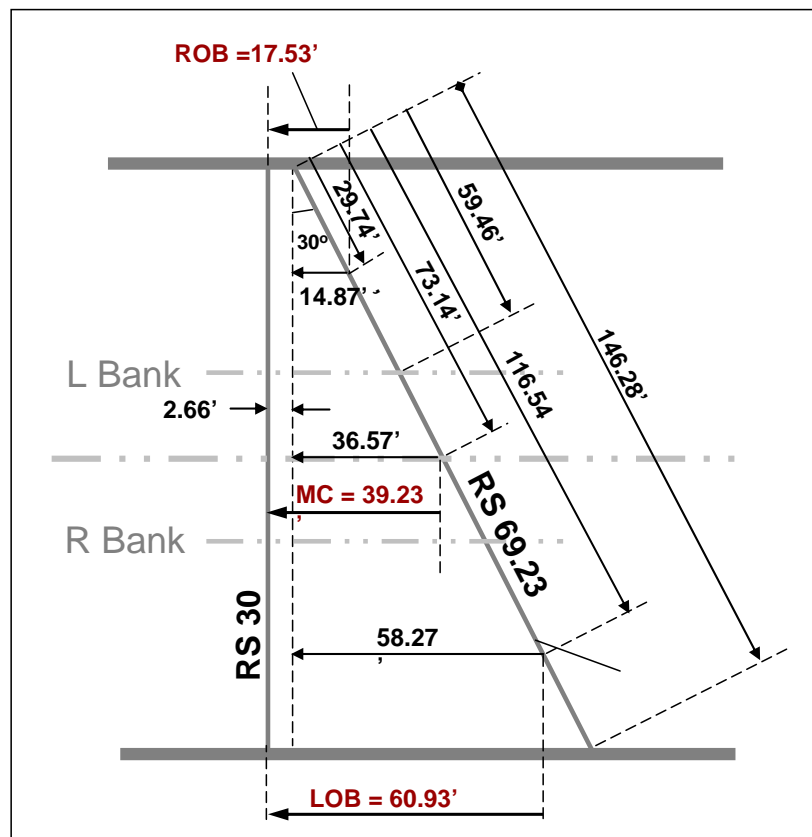





Figure 6.6: Plan View of RS 150 and RS 346.13 for Skewed Bridge

The reach length and contraction/expansion tables are shown in Table 6.2. Ineffective flow options were used at the 1:1 ratio upstream from the bridge and 4:1 downstream from the bridge. Actually, the ineffective flows were not applied upstream to RS 130.

Table 6.2: Reach Length and Contraction/Expansion Coefficient Tables for Type 3 Experiments

Edit Downstream Reach Lengths

River: Type 3 River    ☒ Edit Interpolated XS's

Reach: Only


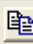

Selected Area Edit Options

Add Constant ... Multiply Factor ... Set Values ... Replace ...

	River Station	LOB	Channel	ROB
1	150	20	20	20
2	130	27.526	49.226	70.926
3	80.77	11.548	11.548	11.548
4	75	Bridge		
5	69.23	60.926	39.226	17.526
6	30	10	10	10
7	20	20	20	20
8	0	0	0	0

OK Cancel Help

Edit Contraction/Expansion Coefficients

River: Type 3 River    ☒ Edit Interpolated XS's

Reach: Only

Selected Area Edit Options

Add Constant ... Multiply Factor ... Set Values ... Replace ...

	River Station	Contraction	Expansion
1	150	0.1	0.3
2	130	0.3	0.5
3	80.77	0.3	0.5
4	75	Bridge	
5	69.23	0.3	0.5
6	30	0.1	0.3
7	20	0.1	0.3
8	0	0.1	0.3

OK Cancel Help

Table 6.3 shows the parameters for the laboratory experiments and the HEC-RAS models for Type 3 experiments.

Table 6.3: Parameter for Type 3 Experiments

Profile No.	Tailwater (RS 0) (ft)	Discharge		
		Laboratory Model (cfs)	Prototype Distorted (cfs)	Prototype Undistorted (cfs)
1	2	3	4	5
1	14.11	2.21	19800	3960
2	16.73	2.21	19800	3960
3	17.78	2.21	19800	3960
4	14.11	2.56	22900	4580
5	16.6	2.56	22900	4580
6	18.04	2.56	22900	4580
7	14.11	2.89	25900	5180
8	16.73	2.89	25900	5180
9	17.78	2.89	25900	5180

Table 6.4 shows the laboratory results given in prototype dimensions for the distorted model. For these studies the HEC-RAS model did not have cross sections corresponding to all the laboratory cross sections. Consequently, Table 6.5 was created to compare Laboratory and HEC-RAS model results for the cross section with corresponding locations. Table 6.6 shows the HEC-RAS results and Table 6.7 shows the differences (HR – Lab) between the values in Tables 6.5 and 6.6. Figures will be presented later together with the Modified HEC-RAS model results.

Table 6.4: Lab Results for Type 3 Experiments

River Station (ft) 1	Laboratory Results								
	Prof 1 (ft) 2	Prof 2 (ft) 3	Prof 3 (ft) 4	Prof 4 (ft) 5	Prof 5 (ft) 6	Prof 6 (ft) 7	Prof 7 (ft) 8	Prof 8 (ft) 9	Prof 9 (ft) 10
750	14.76	17.26	18.24	14.99	17.32	18.83	15.62	17.91	19.03
650	14.76	17.29	18.24	15.26	17.52	19.03	15.72	18.11	19.23
600	14.73	17.26	18.24	15.22	17.49	19.00	15.65	18.08	19.19
550	14.70	17.26	18.21	15.16	17.42	18.96	15.55	18.01	19.13
500	14.60	17.19	18.18	15.06	17.36	18.90	15.42	17.91	19.03
450	14.47	17.13	18.11	14.83	17.26	18.77	15.19	17.75	18.90
400	14.40	17.09	18.04	14.70	17.13	18.67	14.96	17.55	18.70
350	14.40	17.13	18.04	14.50	16.99	18.57	14.73	17.39	18.54
300	14.24	16.93	17.91	14.30	16.86	18.44	14.40	17.13	18.37
250	14.11	16.83	17.85	14.14	16.70	18.31	14.04	16.86	18.18
200	14.11	16.77	17.75	14.11	16.63	18.21	13.98	16.77	18.04
150	14.07	16.73	17.75	14.11	16.60	18.14	14.11	16.73	17.91
100	14.11	16.73	17.75	14.11	16.60	18.08	14.11	16.73	17.85
0	14.11	16.73	17.78	14.11	16.60	18.04	14.11	16.73	17.78

Table 6.5: Lab Results for Type 3 Experiments at HEC-RAS Undistorted Stations

Regular Distorted RS (ft) 1	Laboratory Results								
	Prof 1 (ft) 2	Prof 2 (ft) 3	Prof 3 (ft) 4	Prof 4 (ft) 5	Prof 5 (ft) 6	Prof 6 (ft) 7	Prof 7 (ft) 8	Prof 8 (ft) 9	Prof 9 (ft) 10
150	14.76	17.26	18.24	14.99	17.32	18.83	15.62	17.91	19.03
130	14.76	17.29	18.24	15.26	17.52	19.03	15.72	18.11	19.23
80.77	14.408	17.096	18.050	14.708	17.136	18.676	14.978	17.568	18.716
69.23	14.390	17.129	18.045	14.486	16.985	18.562	14.713	17.376	18.524
30	14.07	16.73	17.75	14.11	16.60	18.14	14.11	16.73	17.91
20	14.11	16.73	17.75	14.11	16.60	18.08	14.11	16.73	17.85
0	14.11	16.73	17.78	14.11	16.60	18.04	14.11	16.73	17.78

 Interpolated Values

 Suspect Points

Table 6.6: Regular Undistorted Type 3 HEC-RAS Results

Regular Undistorted RS (ft) 1	Low Q			Middle Q			High Q		
	Prof 1 (ft) 2	Prof 2 (ft) 3	Prof 3 (ft) 4	Prof 4 (ft) 5	Prof 5 (ft) 6	Prof 6 (ft) 7	Prof 7 (ft) 8	Prof 8 (ft) 9	Prof 9 (ft) 10
150	16.02	17.62	18.48	18.67	18.84	19.54	20.25	20.18	20.25
130	16	17.61	18.48	18.65	18.83	19.53	20.24	20.17	20.24
80.77	14.28	16.54	17.6	15.87	16.39	17.74	17.63	17.44	17.62
69.23	14.2	16.4	17.47	14.31	15.84	17.4	15.1	15.48	16.76
30	14.15	16.61	17.69	14.25	16.3	17.85	15.81	16.23	17.47
20	14.14	16.66	17.72	14.19	16.42	17.93	15.81	16.44	17.6
0	14.11	16.73	17.78	14.11	16.6	18.04	15.8	16.73	17.78

Table 6.7: Differences (HEC-RAS - Lab) for Regular Undistorted Type 3 Model

Regular Undistorted RS (ft) 1	Low Q			Middle Q			High Q		
	Prof 1 (ft) 2	Prof 2 (ft) 3	Prof 3 (ft) 4	Prof 4 (ft) 5	Prof 5 (ft) 6	Prof 6 (ft) 7	Prof 7 (ft) 8	Prof 8 (ft) 9	Prof 9 (ft) 10
150	1.26	0.36	0.24	3.68	1.52	0.71	4.63	2.27	1.22
130	1.24	0.32	0.24	3.39	1.31	0.50	4.52	2.06	1.01
80.77	-0.13	-0.56	-0.45	1.16	-0.75	-0.94	2.65	-0.13	-1.10
69.23	-0.19	-0.73	-0.57	-0.18	-1.14	-1.16	0.39	-1.90	-1.76
30	0.08	-0.12	-0.06	0.14	-0.30	-0.29	1.70	-0.50	-0.44
20	0.03	-0.07	-0.03	0.08	-0.18	-0.15	1.70	-0.29	-0.25
0	0.00	0.00	0.00	0.00	0.00	0.00	1.69	0.00	0.00

 Suspect Points

6.2 Modified Distorted Type 3 HEC-RAS Models

A description of Gary Brunner's Modified Type 3 HEC-RAS model is given below as conveyed to us via e-mail.

Type 3 Model:

1. I interpolated some cross sections upstream of the bridge, and placed ineffective flow areas in a similar manner as what I did in the type 1 models.
2. You were assuming a 4:1 expansion ratio downstream of the bridge. This is causing most of the problems. First off, I think 4:1 is way too high. I think it should be 2:1 or even less. When you use the 4:1 assumption, this requires ineffective flow areas blocking out most of the overbank area in the downstream most cross section. So when you put in a starting water surface equivalent to what you measured, RAS gets an extremely high starting energy. In fact, it is so high, that if you placed that energy in the upstream cross section, normal depth would already results in a water surface higher than your measured values. This tells me that the ineffective flow areas in the downstream boundary cross section are

wrong. I got rid of them completely, which is like assuming a 1.5:1 flow expansion and the results dramatically improved for the 30 degree skewed models. This was the main problem with these models.

3. I also changed the contraction coefficients to 0.1 from 0.3 for the entire model. This is very debatable, as to whether or not it is appropriate. But I do note that on previous research work we conducted on bridge hydraulics with observed data, the calibrated contraction coefficients always came out lower than what was expected.
4. I have a major concern about the measure results at the upstream end of the flume (station 750). All of the graphs for the type 3 runs show the water surface dipping down in the upstream direction over the last two cross sections. This tells me that there is some influence on the water surface due to the close proximity to the flow control at the upstream weir. So I think the measured results at station 750 (distorted, 150 undistorted), are not correct. Without any upstream influence, why would these water surfaces go down in the upstream direction? It does not make sense to me. **(Parr: I agree that something is amiss with the upstream piezometer. As a result, I modified your model by adding a cross section at RS 650distorted and RS 130 undistorted.)**

The undistorted model includes two interpolated cross sections between RS 80.77 and RS 130. (The model GWB worked with did not have RS 130 thus his interpolated cross sections were between RS 80.77 and RS 150. Since the piezometer reading was suspect at RS 150, an additional cross section was added at RS 130.) The

results for the Modified model are presented in Tables 6.9, 6.10 and 6.11. Table 6.9 shows the Modified Undistorted Type 3 HEC-RAS model results. Table 6.10 gives the laboratory measurement and interpolated values at the HEC-RAS stations. The differences (HR – Lab) between the Modified HEC-RAS results and the laboratory values are presented in Table 6.11.

The profile plots for the Regular and Modified Undistorted Type 3 HEC-RAS models are plotted together with the laboratory in Figures 6.7, 6.8 and 6.9 for the low, middle and high flows, respectively. The Modified model is clearly in better agreement with the laboratory data than the Regular model for all discharges. In fact, for the lower discharge shown in Figure 6.7, the Modified HEC-RAS model was in very good agreement with the laboratory data. The middle and high flow runs shows that the profiles upstream from the bridge were clearly influenced by the tailwater elevations. The HEC-RAS models showed a weak dependence on the tailwater condition for the middle flow and no dependence for the high flow. This indicates that the bridge hydraulics in HEC-RAS approaches inlet control-type conditions before the laboratory data as the discharge is increased.

Table 6.8: Modified Undistorted Type 3 HEC-RAS Results

Modified Undistorted RS (ft) 1	Low Q			Middle Q			High Q		
	Prof 1 (ft) 2	Prof 2 (ft) 3	Prof 3 (ft) 4	Prof 4 (ft) 5	Prof 5 (ft) 6	Prof 6 (ft) 7	Prof 7 (ft) 8	Prof 8 (ft) 9	Prof 9 (ft) 10
150	15.57	17.3	18.21	17.88	18.15	18.99	19.39	19.39	19.47
130	15.53	17.29	18.21	17.86	18.13	18.98	19.38	19.38	19.46
113.591	15.43	17.26	18.18	17.81	18.08	18.94	19.33	19.33	19.41
97.1826	15.15	17.16	18.11	17.61	17.91	18.81	19.16	19.16	19.25
80.77	14.24	16.38	17.46	14.99	15.85	17.39	16.68	16.68	16.91
69.2	14.17	16.28	17.36	14.29	15.45	17.12	14.92	14.92	16.17
0	14.11	16.73	17.78	14.11	16.6	18.04	15.8	16.73	17.78

Table 6.9: Lab Results for Type 3 Experiments at HEC-RAS Undistorted Stations

Modified Distorted RS (ft) 1	Low Q			Middle Q			High Q		
	Prof 1 (ft) 2	Prof 2 (ft) 3	Prof 3 (ft) 4	Prof 4 (ft) 5	Prof 5 (ft) 6	Prof 6 (ft) 7	Prof 7 (ft) 8	Prof 8 (ft) 9	Prof 9 (ft) 10
150	14.76	17.26	18.24	14.99	17.32	18.83	15.62	17.91	19.03
130	14.76	17.29	18.24	15.26	17.52	19.03	15.72	18.11	19.23
113.591	14.712	17.257	18.220	15.181	17.445	18.975	15.587	18.035	19.151
97.1826	14.563	17.173	18.157	14.994	17.328	18.861	15.355	17.867	18.992
80.77	14.408	17.096	18.050	14.708	17.136	18.676	14.978	17.568	18.716
69.2	14.390	17.111	18.034	14.486	16.985	18.559	14.706	17.368	18.524
0	14.11	16.73	17.78	14.11	16.60	18.04	14.11	16.73	17.78

 Interpolated Values

 Suspect Points

Table 6.10: Differences (HEC-RAS - Lab) for Modified Undistorted Type 3 Model

Modified Undistorted RS (ft) 1	Low Q			Middle Q			High Q		
	Prof 1 (ft) 2	Prof 2 (ft) 3	Prof 3 (ft) 4	Prof 4 (ft) 5	Prof 5 (ft) 6	Prof 6 (ft) 7	Prof 7 (ft) 8	Prof 8 (ft) 9	Prof 9 (ft) 10
150	0.81	0.04	-0.03	2.89	0.83	0.16	3.77	1.48	0.44
130	0.77	0.00	-0.03	2.60	0.61	-0.05	3.66	1.27	0.23
113.591	0.72	0.00	-0.04	2.63	0.64	-0.04	3.74	1.29	0.26
97.1826	0.59	-0.01	-0.05	2.62	0.58	-0.05	3.80	1.29	0.26
80.77	-0.17	-0.72	-0.59	0.28	-1.29	-1.29	1.70	-0.89	-1.81
69.2	-0.22	-0.83	-0.67	-0.20	-1.53	-1.44	0.21	-2.45	-2.35
0	0.00	0.00	0.00	0.00	0.00	0.00	1.69	0.00	0.00

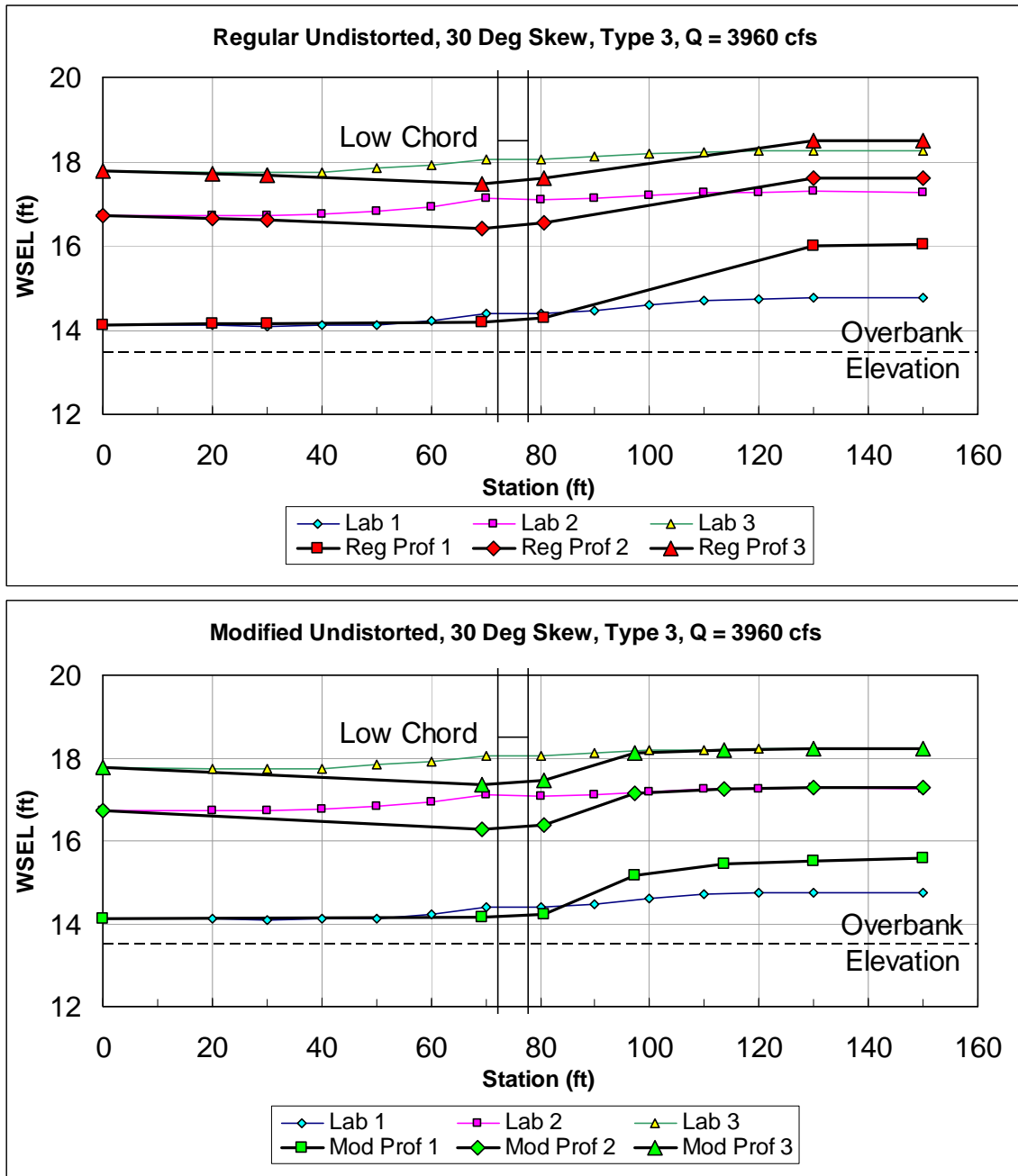


Figure 6.7: Lab and HEC-RAS Undistorted Results for Type 3 Experiments - Low Flow

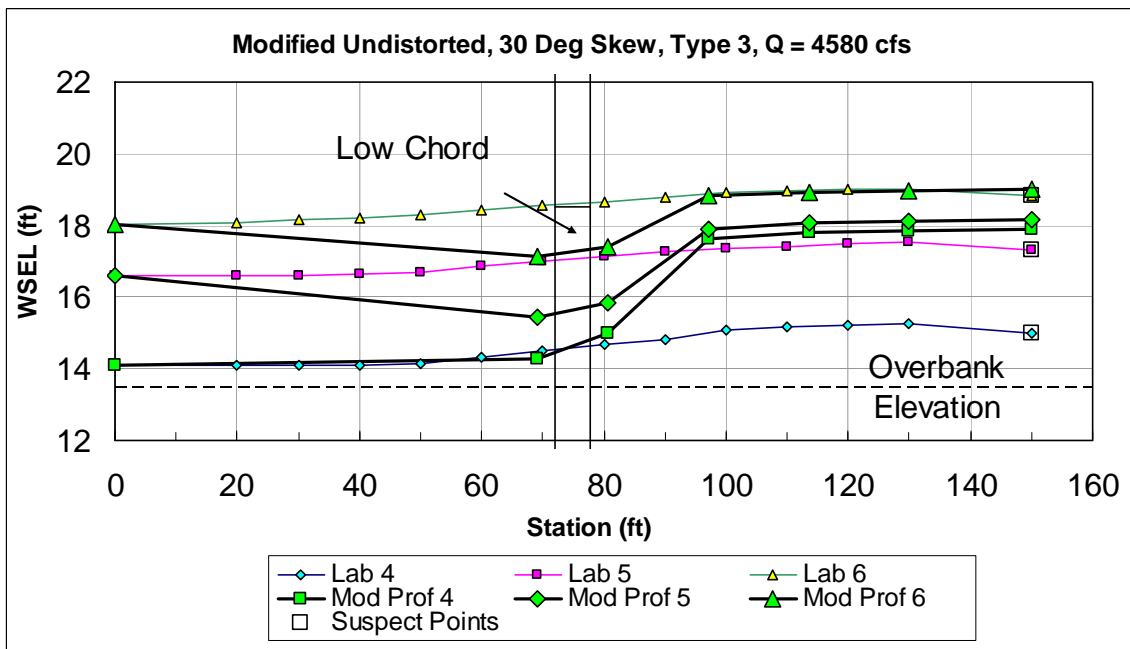
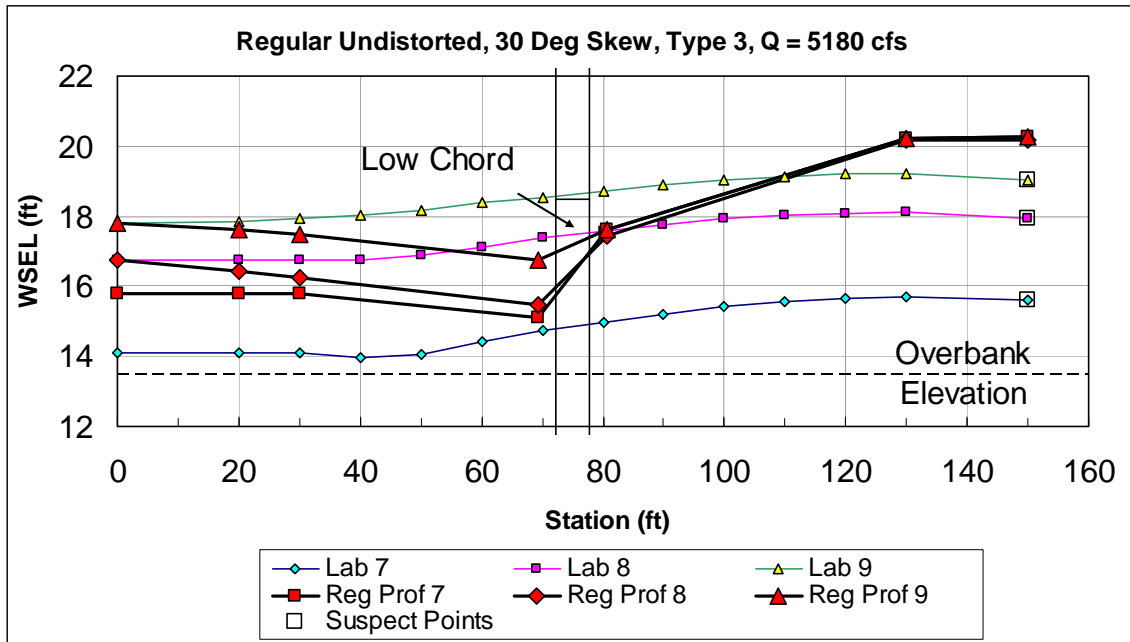


Figure 6.8: Lab and HEC-RAS Undistorted Results for Type 3 Experiments - Middle Flow

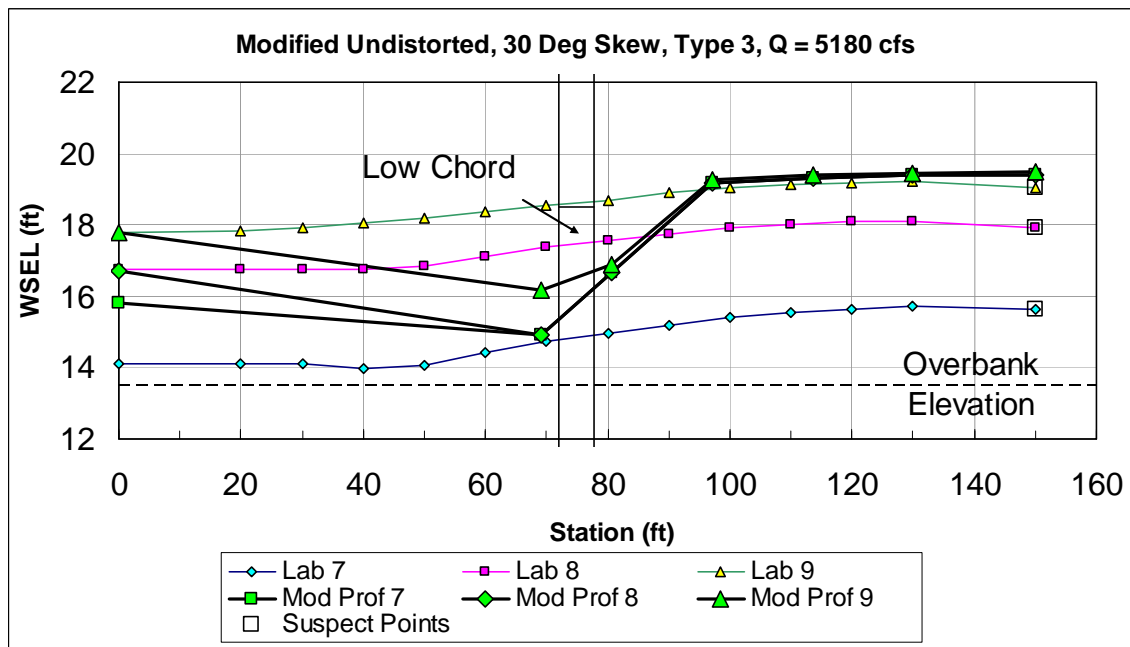
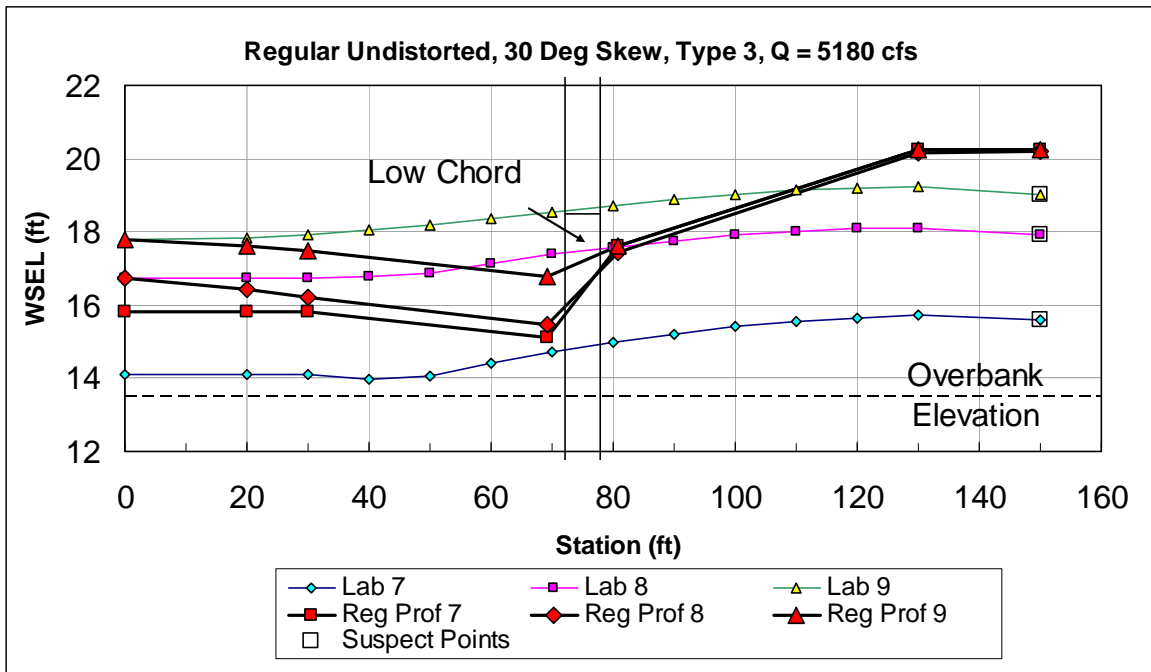


Figure 6.9: Lab and HEC-RAS Undistorted Results for Type 3 Experiments - High Flow

The flow in the laboratory appeared to align to the skewed opening well upstream from the bridge and pass nearly perpendicularly through the bridge opening. The Regular model was modified by selecting 0 degree skew for the bridge (and the bounding cross sections). This is called the Regular No Skew Undistorted Type 3 HEC-RAS model. Figures 6.10, 6.11 and 6.12 compare the results of this model with the Modified model and with the laboratory results. They produce very similar results. The problem with the no skew option is that while the flow in the overbank portions of the bridge opening and the main channel portion above the bank elevations can flow perpendicular to the bridge, the main channel portion below the bank elevations can't since it is constrained by the main channel banks. Nonetheless, the results appear much improved over the Regular model with the 30 degree skew option selected. The crossing of profiles 4 and 5 in Figure 6.11 occurs for the Regular no skew model but not for the Modified model. Overall, the Modified model still appears to be the best one of those models tested.

(No Skew for Regular and 30 Deg Skew for Modified) - Low Flow

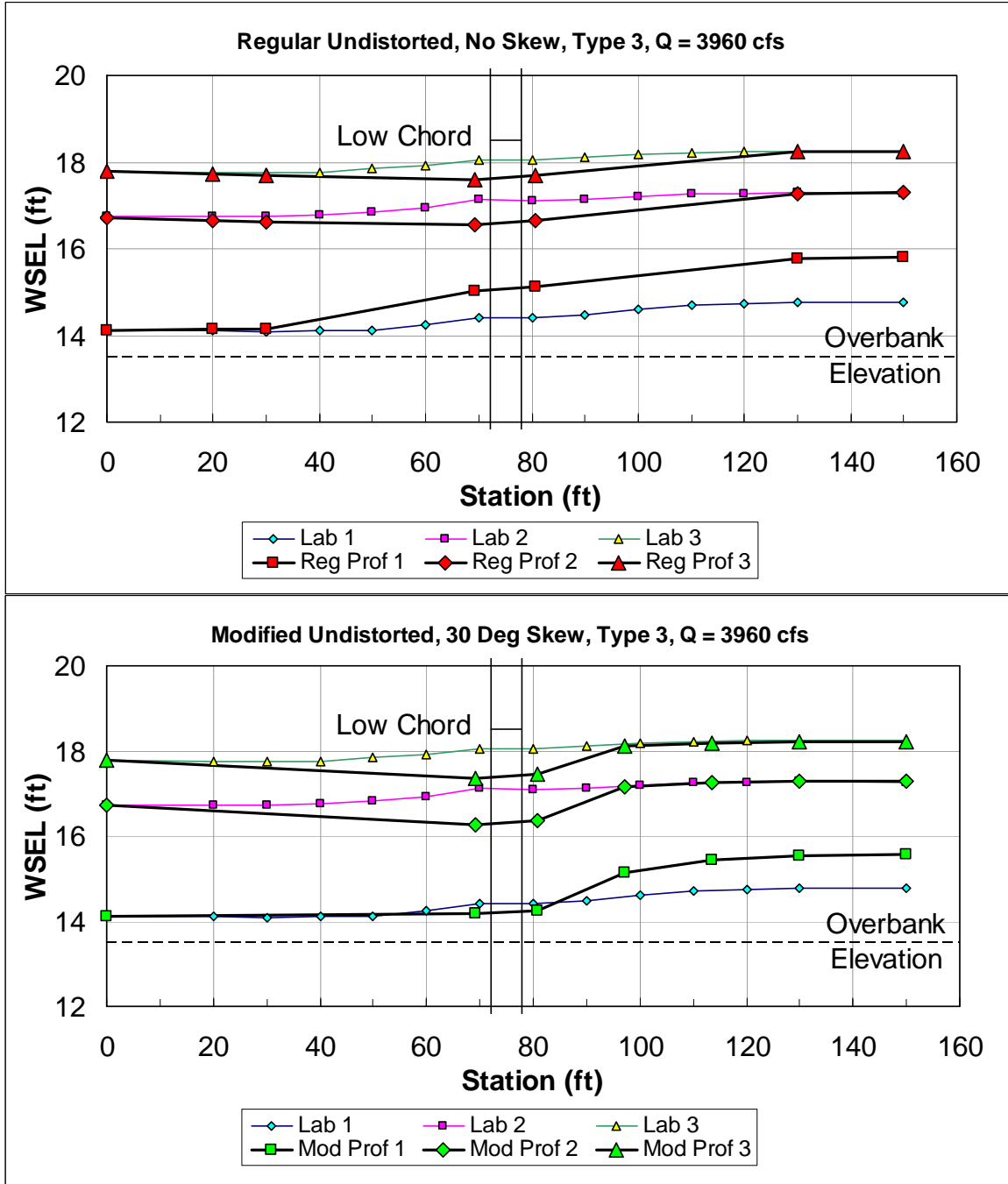


Figure 6.10: Lab and HEC-RAS Undistorted Results for Type 3 Experiments (No Skew for Regular and 30 Deg Skew for Modified) - Low Flow

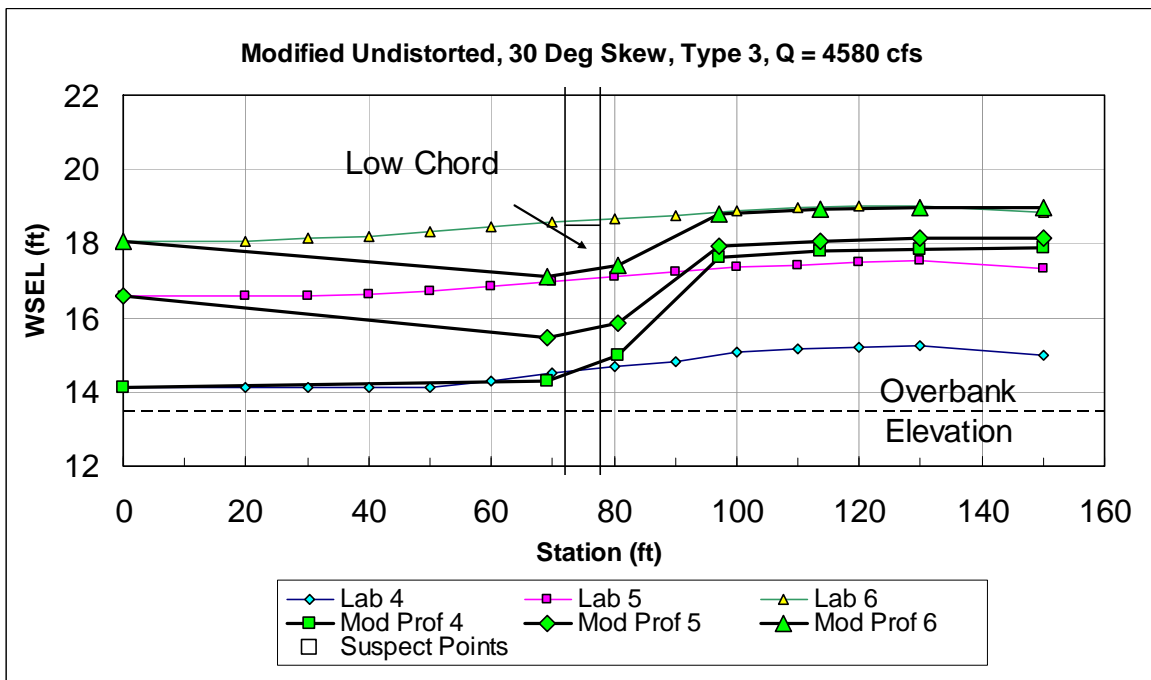
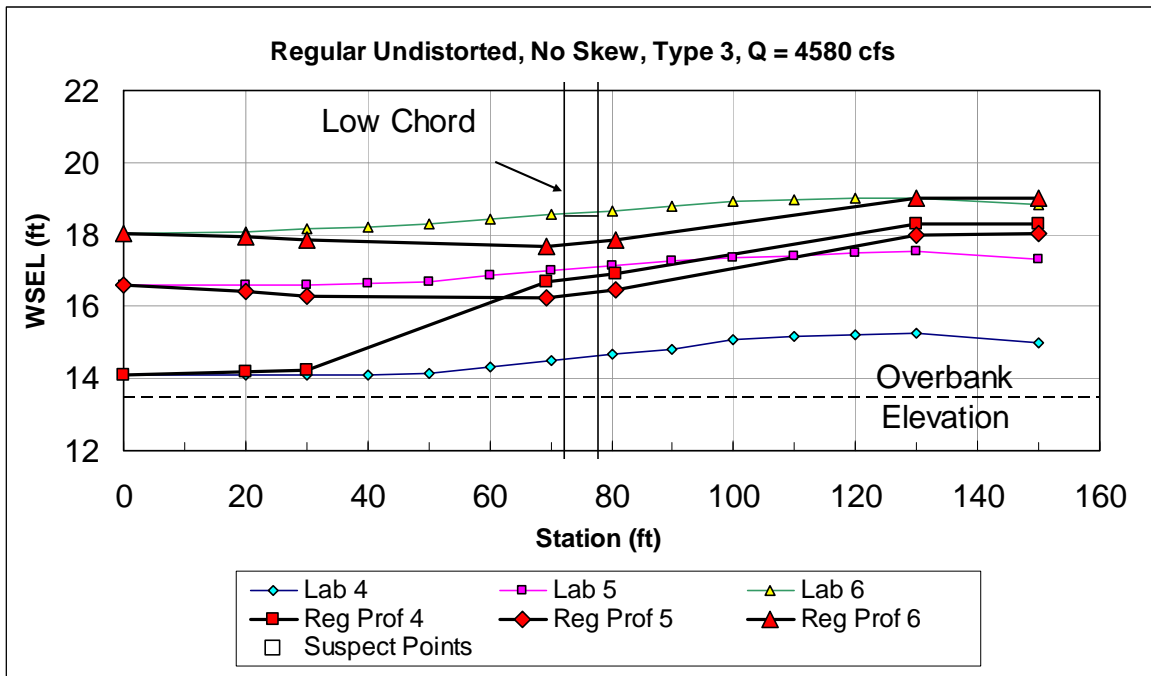


Figure 6.11: Lab and HEC-RAS Undistorted Results for Type 3 Experiments (No Skew for Regular and 30 Deg Skew for Modified) - Middle Flow

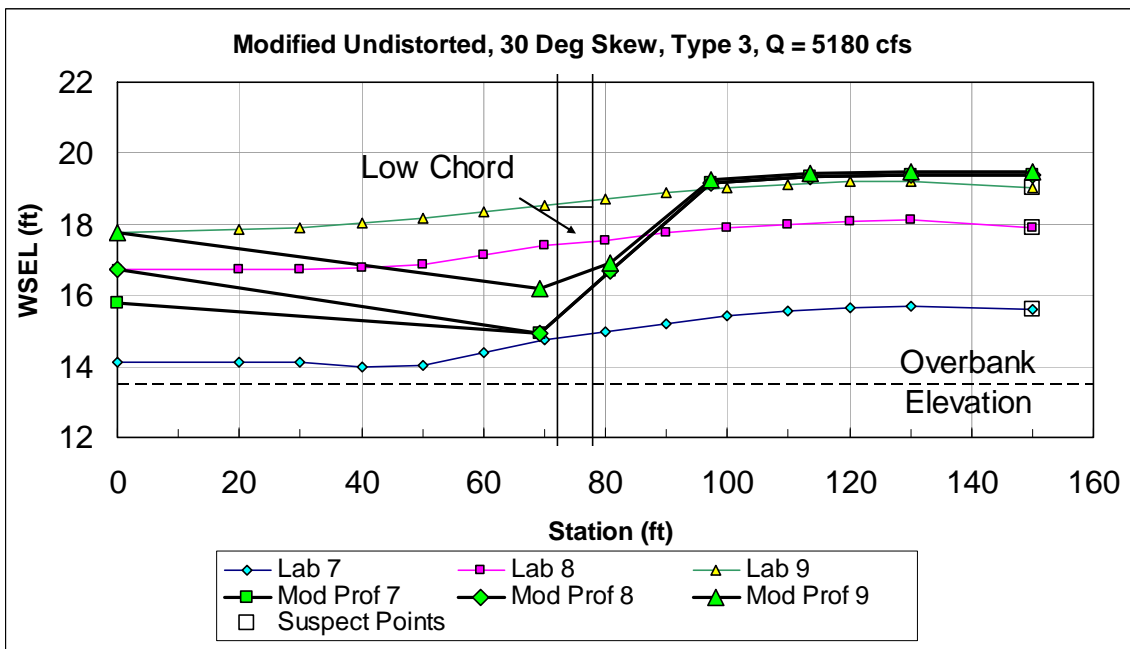
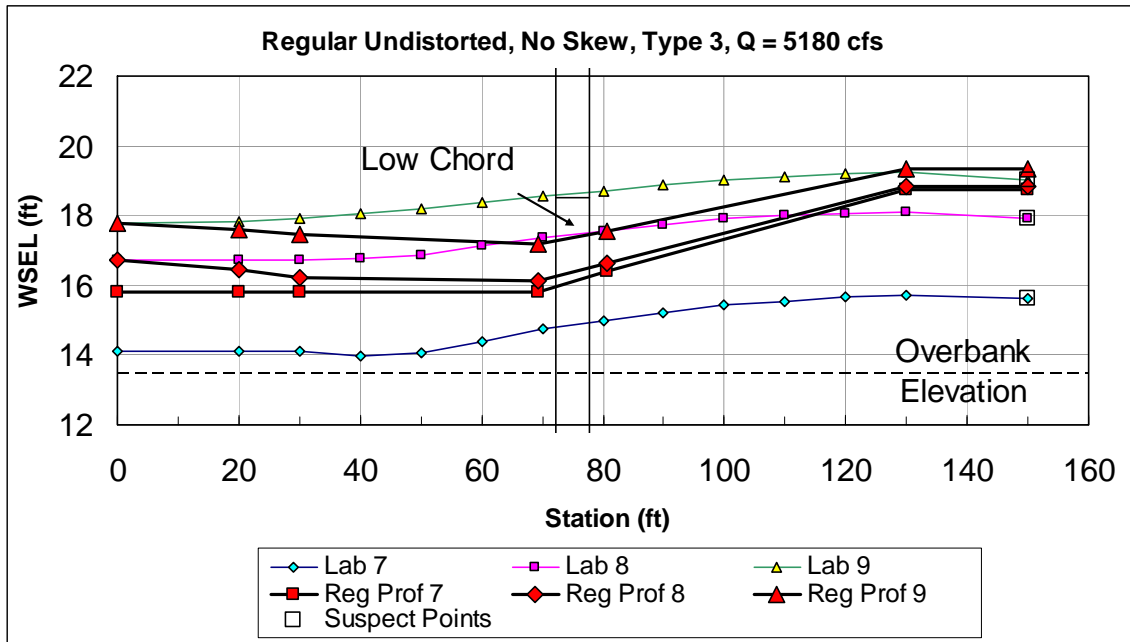


Figure 6.12: Lab and HEC-RAS Undistorted Results for Type 3 Experiments (No Skew for Regular and 30 Deg Skew for Modified) - High Flow

6.3 Distorted Type 3 HEC-RAS Models

The prototype distorted models with $X_r = 100$ and $Y_r = 20$ were created from the prototype undistorted models with $L_r = X_r = Y_r = 20$ by the steps presented in Chapter 4, Section C. Tables 6.11 and 6.12 show the computed water surface elevations for the Regular and Modified distorted and undistorted HEC-RAS models with 30 degree skew, respectively. The agreement is very good for all cross sections. The discrepancies for the distorted model may be due to differences in the Froude number and velocities. Table 6.13 shows the parameters for the Undistorted and Distorted Modified Type 3 HEC-RAS models obtained from the Profile Output tables. Nearly all the parameters are equal for the undistorted and distorted models.

Table 6.11: Results for Modified Undistorted and Distorted Type 3 HEC-RAS Models

Regular Undisorted Type 3 HEC-RAS Model									
Undisorted RS (ft)	Water Surface Elevation (ft) - Undisorted								
	Low Q			Mid Q			High Q		
	PF 1	PF 2	PF 3	PF 4	PF 5	PF 6	PF 7	PF 8	PF 9
150	16.02	17.62	18.48	18.67	18.84	19.54	20.25	20.18	20.25
130	16	17.61	18.48	18.65	18.83	19.53	20.24	20.17	20.24
80.77	14.28	16.54	17.6	15.87	16.39	17.74	17.63	17.44	17.62
69.23	14.2	16.4	17.47	14.31	15.84	17.4	15.1	15.48	16.76
30	14.15	16.61	17.69	14.25	16.3	17.85	15.81	16.23	17.47
20	14.14	16.66	17.72	14.19	16.42	17.93	15.81	16.44	17.6
0	14.11	16.73	17.78	14.11	16.6	18.04	15.8	16.73	17.78

Regular Disorted Type 3 HEC-RAS Model									
Distorted RS (ft)	Water Surface Elevation (ft) - Distorted								
	Low Q			Mid Q			High Q		
	PF 1	PF 2	PF 3	PF 4	PF 5	PF 6	PF 7	PF 8	PF 9
750	15.99	17.62	18.48	18.66	18.84	19.54	20.25	20.18	20.25
650	15.97	17.61	18.47	18.65	18.82	19.53	20.24	20.17	20.24
403.87	14.28	16.54	17.6	15.86	16.39	17.74	17.63	17.44	17.62
346.13	14.2	16.4	17.47	14.31	15.84	17.4	15.1	15.48	16.76
150	14.15	16.61	17.69	14.25	16.3	17.85	15.81	16.23	17.47
100	14.13	16.66	17.72	14.19	16.42	17.93	15.81	16.44	17.6
0	14.11	16.73	17.78	14.11	16.6	18.04	15.8	16.73	17.78

Difference between Regular HEC-RAS Undisorted and Distorted Type 3 HEC-RAS Models										
Distorted RS (ft)	Undisorted RS (ft)	Undisorted - Distorted (ft)								
		Low Q			Mid Q			High Q		
		PF 1	PF 2	PF 3	PF 4	PF 5	PF 6	PF 7	PF 8	PF 9
750	150	0.03	0	0	0.01	0	0	0	0	0
650	130	0.03	0	0.01	0	0.01	0	0	0	0
403.87	80.774	0	0	0	0.01	0	0	0	0	0
346.13	69.22601	0	0	0	0	0	0	0	0	0
150	30	0	0	0	0	0	0	0	0	0
100	20	0.01	0	0	0	0	0	0	0	0
0	0	0	0	0	0	0	0	0	0	0

Table 6.12: Results for Undistorted and Distorted Modified GWB Type 2 HEC-RAS Models

Modified Undisorted Type 3 HEC-RAS Model									
Undistorted RS (ft)	Water Surface Elevation (ft) - Undistorted								
	Low Q			Mid Q			High Q		
	PF 1	PF 2	PF 3	PF 4	PF 5	PF 6	PF 7	PF 8	PF 9
150	15.57	17.3	18.21	17.88	18.15	18.99	19.39	19.39	19.47
130	15.53	17.29	18.21	17.86	18.13	18.98	19.38	19.38	19.46
113.591*	15.43	17.26	18.18	17.81	18.08	18.94	19.33	19.33	19.41
97.1826*	15.15	17.16	18.11	17.61	17.91	18.81	19.16	19.16	19.25
80.77	14.24	16.38	17.46	14.99	15.85	17.39	16.68	16.68	16.91
69.2	14.17	16.28	17.36	14.29	15.45	17.12	14.92	14.92	16.17
0	14.11	16.73	17.78	14.11	16.6	18.04	15.8	16.73	17.78

Modified Disorted Type 3 HEC-RAS Model									
Distorted RS (ft)	Water Surface Elevation (ft) - Distorted								
	Low Q			Mid Q			High Q		
	PF 1	PF 2	PF 3	PF 4	PF 5	PF 6	PF 7	PF 8	PF 9
750	15.53	17.3	18.21	17.87	18.14	18.98	19.39	19.39	19.47
650	15.49	17.29	18.21	17.85	18.13	18.97	19.38	19.38	19.46
567.956*	15.42	17.26	18.18	17.8	18.08	18.94	19.33	19.33	19.41
485.913*	15.15	17.16	18.11	17.6	17.91	18.81	19.16	19.16	19.25
403.87	14.24	16.38	17.46	14.98	15.85	17.38	16.68	16.68	16.91
346.13	14.17	16.28	17.36	14.28	15.45	17.12	14.91	14.91	16.17
0	14.11	16.73	17.78	14.11	16.6	18.04	15.8	16.73	17.78

Difference between Modified HEC-RAS Undistorted and Distorted Type 3 HEC-RAS Models										
Distorted RS (ft)	Undistorted RS (ft)	Undistorted - Distorted (ft)								
		Low Q			Mid Q			High Q		
		PF 1	PF 2	PF 3	PF 4	PF 5	PF 6	PF 7	PF 8	PF 9
750	150	0.04	0	0	0.01	0.01	0.01	0	0	0
650	130	0.04	0	0	0.01	0	0.01	0	0	0
403.87	80.774	0.01	0	0	0.01	0	0	0	0	0
346.13	69.22601	0	0	0	0.01	0	0	0	0	0
150	30	0	0	0	0.01	0	0.01	0	0	0
100	20	0	0	0	0.01	0	0	0.01	0.01	0
0	0	0	0	0	0	0	0	0	0	0

**Table 6.13: HEC-RAS Parameters for Undistorted and Distorted Modified GWB
Type 3 HEC-RAS Models (No Interpolated Xsecs)**

River Sta Und	River Sta Dist	Profile	W.S. Elev Und - Dist (ft)	Crit W.S. Und - Dist (ft)	Vel Total Und/Dist (ft/s)	Hydr Depth Und/Dist (ft)	Fr # XS Und/Dist	Fr # XS Und	Fr # XS Dist
1	2	3	4	5	6	7	8	9	10
150	750	1	0.04	0	0.99	1.01	0.98	0.52	0.53
150	750	2	0	0	1.00	1.00	1.00	0.31	0.31
150	750	3	0	0	1.00	1.00	1.00	0.25	0.25
150	750	4	0.01	0	1.00	1.00	1.00	0.38	0.38
150	750	5	0.01	0	1.00	1.00	1.00	0.36	0.36
150	750	6	0.01	0	1.00	1.00	1.00	0.3	0.30
150	750	7	0	0	1.00	1.00	1.00	0.32	0.32
150	750	8	0	0	1.00	1.00	1.00	0.32	0.32
150	750	9	0	0	1.00	1.00	1.00	0.32	0.32
130	650	1	0.04	0	0.99	1.01	0.98	0.53	0.54
130	650	2	0	0	1.00	1.00	1.00	0.31	0.31
130	650	3	0	0	1.00	1.00	1.00	0.25	0.25
130	650	4	0.01	0	1.00	1.00	1.00	0.38	0.38
130	650	5	0	0	1.00	1.00	1.00	0.36	0.36
130	650	6	0.01	0	1.00	1.00	1.00	0.3	0.30
130	650	7	0	0	1.00	1.00	1.00	0.33	0.33
130	650	8	0	0	1.00	1.00	1.00	0.33	0.33
130	650	9	0	0	1.00	1.00	1.00	0.32	0.32
80.77	403.87	1	0	0.01	1.00	1.00	1.00	0.71	0.71
80.77	403.87	2	0	0.01	1.00	1.00	1.00	0.48	0.48
80.77	403.87	3	0	0.01	1.00	1.00	1.00	0.41	0.41
80.77	403.87	4	0.01	0	1.00	1.00	1.00	0.85	0.85
80.77	403.87	5	0	0	1.00	1.00	1.00	0.73	0.73
80.77	403.87	6	0.01	0	1.00	1.00	1.00	0.57	0.57
80.77	403.87	7	0	0	1.00	1.00	1.00	0.75	0.75
80.77	403.87	8	0	0	1.00	1.00	1.00	0.75	0.75
80.77	403.87	9	0	0	1.00	1.00	1.00	0.72	0.72
75	375	Bridge							
69.2	346.13	1	0	0	1.00	1.00	1.00	0.7	0.70
69.2	346.13	2	0	0	1.00	1.00	1.00	0.49	0.49
69.2	346.13	3	0	0	1.00	1.00	1.00	0.42	0.42
69.2	346.13	4	0.01	0	1.00	1.00	1.00	0.95	0.95
69.2	346.13	5	0	0	1.00	1.00	1.00	0.77	0.77
69.2	346.13	6	0	0	1.00	1.00	1.00	0.6	0.60
69.2	346.13	7	0.01	0.01	1.00	1.00	1.00	0.99	0.99
69.2	346.13	8	0.01	0.01	1.00	1.00	1.00	0.99	0.99
69.2	346.13	9	0	0.01	1.00	1.00	1.00	0.81	0.81
0	0	1	0	0	1.00	1.00	1.00	0.97	0.97
0	0	2	0	0	1.00	1.00	1.00	0.38	0.38
0	0	3	0	0	1.00	1.00	1.00	0.29	0.29
0	0	4	0	0	1.00	1.00	1.00	1.35	1.35
0	0	5	0	0	1.00	1.00	1.00	0.55	0.55
0	0	6	0	0	1.00	1.00	1.00	0.39	0.39
0	0	7	0	0	1.00	1.00	1.00	0.81	0.81
0	0	8	0	0	1.00	1.00	1.00	0.62	0.62
0	0	9	0	0	1.00	1.00	1.00	0.48	0.48

CHAPTER 7 - SUMMARY AND CONCLUSIONS

This study investigated bridge hydraulics for floodplain channels. Laboratory and HEC-RAS modeling were performed for the following bridge scenarios for a range of discharge and tailwater conditions.

- Type 1 - General Bridge Modeling.
- Type 2 - Combination Bridge/Weir Flow.
- Type 3 - Skewed Bridge.

Three different discharges were tested for each of the experiment types. The tailwater elevation was also set at three different values for each discharge. Thus, a total of 27 laboratory tests conditions were studied.

HEC-RAS models were created to simulate the flume data at prototype scales for the assumptions that the laboratory model was (a) undistorted and (b) distorted. Froude number similarity was used to provide “prototype” geometry and discharge. The undistorted HEC-RAS models were based on the assumption of a constant 20:1 model ratio. This means that all geometric dimensions in the model were assumed to be 1/20-th of the prototype dimensions. The distorted modeling was based on the assumption of horizontal and vertical modeling scales of 100:1 (X_r) and 20:1 (X_r), respectively. Thus the vertical and horizontal model dimensions were assumed to be 1/20-th and 1/100-th, respectively, of the prototype dimensions.

Regular HEC-RAS models were created using standard modeling procedures. Modified HEC-RAS models were created using more advanced modeling procedures provided by Gary Brunner of the HEC. Essentially the modified models were created by

him and slightly modified by us by adding adjusted n -values. His models significantly improved the agreement between the laboratory data and HEC-RAS for Types 2 and 3.

The headwater for the Type 1 Regular and Modified HEC-RAS models agreed very well with the laboratory experiments for the low discharge experiments. For the middle and high discharge conditions the HEC-RAS results tended to collapse to a single profile upstream from the bridge implying that that HEC-RAS considered the bridge to be under inlet control with critical flow through the bridge. The headwater for the middle and high flow laboratory experiments distinctly showed the effect of the tailwater. Granted, the middle and high discharge conditions were for relatively high Froude numbers at the bounding cross sections just upstream and downstream from the bridge. There was not much difference between the Regular and Modified Type 1 HEC-RAS models. Table 7.1 shows the Froude numbers for the upstream and downstream bounding cross sections. A check mark designates good agreement between lab and the Modified HEC-RAS models. High Froude numbers exist at the downstream bounding cross sections at the profiles that do not match the laboratory data.

Table 7.1 Portion of Table 4.11 for Type 1 Experiments

Type 1 Modified					
River Sta Undistorted	River Sta Distorted	Profile	Fr # XS Undistorted	Fr # XS Distorted	Match with Lab
1	2	3	9	10	
85.6	428	1	0.36	0.37	x
85.6	428	2	0.41	0.41	x
85.6	428	3	0.51	0.51	x
85.6	428	4	0.53	0.52	x
85.6	428	5	0.52	0.51	
85.6	428	6	0.52	0.51	
85.6	428	7	0.49	0.51	x
85.6	428	8	0.52	0.52	x
85.6	428	9	0.52	0.51	
75	375	Bridge			
64.4	322	1	0.4	0.40	x
64.4	322	2	0.45	0.45	x
64.4	322	3	0.59	0.59	x
64.4	322	4	0.65	0.65	x
64.4	322	5	0.81	0.81	
64.4	322	6	0.93	0.93	
64.4	322	7	0.63	0.63	x
64.4	322	8	0.69	0.69	x
64.4	322	9	0.97	0.97	

x Good match with lab data

The Modified HEC-RAS Type 2 models were much better than the Regular HEC-RAS Type 2 models for all flows (See Figures 5.8, 5.9 and 5.10). The Modified model profiles upstream from the bridge again collapsed to a single curve for each discharge, implying inlet control at the bridge. The laboratory experiments again showed tailwater effects for all discharges. The agreement between the laboratory headwater and the Modified model headwater was good for the low and middle flows but about 2-feet higher for the high flow. Mr. Brunner's use of multiple block ineffective flow areas in lieu of the regular ineffective flow areas was effective. This procedure should be considered at bridge locations where significant road overtopping occurs in the overbank areas.

The Regular models were significantly improved by changing the Pressure and/or Weir Submerged Inlet coefficient C_d to 0.5 as Mr. Brunner did for the Modified models. (Figures 5.11, 5.12 and 5.13). They still were not as good as his Modified models. Table 7.2 below shows high Froude numbers at the downstream bounding cross section for all profiles where there was not a good match with the laboratory data.

Table 7.2 Portion of Table 5.11 for Type 2 Experiments

Type 2 Modified					
Undistorted River Sta	Distorted River Sta	Profile	Undistorted Fr # XS	Distorted Fr # XS	Match with Lab
1	2	3	9	10	
80	400	1	0.28	0.27	x
80	400	2	0.28	0.27	x
80	400	3	0.28	0.28	x
80	400	4	0.28	0.28	x
80	400	5	0.28	0.28	x
80	400	6	0.28	0.28	
80	400	7	0.13	0.13	
80	400	8	0.13	0.13	
80	400	9	0.13	0.13	
75	350	Bridge			
70	350	1	0.76	0.73	x
70	350	2	0.61	0.59	x
70	350	3	0.52	0.51	x
70	350	4	0.62	0.60	x
70	350	5	0.67	0.65	x
70	350	6	0.82	0.78	
70	350	7	0.91	0.89	
70	350	8	0.91	0.89	
70	350	9	0.91	0.89	

x Good match with lab data

The Regular and Modified HEC-RAS Type 3 models were both in good agreement with the laboratory data for the low flow conditions (Figure 6.7). The Modified model was much better than the Regular model for the middle and high flows (Figures 6.8 and 6.9.) At RS 130 the undistorted Modified model agreed almost perfectly for Profiles 6 and 9 of the middle and high flow, respectively. The Regular model was improved by choosing zero skew for the bridge and bounding cross sections directly upstream and downstream from the bridge. (Figures 6.11, 6.10 and 6.12.) This Regular model with no skew gave about the same results as Mr. Brunner's Modified model. These represented the high tailwater condition for each flow. Table 7.3 below shows high Froude numbers at the downstream bounding cross section for all profiles where there was not a good match with the laboratory data.

Table 7.3 Portion of Table 6.13 for Type 3 Experiments

Type 3 Modified					
River Sta Und	River Sta Dist	Profile	Fr # XS Und	Fr # XS Dist	Match with Lab
1	2	3	9	10	
80.77	403.87	1	0.71	0.71	x
80.77	403.87	2	0.48	0.48	x
80.77	403.87	3	0.41	0.41	x
80.77	403.87	4	0.85	0.85	
80.77	403.87	5	0.73	0.73	
80.77	403.87	6	0.57	0.57	x
80.77	403.87	7	0.75	0.75	
80.77	403.87	8	0.75	0.75	
80.77	403.87	9	0.72	0.72	x
75	375	Bridge			
69.2	346.13	1	0.7	0.70	x
69.2	346.13	2	0.49	0.49	x
69.2	346.13	3	0.42	0.42	x
69.2	346.13	4	0.95	0.95	
69.2	346.13	5	0.77	0.77	
69.2	346.13	6	0.6	0.60	x
69.2	346.13	7	0.99	0.99	
69.2	346.13	8	0.99	0.99	
69.2	346.13	9	0.81	0.81	x

x Good match with lab data

Overall, agreement with laboratory and HEC-RAS results were reasonably good when the Froude number at the downstream bounding cross section remained at or below about 0.7. HEC-RAS appears to assume critical depth through the bridge opening when this value is exceeded. Tailwater has negligible effect on the water surface profile upstream from the bridge for critical conditions. Very large discharges create Froude numbers greater than 0.7 at the downstream bounding cross section for properly sized bridges. Froude numbers this high could possibly be found on undersized bridges.

The laboratory models for the analogous conditions distinctly showed that the water surface profiles upstream from the bridges were dependent on tailwater conditions for all runs. This was true for at three types of experiments. It seemed like the capacity of the water to adjust to the impediments created by bridge constrictions was more efficient than the one-dimensional HEC-RAS model simulated and that critical flow conditions (if they existed in the flume) did not dictate inlet control in the laboratory model. For example, visual observation of the Type 3 skewed bridge experiments showed the water adjusting well upstream from the bridge to conform to the skewed opening. The water didn't simply approach the skewed opening directly in the longitudinal direction and "see" the bridge as an opening reduced in area by the cosine of the skew angle. This conforms with the HEC-RAS manuals which state that the skew angle used should be the actual angle of the flow relative to the channel flowline at the bridge. This is difficult to determine unless field observations have been made. Moreover, this angle should vary with discharge.

The HEC-RAS model is a popular program for hydraulic engineers and is a valuable tool for the hydraulic design of bridges. This study showed that HEC-RAS tends to produce conservatively high water surface profiles upstream from bridges when high Froude numbers exist just downstream from the bridge. It may be advisable to use a more physically based model such as FESWMS-2DH (finite-element surface-water modeling system for two-dimensional flow in the horizontal plane, <http://water.usgs.gov/software/feswms.html>) when analyzing a bridge that is experiencing such high flow conditions. In the design mode, it is unlikely that a bridge that produced such high Froude numbers would be considered.

Table 7.4 shows the HEC-RAS project, plan and file names for the Type 1, Type 2 and Type 3 experiments. A CD with the HEC-RAS models is included with this report; HEC-RAS software is required to view these models.

Table 7.4 Project, Plan and File Names

Project Title	Plan Name	Files		
		Plan	Geometry	Flow
		Type1_Feb2010.p (#)	Type1_Feb2010.g (#)	Type1_Feb2010.f (#)
Type 1 February 2010	Type 1, Regular Distorted	15	03	07
	Type 1, Regular Undistorted	17	11	02
	Type 1, Modified Distorted	02	15	07
	Type 1, Modified Undistorted	05	16	02
		Type2_Feb2010.p (#)	Type2_Feb2010.g (#)	Type2_Feb2010.f (#)
Type 2 February 2010	Type 2, Regular Distorted	04	05	06
	Type 2, Regular Undistorted	06	10	08
	Type 2, Modified Distorted	01	15	04
	Type 2, Modified Undistorted	05	16	08
	Type 2, Regular Undistorted Cd = 0.5	03	17	08
		Type3_Feb2010.p (#)	Type3_Feb2010.g (#)	Type3_Feb2010.f (#)
Type 3 February 2010	Type 3, Reg, Distorted, 30 deg Skew	03	15	08
	Type 3, Reg, Undistorted, 30 deg Skew	05	16	09
	Type 3, Mod, Distorted, 30 deg Skew	06	17	08
	Type 3, Mod, Undistorted, 30 deg Skew	11	18	09
	Type 3, Reg, Undistorted, No Skew	18	25	09
	Type 3, Reg, Distorted, No Skew	01	01	08

REFERENCES

Brunner, Gary W., "HEC-RAS River Analysis System User's Manual," Report No. CPD-68, Version 4.0, March 2008, US Army Corps of Engineers, Hydrologic Engineering Center (HEC).

Brunner, Gary W., "HEC-RAS River Analysis System Hydraulic Reference Manual," Report No. CPD-69, Version 4.0, March 2008, US Army Corps of Engineers, Hydrologic Engineering Center (HEC).

Henderson, F. M., "Open Channel Flow," Macmillan Series in Civil Engineering, 1966.

K - TRAN

KANSAS TRANSPORTATION RESEARCH
AND
NEW - DEVELOPMENTS PROGRAM



A COOPERATIVE TRANSPORTATION RESEARCH PROGRAM BETWEEN:

KANSAS DEPARTMENT OF TRANSPORTATION



THE UNIVERSITY OF KANSAS



KANSAS STATE UNIVERSITY

